

PREPARED FOR SUBMISSION TO JHEP

Generalizing event shapes: In search of lost collider time

Gregory P. Korchemsky^a, Emery Sokatchev^{b,c} and Alexander Zhiboedov^b

^a*Institut de Physique Théorique¹, Université Paris Saclay, CNRS, CEA, F-91191 Gif-sur-Yvette, France*

^b*CERN, Theoretical Physics Department, CH-1211 Geneva 23, Switzerland*

^c*Université Grenoble Alpes, USMB, CNRS, LAPTh, F-74000 Annecy, France*

ABSTRACT: We introduce a new class of collider-type observables in conformal field theories which we call generalized event shapes. They are defined as matrix elements of light-ray operators that are sensitive to the longitudinal, or time-dependent, structure of the state produced in the collision. Generalized event shapes can be studied using both correlation functions and scattering amplitudes. They are infrared finite and smoothly transit over to the familiar event shapes. We compute them in planar $\mathcal{N} = 4$ super-Yang-Mills theory at weak and strong coupling, and study their physical properties. We show that at strong coupling both the stringy and quantum-gravitational corrections to the energy-energy correlation exhibit longitudinal broadening that manifests itself through the presence of long-time tails in the energy flux measured by the detectors.

¹Unité Mixte de Recherche 3681 du CNRS

Contents

1	Introduction	1
2	Definition of the observables	7
2.1	ω -deformed light transform	7
2.2	Familiar frames: the null plane	11
2.3	Familiar frames: insertion at spatial infinity	11
2.4	Signature	13
2.5	Generalized event shapes	13
2.6	Special detectors: S, Q, and E	17
2.7	Finiteness, commutativity and non-analyticity in ω	19
3	Detector properties: amplitude definition	20
3.1	Warm up example: free scalar field	22
3.2	One-point functions from amplitudes	25
3.3	Cross-talk	26
3.4	Two-point functions in $\mathcal{N} = 4$ SYM from amplitudes	28
4	Generalized event shapes with scalar detectors	37
4.1	SSC kernel: opposite signs	39
4.2	SSC kernel: same sign	41
4.3	Closing the contour	43
4.4	Detector identity	44
4.5	Bulk point singularity	45
5	$\mathcal{N} = 4$ supersymmetry Ward identities for the kernels	47
5.1	Stress-energy tensor multiplet in $\mathcal{N} = 4$ SYM	47
5.2	Summary of the relationships between the kernels for $\omega_i \neq 0$	50
5.3	Relationship between generalized event shapes in special cases	51
6	Summary of the generalized event shapes in $\mathcal{N} = 4$ SYM	54
6.1	Weak coupling	54
6.2	Strong coupling	57
7	Quantum gravity corrections to event shapes	61
7.1	One-loop supergravity	61
7.2	Dispersive representation of the energy-energy correlator	63
7.3	Small ω and the Regge limit	68

8	Ordinary event shapes at finite λ and finite c_T	69
8.1	Stringy corrections	69
8.2	Gravitational loops	70
9	Conclusions and future directions	71
A	Conformal properties of the deformed light-ray operators	75
B	Reality property of generalized event shapes	78
C	One-point function	79
D	Free scalar field at null infinity	83
E	Derivation of the SSC kernels	84
F	Computing SSC_{++} using correlation functions	89
G	Bulk point singularity	90
H	Details of the derivation in Section 5	91
I	Singular terms in the energy-energy correlation	100
J	Time profile in the detector	101

1 Introduction

In this paper we study a new class of observables in the familiar conformal collider physics setting [1]. They characterize the Lorentzian evolution of a state created by a local operator acting on the vacuum. As time passes, the state evolves in a nontrivial way. Its constituents interact with each other and propagate outwards until they reach the detectors situated at a macroscopic distance from the collision point.

One of the simplest detectors that we can consider is the energy calorimeter. It measures the energy deposited in a given direction at null infinity on the celestial sphere. The observables obtained by considering multiple calorimeters are called energy correlations [1–4]. In field theory terms, the operation of measuring the energy deposited in a certain direction on the celestial sphere corresponds to the insertion of an energy flow operator.¹ In $d = 4$

¹Up to a conformal transformation it is equivalent to the so-called *averaged null energy condition* (ANEC) operator [5].

dimensions it is defined as [1–4]

$$\mathcal{E}(n) = \int_{-\infty}^{\infty} du \lim_{r \rightarrow \infty} r^2 T_{0i} n^i(t = u + r, r\vec{n}), \quad (1.1)$$

where the stress-energy tensor is sent to infinity in the direction of the null vector $n^\mu = (1, \vec{n})$, with the unit vector $\vec{n}^2 = 1$ specifying the location of the energy calorimeter on the celestial sphere. The integral in (1.1) has the meaning of an average over the infinite working time u of the detector. The positivity of the ANEC operator in a unitary QFT, proved in [5, 6], corresponds to the intuitive statement that over an infinite time the energy calorimeter measures a non-negative energy flux in any state.

A hallmark of the detector defined (1.1) is that it probes the *transverse* structure of the state. In other words, if the time evolution produces energy fluxes collimated around particular angular directions, known as jets, these will manifest themselves as peaks in the energy correlations. At the same time, in strong coupling physics the energy calorimeters (1.1) produce, to leading order, a featureless, spherically symmetric energy distribution [1].

One may wonder, on the other hand, what is the *longitudinal* or time-dependent structure of the state? Do energy correlations arise as radiation arrives at future null infinity as a short pulse, or does the dynamical evolution lead to the broadening of the signal in time? The detectors (1.1) are not suited for addressing this question. Indeed, by averaging over time in (1.1) any time-dependent features of the energy flux get lost.

In order to probe the longitudinal aspects of the state, the detector operators should have a finite time resolution. This question has been addressed by the authors of Ref. [7]. They considered deep inelastic scattering, where the state was probed with a stress-energy tensor $T_{\mu\nu}$ localized in a certain region of spacetime and carrying some characteristic four-momentum. The issue of longitudinal broadening was discussed in [7] as well, both at weak and at strong coupling. While the setup of [7] is very physical, the observable in question is quite complicated and it is not directly connected to the more familiar event shapes such as energy correlations.

Inspired by [7], in this paper we would like, on the one hand, to probe the longitudinal structure of the state, and on the other hand, to stay as close as possible to the well-studied event shapes, such as energy correlations. To this end we consider the following generalization of the energy calorimeter

$$\mathcal{E}(\hat{\omega}, n) = \int_{-\infty}^{\infty} du e^{-i\hat{\omega}u} \lim_{r \rightarrow \infty} r^2 T_{0i} n^i(t = u + r, r\vec{n}), \quad (1.2)$$

which probes the state at the characteristic timescale $1/\hat{\omega}$. The deformation parameter $\hat{\omega}$ is interpreted as the energy (or ‘frequency’) transferred from the detector to the particles that it probes (see (1.7) below). We call the matrix elements of products of operators (1.2) *generalized event shapes*. Their study is the main subject of the present paper.²

²This operator appeared recently in [8], where $\hat{\omega}$ played the role of a regulator in the computation of

The generalized event shapes are not standard differential cross sections. To elucidate this point, let us denote the quantum state by $|\Psi\rangle$, and write the corresponding density matrix $\rho_\Psi = |\Psi\rangle\langle\Psi|$. Physical observables are then associated to hermitian operators $X = X^\dagger$ and are computed as their expectation values,

$$\langle X \rangle_\Psi \equiv \text{Tr} [\rho_\Psi X] . \quad (1.3)$$

In fact, the observables normally studied in collider experiments, the so-called event shapes, are more restrictive than (1.3). To understand this, it is useful to write the density matrix in a multi-particle basis $|n\rangle$,

$$\rho_\Psi = \sum_{n,n'} |n\rangle\langle n'| \times \langle n|\Psi\rangle\langle\Psi|n'\rangle . \quad (1.4)$$

A standard event shape is then defined by restricting to a measurement protocol, or detector, X that is diagonal in the multi-particle basis $X_{\text{standard}} = \sum_n x_n |n\rangle\langle n|$. Such detectors are natural since they can be easily realized in an experimental setting. These measurements are classical in the sense that they only probe the probability $|\langle\Psi|n\rangle|^2$, also known as differential cross section, and are not sensitive to the phases $\phi_{\Psi,n}$ of the scattering amplitudes $\langle\Psi|n\rangle = |\langle\Psi|n\rangle|e^{i\phi_{\Psi,n}}$.³ In the language of conformal field theory, the standard event shape distributions, or weighted cross sections, correspond to the matrix elements of the so-called light-ray operators [10], of which the ANEC operator (1.1) is an important example. Thinking about event shapes in terms of the matrix elements of light-ray operators has proved very fruitful and has led to new insights into the structure of event shapes even in theories without conformal symmetry such as QCD, see e.g. [11–13].

Conceptually nothing prevents us from considering more general detectors X with non-vanishing non-diagonal elements $\langle n|X|n'\rangle$ in the multi-particle basis. The corresponding observables (1.3) are sensitive to the phases of the scattering amplitudes $\langle n|\Psi\rangle$.⁴ In fact, in a measurement of finite duration this is essentially unavoidable.

The consequences of this fact are probably most dramatic in a gapless theory. Indeed, due to the uncertainty principle, any finite-time T measurement necessarily perturbs the system at the energy scale $\delta E \sim 1/T$. This causes transitions inside the physical detector

various commutators of light-ray operators. Our motivation here is different. In particular, in this paper we only study the matrix elements of light-ray operators of the type (1.2) at non-coincident points, for which all the commutators vanish, see e.g. (1.5).

³The question to what extent the phase of an amplitude is uniquely fixed by the differential cross section has a long history in the S -matrix bootstrap, see [9] for a recent review. In this context it was rigorously shown that in some special situations, namely elastic scattering of massive particles at low energies where no particle production is possible and with some extra technical assumptions, knowing the differential cross section does uniquely specify the phase. For such cases the observables discussed here can be computed in the standard collider setting by first reconstructing the phase of the amplitude from the measured differential cross section and then evaluating (1.3).

⁴More precisely, they are sensitive to the relative phases of the scattering amplitudes since the overall phase of the S -matrix is not observable.

$\langle n|X|n'\rangle$ with $E_n - E_{n'} \sim 1/T$. The observables of this type with a finite time resolution are the main subject of the present paper. To realize such observables in practice, one would need to devise an experiment that measures the phases of the scattering amplitudes $\langle \Psi|n\rangle$ and not just the cross sections $|\langle \Psi|n\rangle|^2$, since from (1.4) we have $\rho_\Psi = |n\rangle\langle n'| \cdot |\langle \Psi|n\rangle| |\langle \Psi|n'\rangle| e^{i(\phi_{\Psi,n'} - \phi_{\Psi,n})}$.⁵ This is precisely the effect of introducing a non-zero $\hat{\omega}$ in (1.2).

Still, the generalized detector operators (1.2) share many properties with the standard energy calorimeter (1.1). For example, they commute when placed at different points on the celestial sphere,

$$[\mathcal{E}(\hat{\omega}_1, n_1), \mathcal{E}(\hat{\omega}_2, n_2)] = 0, \quad n_1 \neq n_2. \quad (1.5)$$

This follows directly from the arguments of [15]. For non-positive (non-negative) $\hat{\omega}$ the operators (1.2) annihilate the right (left) vacuum

$$\begin{aligned} \mathcal{E}(\hat{\omega}, n)|\Omega\rangle &= 0, & \hat{\omega} &\leq 0, \\ \langle\Omega|\mathcal{E}(\hat{\omega}, n) &= 0, & \hat{\omega} &\geq 0. \end{aligned} \quad (1.6)$$

The relations (1.5) and (1.6) are familiar from the study of ordinary event shapes.

Finally, a new feature of (1.2) compared to (1.1) is that $\mathcal{E}(\hat{\omega}, n)$ carries a nonzero momentum $\hat{\omega}n^\mu$,

$$[P^\mu, \mathcal{E}(\hat{\omega}, n)] = \hat{\omega}n^\mu \mathcal{E}(\hat{\omega}, n). \quad (1.7)$$

In other words, when an excitation goes through the detector (1.2), it acquires an energy ‘kick’. In particular, such detectors can use part of their energy to create or annihilate particles. This leads to various new and interesting effects that we describe below.

The generalized event shapes have a much richer structure than the standard ones. This is not surprising since no information is lost from the stress-energy tensor after the Fourier transform in (1.2), which is to be contrasted with the averaging over time in (1.1). From this point of view the generalized event shapes are nothing but the familiar Wightman functions understood through the prism of a collider-type experiment. We believe that this point of view is useful since it reveals the dynamical information contained in the Wightman function in a more intuitive form.

Importantly, the generalized event shapes are IR finite if the underlying undeformed event shapes are IR finite. In fact, we expect them to be IR finite even when the undeformed event shapes are not. We present explicit examples of this type in the paper. This might be interesting in the context of QCD, where by considering generalized event shapes one can study a broader class of observables.⁶ In weakly coupled theories, generalized event shapes can be computed using either the standard scattering amplitudes techniques, or equivalently

⁵This is different from the interference effect between different intermediate states that contribute to the same final state, recently discussed in [14].

⁶A natural example is the generalized charge-charge correlation which is not IR safe in the ordinary setup.

from correlation functions. In a strongly coupled CFT only the correlation function picture is available.

After considering the general properties of the generalized event shapes, we analyze them in the planar $\mathcal{N} = 4$ SYM theory both at weak and at strong coupling. For $\hat{\omega}_i = 0$ these event shapes were studied in a series of papers [16–19], of which the present paper is a natural continuation. More precisely, we consider two-point generalized event shape distributions which are given by an expectation value of the product of two detector operators over the state created out of the vacuum by a local operator. We work in Mellin space and obtain a concise representation for these distributions in the form of a convolution of the Mellin amplitude for four-point correlation function and certain kinematical kernel depending on the choice of the detector. We use $\mathcal{N} = 4$ supersymmetry Ward identities to relate to each other the results for different detectors, generalizing the $\hat{\omega}_i = 0$ analysis of [16, 17, 20, 21].

Below we quote our results for the energy-energy correlation (EEC) at weak and at strong coupling. It is convenient to introduce dimensionless frequencies ω_i (related to $\hat{\omega}_i$ above by a simple rescaling $\omega_i = 2\hat{\omega}_i(qn_i)/q^2$) and the conformal version of the angle between the detectors z ,⁷ see Section 4 for the detailed definitions.

- At weak coupling, to leading order in the 't Hooft coupling $a = g^2 N_c / (4\pi^2)$ we get for $0 < z < 1$

$$\begin{aligned} \text{EEC}_{+-}^{\text{weak}} = & \frac{a}{4} \left[-\frac{\omega_1^2 \omega_2^2}{36(\omega_2 + 1)z} \log \left(\frac{z(\omega_2 + 1)}{\omega_2 z + 1} \right) \right. \\ & + \frac{(\omega_1^2 \omega_2^2 z^2 + 6\omega_1 \omega_2 z (\omega_1 + \omega_2 + 3) + 6(\omega_1^2 + \omega_2^2 + 3\omega_1 \omega_2 + 6(\omega_1 + \omega_2) + 6)) \log \left(\frac{\omega_2 z + 1}{1 - z} \right)}{36(1 - z)z^2} \\ & \left. + \frac{(\omega_2 + 1)(\omega_2^2 + 6\omega_2 + 6) \left(\frac{\omega_1^2 (\omega_2 z + 1)^2}{(\omega_2 + 1)^2} + \frac{6\omega_1 (\omega_2 z + 1)}{(\omega_2 + 1)} + 6 \right) \log \left(\frac{\omega_1 \omega_2 z + \omega_1 + \omega_2 + 1}{(\omega_2 + 1)^2} \right)}{72(1 - z)z(\omega_2 z + 1)} \right]. \quad (1.8) \end{aligned}$$

- At strong coupling, we get from tree-level supergravity for $0 < z < 1$

$$\text{EEC}_{+-}^{\text{sugra}} = \frac{(\omega_2 + 1)^2 (\omega_2^2 + 6\omega_2 + 6) \left(\frac{\omega_1^2 (\omega_2 z + 1)^2}{(\omega_2 + 1)^2} + \frac{6\omega_1 (\omega_2 z + 1)}{\omega_2 + 1} + 6 \right)}{72(\omega_2 z + 1)^3}. \quad (1.9)$$

The subscript ‘+−’ in the formulas above refers to the particular choice $\omega_1 \geq 0$ and $-1 < \omega_2 \leq 0$. Setting $\omega_i = 0$ we reproduce the previously known results for the (undeformed) energy-energy correlation [1, 16, 17]. We will show that the expressions for $\text{EEC}(\omega_1, \omega_2)$ are sensitive to the signs of ω_i and are not analytic around $\omega_i = 0$.⁸ This is a common feature of the generalized event shapes. The complete set of our results is summarized in Section 6. The expressions above should be completed by contact terms at $z = 0$, i.e. when

⁷In the rest frame of the source $z = (1 - (\vec{n}_1 \vec{n}_2))/2 = \sin^2(\theta/2)$, where θ is the angle between \vec{n}_1 and \vec{n}_2 .

⁸This property is not obvious from the expressions above but can be seen from the results collected in Section 6.

the detectors are on top of each other. Such terms require a more careful treatment and will be the subject of a separate paper [22]. At weak coupling there are also terms localized in the back-to-back region $z = 1$ which we discuss below.

As we mentioned above, the generalized event shapes can be computed even in the cases in when the ordinary event shapes are not well defined. One notable example is the computation of stringy and quantum-gravitational (QG) corrections to the energy-energy correlation at strong coupling. More precisely, computing the $1/\lambda$ (stringy) or $1/c_T$ (quantum-gravitational) corrections to the correlation function of local operators, one finds that they produce an infinite contribution to the energy-energy correlation.⁹ On the other hand, based on general grounds, the energy-energy correlation should be finite at finite c_T and finite λ , see [15]. Introducing non-zero ω_i solves the problem and makes the corrections to the generalized event shapes finite and systematically computable.

A distinctive feature of the stringy and QG corrections to the generalized event shapes is the presence of divergences in the $\omega_i \rightarrow 0$ limit. By means of a Fourier transform these can be interpreted as long-time effects in the detectors, which continue to detect the non-zero energy flux at arbitrarily late times. This is an artifact of perturbation theory because in the complete theory the energy flux eventually goes to zero. From this point of view, the correct physical interpretation of the $\omega_i \rightarrow 0$ divergences is the presence of a long-time tail of radiation measured by the detectors. As we will see below, the presence of such long-time tails is typical for theories with a gravity dual. This is very different from what is measured by the detectors at weak coupling where the radiation is localized on timescales determined by the characteristic size of the wave packet that creates the state. Moreover, by focusing on the different types of time (or, equivalently, frequency) dependence of the energy flux one can distinguish different underlying physics: classical gravity, stringy corrections, and quantum-gravitational effects.

Choosing only one non-vanishing ω_i , say $\omega_2 \neq 0$, and making use of the recent progress in the understanding of gravitational loops in AdS [23–25], in Section 7 we analyze the leading correction to the energy-energy correlation in $\mathcal{N} = 4$ SYM from the one-loop supergravity Mellin amplitude [26]. As expected, the correction is divergent in the $\omega_2 \rightarrow 0$ limit. We compute all the divergent terms explicitly, the result given by (7.6). To better understand the origin of the divergences (and how they disappear at finite c_T and λ) we use the Mellin space dispersion relations [27] to derive a dispersive representation for the energy-energy correlation, see (7.17).

Equipped with the perturbative results at $\omega_i \neq 0$, in Section 8 we discuss corrections to the undeformed event shapes ($\omega_i = 0$) at finite λ and finite c_T . Closely related to the discussion of long-time effects above, a characteristic feature of the perturbative corrections to the undeformed event shapes at strong coupling is that they are enhanced compared to the perturbative expansion of the correlation function. We review the stringy contributions

⁹In a gauge theory c_T is related to the number of colors N_c . In what follows, in the framework of $\mathcal{N} = 4$ SYM we set $c_T = (N_c^2 - 1)/4$.

to the energy-energy correlation, emphasizing on the enhancement of the leading stringy correction to the energy-energy correlation compared to the analogous correction to the correlation function. We point out that these corrections have a long-time origin and are drastically different from the pattern of radiation produced in classical gravity. Finally, we discuss the finite c_T corrections to the ordinary event shapes. Here again we observe that the explicit one-loop computation from Section 7 predicts the existence of both λ - and c_T -enhanced terms in the expansion of the energy-energy correlation. We speculate on the possible form of the leading $1/c_T$ correction to the energy-energy correlation, see (8.6).

The structure of the paper is as follows. In Section 2 we introduce the generalized detector operators as the ω -deformed light-ray transform of local operators. We then define the generalized event shapes and discuss their general properties in a conformal field theory. In Section 3, we compute one- and two-point correlations at weak coupling using the amplitude approach. In Section 4, we employ the correlation function approach to study the properties of the scalar-scalar correlation both at weak and strong coupling in $\mathcal{N} = 4$ SYM. In Section 5 we extend our analysis to more complicated correlation functions involving the conserved R -current and the stress-energy tensor. We also establish an interesting relation between the event shape correlations involving energy and charge detectors. Section 6 contains a summary of our results for various event shapes in $\mathcal{N} = 4$ SYM at weak and strong coupling. In Section 7 we discuss the corrections to the generalized energy-energy correlation at strong coupling coming from gravitational loops. In Section 8 we discuss stringy and gravitational corrections to the undeformed energy-energy correlation at finite λ and finite c_T . Section 9 contains concluding remarks and a list of interesting open questions to pursue. The technical details are presented in several appendices.

2 Definition of the observables

In this section we define the generalized event shapes that will be the main subject of the paper. We start by introducing the ω -deformed light-ray transform (which is a one-parameter generalization of the usual light transform of [10]) and review its basic properties in the context of d -dimensional CFT.¹⁰ The new objects have slightly unusual conformal transformation properties but preserve some of the salient features of the familiar, $\hat{\omega} = 0$, light-ray operators. Physically, the main new feature of the ω -deformed detectors is that they can create and annihilate particles depending on the sign of $\hat{\omega}$. This leads to various new interesting effects.

2.1 ω -deformed light transform

Eventually, we will be interested in placing symmetric traceless primary operators at future null infinity and integrating them over time with a plane wave profile. It is appropriate to

¹⁰In the following sections we will focus on the generalized event shapes in $d = 4$ $\mathcal{N} = 4$ SYM.

start with a general discussion of the conformal properties of such objects and specify their insertion at null infinity later.

To describe the conformal properties of the ω -deformed calorimeters it is convenient to use the embedding space formalism in which Minkowski space is realized as a subset of the projective null cone in $\mathbb{R}^{2,d}$. We denote $(d+2)$ -dimensional vectors in the embedding space as $X = (X^+, X^-, X^\mu)$ where $X^\pm = X^{d+2} \pm X^{d+1}$ and $X^\mu = X^0, \dots, X^{d-1}$. The scalar product in these coordinates looks as

$$X \cdot X = X^+ X^- + (X^0)^2 - (X^1)^2 - \dots - (X^{d-1})^2. \quad (2.1)$$

The projective null cone is defined as $X \cdot X = 0$ modulo rescaling $X \sim \lambda X$, where $\lambda \in \mathbb{R}_+$. Minkowski space arises as the locus $(X^+, X^-, X^\mu) = (1, -x^2, x^\mu)$, where $x^2 = (x^0)^2 - (\vec{x})^2$ and $\vec{x} = (x^1, \dots, x^{d-1})$.

To describe local operators with spin we introduce the familiar index-free notation

$$O(x, z) \equiv O_{\mu_1 \dots \mu_J}(x) z^{\mu_1} \dots z^{\mu_J}, \quad (2.2)$$

where the Lorentz indices of the operator are contracted with a future-pointing null polarization vector z^μ .¹¹ In the embedding space $O(x, z)$ gets lifted to a *homogeneous* (see (2.4) below) function $O(X, Z)$, where $X^2 = Z^2 = X \cdot Z = 0$. It is related to the operator $O(x, z)$ as follows

$$O(X, Z) = (X^+)^{-\Delta} O\left(x = \frac{X}{X^+}, z = Z - \frac{Z^+}{X^+} X\right). \quad (2.3)$$

Here on the left-hand side $O(X, Z)$ is written in terms of the $(d+2)$ -dimensional vectors X and Z , while on the right-hand side $O(x, z)$ depends on the d -dimensional coordinate $x^\mu = X^\mu/X^+$ and the auxiliary d -dimensional null polarization vector $z^\mu = Z^\mu - X^\mu Z^+/X^+$. Up to gauge fixing, the two representations encode the same information. We will switch between the embedding and physical coordinates interchangeably, hoping that this will not cause confusion.

The conformal transformations act linearly on the vectors X and Z by multiplying them by $SO(2, d)$ matrices.¹² The primary operators $O(X, Z)$ are invariant under such transformations. They are homogeneous functions,

$$O(\lambda X, \rho Z) = \lambda^{-\Delta} \rho^J O(X, Z), \quad \lambda, \rho > 0, \quad (2.4)$$

and the degrees of homogeneity Δ and J define the quantum numbers of the operator (or representation labels) – dimension and spin, respectively. In addition, $O(X, Z)$ is invariant under the following shifts

$$O(X, Z + \beta X) = O(X, Z). \quad (2.5)$$

¹¹The notation z^μ for the polarization vector is quite common. Later in this section z will also denote an angular variable, see Eq. (2.42), but this should not lead to confusion.

¹²See appendix A for further details.

The light transform of a primary operator $O(X, Z)$ is defined as [10]

$$\mathbf{L}[O](X, Z) := \int_{-\infty}^{\infty} d\alpha O(Z - \alpha X, -X). \quad (2.6)$$

The light-ray operator $\mathbf{L}[O](X, Z)$ defined in such a way is a primary operator with the scaling dimension $1 - J$ and spin $1 - \Delta$. The conventional event shapes can be understood as matrix elements of the light-ray operators inserted at spatial infinity X_∞ [15], see Section 2.3 for the precise definition.

As discussed in the introduction, in this paper we are interested in generalized event shapes which are sensitive to the longitudinal structure of the state. We would therefore like to consider a generalization of (2.6), where instead of simply integrating over α with weight 1 we insert some nontrivial weight function. As we will see below, a natural choice is to consider the Fourier transform with respect to α .¹³ We thus define the ω -deformed light transform as follows

$$\mathbf{L}_{\hat{\omega}}[O](X, Z) \equiv \int_{-\infty}^{\infty} d\alpha e^{-i\hat{\omega}\alpha} O(Z - \alpha X, -X). \quad (2.7)$$

In the context of a collider experiment the insertion of the phase $e^{-i\hat{\omega}\alpha}$ in (2.7) leads to two important new properties of the detectors. Firstly, the detector carries a non-vanishing null momentum, which is quite natural if the source and the sink are momentum eigenstates. Secondly, the phase $e^{-i\hat{\omega}\alpha}$ improves the convergence of the integral at large α , which is related to the IR safety of the observables in question [15].

Let us find out how the $\hat{\omega}$ -deformed light-ray operators $\mathbf{L}_{\hat{\omega}}[O](X, Z)$ transform under (2.4) and (2.5). Using the definition (2.7) it is easy to check that

$$\mathbf{L}_{\hat{\omega}}[O](\lambda X, \lambda Z) = \lambda^{J-\Delta} \mathbf{L}_{\hat{\omega}}[O](X, Z), \quad (2.8)$$

$$\mathbf{L}_{\hat{\omega}}[O](X, Z + \beta X) = e^{-i\hat{\omega}\beta} \mathbf{L}_{\hat{\omega}}[O](X, Z). \quad (2.9)$$

In addition, we use (2.4) to find

$$\mathbf{L}_{\hat{\omega}}[O](X, \gamma Z) = \int_{-\infty}^{\infty} d\alpha e^{-i\hat{\omega}\alpha} O(\gamma Z - \alpha X, -X) = \gamma^{1-\Delta} \mathbf{L}_{\gamma\hat{\omega}}[O](X, Z). \quad (2.10)$$

Comparing (2.8), (2.9) and (2.10) to the transformation properties of the primary operators (2.4) and (2.5), one deduces that for $\hat{\omega} \neq 0$ the operator $\mathbf{L}_{\hat{\omega}}[O](X, Z)$ does not transform like an ordinary primary operator. At the same time, for $\hat{\omega} = 0$ it is a primary operator with the quantum numbers $(1 - J, 1 - \Delta)$.

To better understand the properties of $\mathbf{L}_{\hat{\omega}}[O](X, Z)$ for $\hat{\omega} \neq 0$ let us rewrite (2.7) in Poincaré coordinates. Using the correspondence formula (2.3) and the scaling property (2.4), and fixing the gauge as $X = (1, -x^2, x^\mu)$ and $Z = (0, -2(z \cdot x), z)$, we get

$$\mathbf{L}_{\hat{\omega}}[O](x, z) = \int_{-\infty}^{\infty} d\alpha (-\alpha)^{-\Delta-J} e^{-i\hat{\omega}\alpha} O\left(x - \frac{z}{\alpha}, z\right). \quad (2.11)$$

¹³We thank Petr Kravchuk for discussions related to the material in this section.

Let us now act on this operator with the generators of conformal transformations in x -space. We focus on their action at the origin $x = 0$, since $\mathbf{L}_{\hat{\omega}}[O](x, z) = e^{iP \cdot x} \mathbf{L}_{\hat{\omega}}[O](0, z) e^{-iP \cdot x}$. For the generator of the special conformal transformation K_{μ} we get

$$[K_{\mu}, \mathbf{L}_{\hat{\omega}}[O](0, z)] = 2\hat{\omega} z_{\mu} \mathbf{L}_{\hat{\omega}}[O](0, z). \quad (2.12)$$

To derive this relation, we applied the special conformal transformation to the local operator under the integral in (2.11), used the identity

$$\left[K_{\mu}, O\left(-\frac{z}{\alpha}, z\right) \right] = -i \left[2z_{\mu} \partial_{\alpha} O\left(-\frac{z}{\alpha}, z\right) - 2(\Delta + J) \frac{z_{\mu}}{\alpha} O\left(-\frac{z}{\alpha}, z\right) \right], \quad (2.13)$$

and finally integrated by parts.¹⁴

It follows from (2.12) that the light-ray operators $\mathbf{L}_{\hat{\omega}}[O](0, z)$ are eigenstates of the special conformal generator with a non-zero eigenvalue $2\hat{\omega} z_{\mu}$. The significance of this fact is that, when placed at spatial infinity as discussed in detail in the next section, $\mathbf{L}_{\hat{\omega}}[O](\infty, z)$ becomes an eigenstate of the momentum generator P_{μ} , or in other words it carries a definite momentum. This is what motivates our choice of the factor $e^{-i\hat{\omega}\alpha}$ in (2.7) versus some more general weight function $f(\alpha)$. In particular, when studying event shapes or matrix elements of the ω -deformed light transform operators between momentum eigenstates, we will find a simple selection rule or, equivalently, an overall momentum-preserving delta function.

For the dilatations we get

$$\begin{aligned} \lambda^{iD} \mathbf{L}_{\hat{\omega}}[O](0, z) \lambda^{-iD} &= \int_{-\infty}^{\infty} d\alpha (-\alpha)^{-\Delta-J} e^{-i\hat{\omega}\alpha} \lambda^{iD} O\left(-\frac{z}{\alpha}, z\right) \lambda^{-iD} \\ &= \int_{-\infty}^{\infty} d\alpha (-\alpha)^{-\Delta-J} e^{-i\hat{\omega}\alpha} \lambda^{\Delta} O\left(-\lambda \frac{z}{\alpha}, z\right) \\ &= \lambda^{1-J} \int_{-\infty}^{\infty} d\alpha (-\alpha)^{-\Delta-J} e^{-i\lambda\hat{\omega}\alpha} O\left(-\frac{z}{\alpha}, z\right) = \lambda^{1-J} \mathbf{L}_{\lambda\hat{\omega}}[O](0, z). \end{aligned} \quad (2.14)$$

Finally, under the Lorentz transformation by an identical argument we get

$$U_{\Lambda} \mathbf{L}_{\hat{\omega}}[O](0, z) U_{\Lambda}^{-1} = \mathbf{L}_{\hat{\omega}}[O](0, \Lambda z). \quad (2.15)$$

It is easy to check that the relations (2.12), (2.14) and (2.15) are consistent with the conformal algebra, $[D, K_{\mu}] = -iK_{\mu}$ and $[D, L_{\mu\nu}] = 0$, where $L_{\mu\nu}$ are the generators of the Lorentz transformations. In the standard discussion of the representations of the conformal group, see for example [28], it is assumed that operators placed at the origin transform in a finite-dimensional representation of the Lorentz group. In this case, applying Schur's lemma one would conclude from $[D, L_{\mu\nu}] = 0$ that D has to be proportional to the identity matrix. The light-ray operators discussed here transform in an infinite-dimensional representation of the Lorentz group (2.15) and therefore the above argument does not apply. Indeed, it follows from (2.14) that D acts nontrivially on $\mathbf{L}_{\hat{\omega}}[O](0, z)$. Moreover, if D were proportional to the identity matrix, one would deduce from $[D, K_{\mu}] = -iK_{\mu}$ that K_{μ} has to annihilate the operator $\mathbf{L}_{\hat{\omega}}[O](0, z)$, in contradiction to (2.12).

¹⁴An alternative derivation of (2.12) and (2.14) within the embedding formalism is presented in appendix A.

2.2 Familiar frames: the null plane

To get a better intuition regarding (2.7) it is useful to write it in various conformal frames. Let us first consider the insertion at past null infinity,

$$X_0 = \left(0, 0, -\frac{1}{2}, \frac{1}{2}, \vec{0}\right), \quad Z_0 = (1, \vec{y}^2, 0, 0, \vec{y}), \quad (2.16)$$

where $\vec{y} = (y^2, y^3, \dots, y^{d-1})$. In this frame we get (defining $u = t - y^1$, $v = t + y^1$)

$$\begin{aligned} \mathbf{L}_{\hat{\omega}}[O](X_0, Z_0) &= \int_{-\infty}^{\infty} d\alpha e^{-i\hat{\omega}\alpha} O(Z_0 - \alpha X_0, -X_0) \\ &= \int_{-\infty}^{\infty} du e^{-i\hat{\omega}u} O_{u\dots u}(u, v=0, \vec{y}), \end{aligned} \quad (2.17)$$

where we applied the relations (2.3) and (2.2) and used that $O_u = \frac{1}{2}O^v = \frac{1}{2}(O^t + O^{y^1})$. In this way we have recovered a definition of the light-ray operator on the null hyperplane $v=0$.

It follows from (2.17) that the operator $\mathbf{L}_{\hat{\omega}}[O](X_0, Z_0)$ annihilates the right (left) vacuum for $\hat{\omega} \leq 0$ ($\hat{\omega} \geq 0$), e.g.

$$\mathbf{L}_{\hat{\omega}}[O](X_0, Z_0)|\Omega\rangle = 0, \quad \hat{\omega} \leq 0. \quad (2.18)$$

Indeed the state on the left-hand side of this relation has the momentum $P_u = \hat{\omega}$. In a unitarity QFT it has to satisfy the condition $P_u > 0$ or vanish otherwise.

2.3 Familiar frames: insertion at spatial infinity

In this paper we will be interested in a setup when the detectors are placed at spatial infinity. In terms of $\mathbf{L}_{\hat{\omega}}[O](X, Z)$ this corresponds to (see (2.3))

$$X_{\infty} = (0, 1, 0^{\mu}), \quad Z_{\infty} = (0, 0, n^{\mu}), \quad (2.19)$$

where $n^2 = 0$. It is easy to verify that $Z_{\infty} \cdot X_{\infty} = 0$, as well as $Z_{\infty}^2 = X_{\infty}^2 = 0$.

It is convenient to place the detector at finite distance in the Poincaré coordinates and then approach the spatial infinity point (2.19) by taking a ‘detector limit’. To achieve this, we consider the following r -dependent points

$$X_r \equiv \left(0, 1, -\frac{\bar{n}}{2(n\bar{n})r}\right), \quad Z_r \equiv \left(\frac{1}{r}, 0, n\right), \quad (2.20)$$

satisfying $Z_r \cdot X_r = Z_r^2 = X_r^2 = 0$. Here we introduced an arbitrary null vector $\bar{n}^2 = 0$ such that $(n\bar{n}) \neq 0$. Eq. (2.20) becomes (2.19) in the detector limit $r \rightarrow \infty$ and the dependence on \bar{n} drops out. With this choice of the conformal frame we get from (2.7)

$$\mathbf{L}_{\hat{\omega}}[O](X_{\infty}, Z_{\infty}) = \lim_{r \rightarrow \infty} \mathbf{L}_{\hat{\omega}}[O](X_r, Z_r)$$

$$= \int_{-\infty}^{\infty} d\alpha e^{-2i(n\bar{n})\hat{\omega}\alpha} \lim_{r \rightarrow \infty} \frac{r^{\Delta-J}}{[2(n\bar{n})]^{J-1}} O_{\mu_1 \dots \mu_J}(rn + \alpha\bar{n}) \bar{n}^{\mu_1} \dots \bar{n}^{\mu_J}, \quad (2.21)$$

where we substituted (2.20) into $O(Z_r - \alpha X_r, -X_r)$ and applied (2.3) and (2.2) for $x^\mu = rn^\mu + \frac{\alpha \bar{n}^\mu}{2(n\bar{n})}$ and $z^\mu = \frac{\bar{n}^\mu}{2(n\bar{n})r}$.

The careful reader might have noticed that in the last line of (2.21) we exchanged the order of the integration and the limit $r \rightarrow \infty$. The justification is as follows. Physically, we imagine placing the detectors at some finite distance r from the collision point, integrating over working time of the detectors and, then, taking the limit $r \rightarrow \infty$. In practice, however, it is much easier to send the detectors to infinity first and only then integrate over time. This is what we do in the present paper. We expect that the order of operations does not matter as long as the detectors do not communicate with each other, namely for $n_i \neq n_j$. This is the regime that we study in the present paper. In other words, exchanging the limit and the integration in (2.21) can lead to results that differ by contact terms localized at $n_i = n_j$, see [22].

In the sections below we consider a slightly different definition of the ω -detectors. We change $\hat{\omega} \rightarrow \hat{\omega}/2$ in the formula above and consider $O_J(\hat{\omega}, n) \equiv 2^{J-1} \mathbf{L}_{\frac{\hat{\omega}}{2}}[O](X_\infty, Z_\infty)$, so that

$$\mathcal{O}_J(\hat{\omega}, n) \equiv \int_{-\infty}^{\infty} d\alpha e^{-i(n\bar{n})\hat{\omega}\alpha} \lim_{r \rightarrow \infty} \frac{r^{\Delta-J}}{(n\bar{n})^{J-1}} O_{\mu_1 \dots \mu_J}(rn + \alpha\bar{n}) \bar{n}^{\mu_1} \dots \bar{n}^{\mu_J}, \quad (2.22)$$

where $n^2 = \bar{n}^2 = 0$. Let us emphasize again that the precise choice of \bar{n} is immaterial since the result does not depend on it. We will always assume that n^μ is a *future-pointing* null vector, namely $n^0 > 0$. The advantage of rescaling $\hat{\omega}$ by a factor of $1/2$ comes from noticing that

$$[P^\mu, \mathcal{O}_J(\hat{\omega}, n)] = \hat{\omega} n^\mu \mathcal{O}_J(\hat{\omega}, n), \quad (2.23)$$

which is an immediate consequence of (2.12) because the special conformal transformations at infinity correspond to translations around the origin. In other words, the detectors (2.22) carry a definite null momentum $\hat{\omega} n^\mu$.¹⁵

The momentum operator acts on the local operator as $[P^\mu, O_{\mu_1 \dots \mu_J}(x)] = i\partial^\mu O_{\mu_1 \dots \mu_J}(x)$. For $x = rn + \alpha\bar{n}$ and $r \rightarrow \infty$ the leading contribution only comes from the light-cone component $n^\mu(P\bar{n})/(n\bar{n}) = in^\mu \partial_\alpha/(n\bar{n})$. The contribution of the remaining components of P^μ is suppressed by a power of $1/r$. Integrating by parts in (2.22) we obtain (2.23).

From (2.10) we derive the scaling property

$$\mathcal{O}_J(\lambda^{-1}\hat{\omega}, \lambda n) = \lambda^{1-\Delta} \mathcal{O}_J(\hat{\omega}, n). \quad (2.24)$$

Setting $\hat{\omega} = 0$ and $n^\mu = (1, \vec{n})$ in (2.22) and replacing $O_{\mu_1 \dots \mu_J}$ with a conserved current or to the stress-energy tensor we recover the familiar charge $\mathcal{Q}(n)$ and energy $\mathcal{E}(n)$ detector

¹⁵Our convention for the symmetry generators is such that $[P^\mu, O(q)] = q^\mu O(q)$, where $O(q) \equiv \int d^d x e^{-iq \cdot x} O(x)$ and here we work in the mostly minus signature.

operators from [1, 16, 17]. From (2.23) it follows immediately that

$$\begin{aligned}\mathcal{O}_J(\hat{\omega}, n)|\Omega\rangle &= 0, \quad \hat{\omega} \leq 0, \\ \langle\Omega|\mathcal{O}_J(\hat{\omega}, n) &= 0, \quad \hat{\omega} \geq 0,\end{aligned}\tag{2.25}$$

where $|\Omega\rangle$ is the CFT vacuum. Eq. (2.25) is an obvious generalization of the corresponding property of light-ray operators at $\hat{\omega} = 0$, see [10] for the detailed argument.

2.4 Signature

Every relativistic quantum field theory has an anti-unitary symmetry which we denote by CRT, see e.g. [29]. This transformation reverses time T , one spatial direction R , as well as all charges C . Combining CRT with Hermitian conjugation we can classify operators into eigenspaces of $((\text{CRT})\dots(\text{CRT})^{-1})^\dagger$ [10]. The corresponding eigenvalue ± 1 is called the signature of the operator.

Let us examine the action of CRT on the ω -deformed light-ray transforms (2.17). CRT is an anti-unitary symmetry that acts as

$$(u, v, \vec{y}) \rightarrow (-u, -v, \vec{y}).\tag{2.26}$$

Combining CRT with Hermitian conjugation we get

$$\begin{aligned}\left((\text{CRT}) \int_{-\infty}^{\infty} du e^{-i\hat{\omega}u} \mathcal{O}_{u\dots u}(u, 0, \vec{y})(\text{CRT})^{-1}\right)^\dagger &= \eta_O(-1)^J \int_{-\infty}^{\infty} du e^{i\hat{\omega}u} \mathcal{O}_{u\dots u}(-u, 0, \vec{y}) \\ &= \eta_O(-1)^J \int_{-\infty}^{\infty} du e^{-i\hat{\omega}u} \mathcal{O}_{u\dots u}(u, 0, \vec{y}),\end{aligned}\tag{2.27}$$

where η_O is an arbitrary phase factor. Depending on the definition of the operator, the latter can be set to 1.¹⁶ For $\hat{\omega} = 0$ the eigenvalue $\eta_O(-1)^J$ is called the ‘signature’ of the light-ray operator. As follows from (2.27), the signature of the operator does not depend on $\hat{\omega}$.

We review the implications of CRT for the one- and two-point generalized event shapes in appendix B.

2.5 Generalized event shapes

Having defined the ω -deformed light-ray operators (2.22), we can now consider their matrix elements over physical states

$$\begin{aligned}\langle\phi_2(\tilde{q})\mathcal{O}_{J_1}(\hat{\omega}_1, n_1)\dots\mathcal{O}_{J_k}(\hat{\omega}_k, n_k)\phi_1(q)\rangle &= (2\pi)^d \delta^d(\tilde{q} - \sum_{i=1}^k \hat{\omega}_i n - q) \theta(q) \theta(q + \sum_{i=1}^k \hat{\omega}_i n) \\ &\times \langle\langle\phi_2(\tilde{q})\mathcal{O}_{J_1}(\hat{\omega}_1, n_1)\dots\mathcal{O}_{J_k}(\hat{\omega}_k, n_k)\phi_1(q)\rangle\rangle.\end{aligned}\tag{2.28}$$

¹⁶However this is not always a natural choice. For example, for the conserved current in a free scalar theory, $J_\mu = (J_\mu)^\dagger = i(\bar{\phi}\partial_\mu\phi - \partial_\mu\bar{\phi}\phi)$ we get $\eta_{J_\mu} = -1$. In fact this is the choice that we make for the charge detector operator $\mathcal{Q}(\hat{\omega}, n)$ in this paper.

Here $\mathcal{O}_{J_i}(\hat{\omega}_i, n_i)$ are identified as the ‘detectors’, $\phi_1(q)$ as the ‘source’ and $\phi_2(\tilde{q})$ as the ‘sink’. To describe a nontrivial physical state, q and \tilde{q} have to be future-pointing timelike momenta. The overall momentum conservation delta function in (2.28) takes into account the fact that each detector carries momentum $\hat{\omega}_i n_i^\mu$. The step function

$$\theta(q) \equiv \theta(q^0)\theta(q^2) \quad (2.29)$$

ensures that the relevant momenta are future-pointing time-like. This puts a constraint on the values of $\hat{\omega}_i$ for which the correlation function (2.28) is non-zero.

Below we choose the source and sink to be described by a scalar primary operator $\phi_1 = \phi_2^\dagger = \phi$ with the scaling dimension Δ_ϕ . We define the properly normalized correlation function

$$\langle \mathcal{O}_{J_1}(\hat{\omega}_1, n_1) \dots \mathcal{O}_{J_k}(\hat{\omega}_k, n_k) \rangle_q \equiv \frac{(q^2)^{\Delta_\phi - \frac{d}{2}}}{\sigma_{tot}(q)} \langle \langle \phi^\dagger(\tilde{q}) \mathcal{O}_{J_1}(\hat{\omega}_1, n_1) \dots \mathcal{O}_{J_k}(\hat{\omega}_k, n_k) \phi(q) \rangle \rangle, \quad (2.30)$$

which we shall call a *generalized event shape*. Here we made the left-hand side of (2.30) independent on the normalization of the operator $\phi(x)$ by dividing the right-hand side by the Fourier transform of the Wightman two-point function

$$\sigma_{tot}(q) \equiv \int d^d x e^{-iq \cdot x} \langle \phi^\dagger(x) \phi(0) \rangle. \quad (2.31)$$

It has the meaning of the total cross section of the process source \rightarrow anything. Choosing $\langle \phi^\dagger(x) \phi(0) \rangle = 1/(-x^2 + i0x^0)^{\Delta_\phi}$ we get

$$\sigma_{tot}(q) = \theta(q) \frac{2\pi^{d/2+1}(q^2/4)^{\Delta_\phi - d/2}}{\Gamma(\Delta_\phi)\Gamma(\Delta_\phi + 1 - d/2)}. \quad (2.32)$$

One-point function

Let us consider some simple examples of (2.30). We start with the one-point event shape. Its form is fixed by symmetry up to an arbitrary function of dimensionless argument

$$\langle \mathcal{O}_J(\hat{\omega}, n) \rangle_q = \frac{1}{S_{d-2}} \frac{(q^2)^{\Delta_\phi - \frac{d}{2} + \frac{J+\Delta_O}{2} - 1}}{(qn)^{\Delta_O - 1}} f_{\mathcal{O}_J}\left(\hat{\omega} \frac{2(qn)}{q^2}\right), \quad (2.33)$$

where the power of (qn) and q^2 is dictated by the relation (2.24) and by the scaling dimension of the observable, respectively. In this relation (Δ_O, J) are the quantum numbers of the detector operator. The normalization factor involving the area of the unit sphere $S_{d-2} = 2\pi^{\frac{d-1}{2}}/\Gamma(\frac{d-1}{2})$ was introduced for convenience (see e.g. (2.49) and (2.50) below).

It is convenient to replace the argument of the function $f_{\mathcal{O}_J}$ in (2.33) by the dimensionless frequency

$$\omega = \frac{2(qn)}{q^2} \hat{\omega}. \quad (2.34)$$

The constraint (2.29) that the sink carries a time-like momentum becomes $\theta(1 + \omega)$, or $\omega \geq -1$. The rescaled frequency makes the transformation property (2.24) look simpler,

$$\mathcal{O}_J(\omega, \lambda n) = \lambda^{1-\Delta} \mathcal{O}_J(\omega, n). \quad (2.35)$$

In what follows we will interchange freely between $\hat{\omega}$ and ω , keeping in mind the relation (2.34) between them. We hope this will not cause any confusion.

In the present paper we consider the detector operators (2.22) made out of Hermitian local operators. We then have the following relation

$$\left[\mathcal{O}_J(\hat{\omega}, n) \right]^\dagger = \mathcal{O}_J(-\hat{\omega}, n), \quad (2.36)$$

which relates the event shapes for positive and negative ω . In the case of the one-point function we have

$$\left[\langle \mathcal{O}_J(\hat{\omega}, n) \rangle_q \right]^* = \left[\mathcal{O}_J(\hat{\omega}, n) \right]^\dagger_{q+\hat{\omega}n} = \langle \mathcal{O}_J(-\hat{\omega}, n) \rangle_{q+\hat{\omega}n}. \quad (2.37)$$

We can also derive a similar relation using the CRT transformation and the Hermitian conjugation (2.27), see appendix B for details,

$$\text{CRT} : \quad \langle \mathcal{O}_J(\hat{\omega}, n) \rangle_q = \pm \langle \mathcal{O}_J(-\hat{\omega}, n) \rangle_{q+\hat{\omega}n}, \quad (2.38)$$

where the sign \pm on the right-hand side corresponds to the signature of the detector operator $\mathcal{O}_J(\hat{\omega}, n)$ discussed in Section 2.4. Combining together (2.37) and (2.38) we find that that $\langle \mathcal{O}_J(\hat{\omega}, n) \rangle_q$, or equivalently the function $f_{\mathcal{O}_J}(\omega)$ in (2.33), is real for the detector operators of positive signature.

We can now use (2.33) to rewrite the relation (2.38) as follows

$$\frac{(q^2)^{\Delta_\phi - \frac{d}{2} + \frac{J+\Delta_{\mathcal{O}}}{2} - 1}}{(qn)^{\Delta_{\mathcal{O}} - 1}} f_{\mathcal{O}_J}\left(\hat{\omega} \frac{2(qn)}{q^2}\right) = \frac{(\hat{q}^2)^{\Delta_\phi - \frac{d}{2} + \frac{J+\Delta_{\mathcal{O}}}{2} - 1}}{(\hat{q}n)^{\Delta_{\mathcal{O}} - 1}} f_{\mathcal{O}_J}\left(-\hat{\omega} \frac{2(\hat{q}n)}{\hat{q}^2}\right), \quad (2.39)$$

where $\hat{q} = q + \hat{\omega}n$. It simplifies to

$$f_{\mathcal{O}_J}(\omega) = (1 + \omega)^{\Delta_\phi - \frac{d}{2} + \frac{J+\Delta_{\mathcal{O}}}{2} - 1} f_{\mathcal{O}_J}\left(-\frac{\omega}{\omega + 1}\right). \quad (2.40)$$

Some explicit examples of $f_{\mathcal{O}_J}(\omega)$ can be found in Section 2.6.

Two-point functions

The two-point correlation (2.30) takes the following general form

$$\langle \mathcal{O}_{J_1}(\omega_1, n_1) \mathcal{O}_{J_2}(\omega_2, n_2) \rangle_q = \frac{1}{S_{d-2} S_{d-3}} \frac{(q^2)^{\Delta_\phi - \frac{d}{2} + \sum_{i=1}^2 \frac{J_i + \Delta_{\mathcal{O}_i} - 2}{2}}}{(qn_1)^{\Delta_{\mathcal{O}_1} - 1} (qn_2)^{\Delta_{\mathcal{O}_2} - 1}} f_{\mathcal{O}_{J_1} \mathcal{O}_{J_2}}(\omega_1, \omega_2, z), \quad (2.41)$$

where the scaling function $f_{\mathcal{O}_{J_1}\mathcal{O}_{J_2}}$ depends on the rescaled dimensionless frequencies (2.34) of the detectors and on the cross-ratio

$$z = \frac{q^2(n_1 n_2)}{2(qn_1)(qn_2)}, \quad 0 \leq z \leq 1. \quad (2.42)$$

It captures the dependence on the relative angle between the detectors. To derive the condition $0 \leq z \leq 1$ recall that q^μ is a future-pointing time-like vector and n_i^μ are future-pointing null vectors. Like in (2.33), the normalization factor in (2.41) helps simplify the expressions for the scaling functions $f_{\mathcal{O}_{J_1}\mathcal{O}_{J_2}}$.

Like for the one-point function, the condition that both the sink and the source carry time-like momenta, q and $\tilde{q} = q + \hat{\omega}_1 n_2 + \hat{\omega}_2 n_2$, respectively, restricts the values of ω_i as follows

$$\theta\left(q + \sum_{i=1}^2 \hat{\omega}_i n_i\right) : \quad 1 + z\omega_i \geq 0, \quad 1 + \omega_1 + \omega_2 + z\omega_1\omega_2 \geq 0. \quad (2.43)$$

These relations are obtained from (2.29) by switching to $\omega_i = 2(qn_i)/q^2 \hat{\omega}_i$ and using (2.42).

Repeating the argument in Section 2.5, namely considering the Hermitian conjugation and CRT transformation of the positive signature detector operators, we get (see appendix B for details)

$$\begin{aligned} \left[\langle \mathcal{O}_{J_1}(\omega_1, n_1) \mathcal{O}_{J_2}(\omega_2, n_2) \rangle_q \right]^* &= \langle \mathcal{O}_{J_1}(\omega_1, n_1) \mathcal{O}_{J_2}(\omega_2, n_2) \rangle_q \\ &= \langle \mathcal{O}_{J_1}(-\omega_1, n_1) \mathcal{O}_{J_2}(-\omega_2, n_2) \rangle_{q+\hat{\omega}_1 n_1+\hat{\omega}_2 n_2}. \end{aligned} \quad (2.44)$$

Combining this relation with (2.41) we find

$$f_{\mathcal{O}_{J_1}\mathcal{O}_{J_2}}(\omega_1, \omega_2, z) = \frac{(1 + \omega_1 + \omega_2 + \omega_1\omega_2 z)^{\Delta_\phi - \frac{d}{2} + \sum_{i=1}^2 \frac{J_i + \Delta_{\mathcal{O}_i} - 2}{2}}}{(1 + \omega_2 z)^{\Delta_{\mathcal{O}_1} - 1} (1 + \omega_1 z)^{\Delta_{\mathcal{O}_2} - 1}} f_{\mathcal{O}_{J_1}\mathcal{O}_{J_2}}(\omega'_1, \omega'_2, z'), \quad (2.45)$$

where $f_{\mathcal{O}_{J_1}\mathcal{O}_{J_2}}(\omega_1, \omega_2, z)$ is real for the ω -deformed light transform of the hermitian operators \mathcal{O}_i of positive signature and

$$\begin{aligned} \omega'_1 &= -\omega_1 \frac{1 + \omega_2 z}{1 + \omega_1 + \omega_2 + \omega_1\omega_2 z}, \\ \omega'_2 &= -\omega_2 \frac{1 + \omega_1 z}{1 + \omega_1 + \omega_2 + \omega_1\omega_2 z}, \\ z' &= z \frac{1 + \omega_1 + \omega_2 + \omega_1\omega_2 z}{(1 + \omega_1 z)(1 + \omega_2 z)}. \end{aligned} \quad (2.46)$$

The quantity $1 + \omega_1 + \omega_2 + \omega_1\omega_2 z$ is the dimensionless version of $\tilde{q}^2 = (q + \hat{\omega}_1 n_2 + \hat{\omega}_2 n_2)^2$, which already appeared above in (2.43).

The crucial feature of (2.45) is that it relates the two-point functions defined for ω_i and ω'_i of opposite signs. In the context of the S -matrix this relation corresponds to the crossing

transformation which exchanges particles and anti-particles. We can therefore call (2.45) a *crossing relation*. It will serve as a nontrivial consistency check for our computations in the following sections. Note that for $\omega_i = 0$ the relation (2.45) becomes trivial.

Finally, if the detectors are identical, the following relation holds

$$f_{\mathcal{O}_J \mathcal{O}_J}(\omega_1, \omega_2, z) = f_{\mathcal{O}_J \mathcal{O}_J}(\omega_2, \omega_1, z), \quad z \neq 0. \quad (2.47)$$

It expresses the fact that the ω -deformed event shape (2.30) is invariant under the permutation of the detectors. For $z = 0$ the detectors do not necessarily commute, see [22].

2.6 Special detectors: S, Q, and E

In the framework of $d = 4$, $\mathcal{N} = 4$ SYM we consider three types of detector operators:

- *Scalar detector* $\mathcal{O}(\hat{\omega}, n)$, denoted by S, obtained from the local operator with $J = 0$ and $\Delta = 2$;
- *Charge detector* $\mathcal{Q}(\hat{\omega}, n)$, denoted by Q, obtained from the R -current with $J = 1$ and $\Delta = 3$;
- *Energy detector* $\mathcal{E}(\hat{\omega}, n)$, denoted by E, obtained from the stress-energy tensor with $J = 2$ and $\Delta = 4$.

They all have positive signature and the corresponding generalized event shapes will be real, in agreement with the general discussion in the previous subsection. When elaborating the detailed form of the correlators in $\mathcal{N} = 4$ SYM we will need to carefully specify the R -symmetry structure. This will be done in Section 3 below but for the purpose of this section it is not important.

The one-point functions of such detectors, evaluated in a state created by a scalar primary with scaling dimension Δ_ϕ , are completely fixed by conformal invariance (see Appendix C). Applying (2.33) for $d = 4$ and $\Delta_O = J + 2$ we get

$$\langle \mathcal{O}_J(\hat{\omega}, n) \rangle_q = \frac{1}{4\pi} \frac{(q^2)^{\Delta_\phi - 2 + J}}{(qn)^{J+1}} f_{\mathcal{O}_J}(\omega), \quad (2.48)$$

where ω is defined in (2.34).

The calculation in Appendix C shows that the scaling function $f_{\mathcal{O}_J}$ takes different form for positive and negative ω :

$$\begin{aligned} \omega > 0 : \quad f_S(\omega) &= 1, \\ f_Q(\omega) &= 1 + \frac{\omega}{2}(\Delta_\phi - 1), \\ f_E(\omega) &= 1 + \frac{\omega}{2}\Delta_\phi + \frac{\omega^2}{12}(\Delta_\phi - 1)\Delta_\phi; \end{aligned} \quad (2.49)$$

$$\begin{aligned}
-1 < \omega < 0 : \quad f_S(\omega) &= (1 + \omega)^{\Delta_\phi - 2}, \\
f_Q(\omega) &= (1 + \omega)^{\Delta_\phi - 2} \left[1 - \frac{\omega}{2}(\Delta_\phi - 3) \right], \\
f_E(\omega) &= (1 + \omega)^{\Delta_\phi - 2} \left[1 - \frac{\omega}{2}(\Delta_\phi - 4) + \frac{\omega^2}{12}(\Delta_\phi - 4)(\Delta_\phi - 3) \right]. \quad (2.50)
\end{aligned}$$

For $\omega = 0$ we have $f_{\mathcal{O}_J}(0) = 1$. In this case, in the rest frame of the source, for $q^\mu = (q, \vec{0})$, the integral of the one-point function over the unit sphere, $\int d^2\vec{n} \langle \mathcal{O}_J(0, n) \rangle_q$, yields the total charge of the source. It is easy to check that the formulas above satisfy the relation (2.40). We remark that the ω -deformed event shapes are not analytic around $\omega = 0$. This is very intuitive because, depending on the sign of ω , the detectors either create or annihilate particles. We discuss this property further in Section 2.7.

The relations (2.49) and (2.50) are valid for a source of arbitrary scaling dimension Δ_ϕ . In $\mathcal{N} = 4$ SYM we choose the source to be the half-BPS scalar operator with dimension $\Delta_\phi = 2$ (see Eq. (3.31) below). In this case, the one-point functions (2.49) and (2.50) simplify as

$$f_S(\omega) = 1, \quad f_Q(\omega) = 1 + \frac{\omega}{2}, \quad f_E(\omega) = 1 + \omega + \frac{\omega^2}{6}. \quad (2.51)$$

We will derive these expressions in the next section where we compute the generalized event shapes using the amplitude method.

Likewise, for $\Delta_\phi = 2$ the two-point function (2.41) simplifies as

$$\langle \mathcal{O}_{J_1}(\omega_1, n_1) \mathcal{O}_{J_2}(\omega_2, n_2) \rangle_q = \frac{1}{8\pi^2} \frac{(q^2)^{J_1+J_2}}{(qn_1)^{J_1+1} (qn_2)^{J_2+1}} f_{\mathcal{O}_{J_1} \mathcal{O}_{J_2}}(\omega_1, \omega_2, z), \quad (2.52)$$

where we replaced $\Delta_{\mathcal{O}_i} = 2 + J_i$.

For the detectors described above we will follow the tradition in the literature and will call the two points functions (2.41) *correlations*. For example, for the correlations of scalar, charge and energy we write

$$\begin{aligned}
\text{SSC} &\equiv f_{\mathcal{O}\mathcal{O}}(\omega_1, \omega_2, z), & \text{QQC} &\equiv f_{\mathcal{Q}\mathcal{Q}}(\omega_1, \omega_2, z), \\
\text{QSC} &\equiv f_{\mathcal{Q}\mathcal{O}}(\omega_1, \omega_2, z), & \text{ESC} &\equiv f_{\mathcal{E}\mathcal{O}}(\omega_1, \omega_2, z), \\
\text{EQC} &\equiv f_{\mathcal{E}\mathcal{Q}}(\omega_1, \omega_2, z), & \text{EEC} &\equiv f_{\mathcal{E}\mathcal{E}}(\omega_1, \omega_2, z). \quad (2.53)
\end{aligned}$$

Again in $\mathcal{N} = 4$ SYM we would need to specify the choice of the R-symmetry components of the scalar and the current operators, this will be done below.

The factor of $1/(8\pi^2)$ on the right-hand side of (2.52) was inserted to simplify the normalization conditions for the scaling function $f_{\mathcal{O}_{J_1} \mathcal{O}_{J_2}}(\omega_1, \omega_2, z)$ at $\omega_i = 0$. In the case of the energy-energy correlations these conditions take the form [12, 30, 31]

$$\int_0^1 dz \text{EEC}(0, 0, z) = \frac{1}{2}, \quad \int_0^1 dz z \text{EEC}(0, 0, z) = \frac{1}{4}. \quad (2.54)$$

These relations follow from the requirement that the total momentum of the particles produced in the rest frame of the source should be equal to $q^\mu = (q, \vec{0})$. Relations (2.54) follow from the Ward identities satisfied by the stress-energy tensor.

Since the ω -deformed event shapes are not analytic around $\omega = 0$, we should be more specific about the choice of the signs of ω . Let us for example consider SSC defined in (2.53). We have four choices SSC_{++} , SSC_{+-} , SSC_{-+} , SSC_{--} . As argued in the previous subsection, these functions are real. Moreover, due to (2.45) only two of them are independent.

More precisely, in the main case of interest that we consider in detail below, namely $d = 4$ and $\Delta_\phi = 2$, we get from (2.45)

$$\begin{aligned}\text{SSC}_{-+}(\omega_1, \omega_2, z) &= \frac{1}{(1 + \omega_1 z)(1 + \omega_2 z)} \text{SSC}_{+-}(\omega'_1, \omega'_2, z'), \\ \text{SSC}_{--}(\omega_1, \omega_2, z) &= \frac{1}{(1 + \omega_1 z)(1 + \omega_2 z)} \text{SSC}_{++}(\omega'_1, \omega'_2, z'),\end{aligned}\tag{2.55}$$

where ω'_i and z' were defined in (2.46). These relations allow us to restrict the discussion only to SSC_{+-} and SSC_{++} . The same applies to other event shapes:

$$\begin{aligned}\text{QSC}(\omega_1, \omega_2, z) &= \frac{(1 + \omega_1 + \omega_2 + \omega_1 \omega_2 z)}{(1 + \omega_2 z)^2(1 + \omega_1 z)} \text{QSC}(\omega'_1, \omega'_2, z'), \\ \text{QQC}(\omega_1, \omega_2, z) &= \frac{(1 + \omega_1 + \omega_2 + \omega_1 \omega_2 z)^2}{(1 + \omega_1 z)^2(1 + \omega_2 z)^2} \text{QQC}(\omega'_1, \omega'_2, z'), \\ \text{ESC}(\omega_1, \omega_2, z) &= \frac{(1 + \omega_1 + \omega_2 + \omega_1 \omega_2 z)^2}{(1 + \omega_2 z)^3(1 + \omega_1 z)} \text{ESC}(\omega'_1, \omega'_2, z'), \\ \text{EQC}(\omega_1, \omega_2, z) &= \frac{(1 + \omega_1 + \omega_2 + \omega_1 \omega_2 z)^3}{(1 + \omega_2 z)^3(1 + \omega_1 z)^2} \text{EQC}(\omega'_1, \omega'_2, z'), \\ \text{EEC}(\omega_1, \omega_2, z) &= \frac{(1 + \omega_1 + \omega_2 + \omega_1 \omega_2 z)^4}{(1 + \omega_1 z)^3(1 + \omega_2 z)^3} \text{EEC}(\omega'_1, \omega'_2, z').\end{aligned}\tag{2.56}$$

2.7 Finiteness, commutativity and non-analyticity in ω

One might wonder to what extent the generalized event shapes (2.30) are well defined. To understand this issue it is convenient to go to the conformal frame (2.17) and to consider the product of the detector operators inserted at the same null plane,

$$\int_{-\infty}^{\infty} du_1 e^{-i\hat{\omega}_1 u_1} O_{\underbrace{u \dots u}_{j_1}}(u_1, v = 0, \vec{y}_1) \int_{-\infty}^{\infty} du_2 e^{-i\hat{\omega}_2 u_2} O_{\underbrace{u \dots u}_{j_2}}(u_2, v = 0, \vec{y}_2). \tag{2.57}$$

The conditions for the existence of this product for $\hat{\omega}_i = 0$ were discussed in detail in [15]. The basic observation is that the product of operators (2.57) is potentially ill-defined because the two operators in (2.57) become light-like separated when one of the detectors reaches infinity $u_i = \pm\infty$. An avatar of this in a collider experiment is that the corresponding observable is not IR safe.

In the case $\omega_i = 0$ the situation is discussed in Section 4.4 in [15]. An important condition that guarantees the existence and commutativity of the product (2.57) for $\vec{y}_1 \neq \vec{y}_2$ is

$$J_1 + J_2 \geq 1 + J_0, \quad (2.58)$$

where J_0 is the Regge intercept of the theory and J_1, J_2 are the spins of the operators in (2.57).¹⁷

The insertion of ω -dependent phase factors in (2.57) does not affect the analysis of [15] and therefore all the results apply directly. This fact immediately implies that the ω -deformed event shapes are finite and commutative for $\vec{y}_1 \neq \vec{y}_2$, or, equivalently, for $n_1 \neq n_2$ in the collider experiment frame, as long as the condition (2.58) is satisfied.

There is a difference between the two cases in the situation when (2.58) is violated. For $\omega_i = 0$ the product (2.57) is ill-defined. The reason is that the integrals over u_i diverge polynomially at large $|u_i| \gg 1$, see [32] for a recent discussion of this point. For $\omega_i \neq 0$ the rapidly oscillating phases damp the contribution at $|u_i| \gg 1$ in (2.57). As a consequence, the product of operators in (2.57) is well defined (at least in the distributional sense) and commutative for $\vec{y}_1 \neq \vec{y}_2$,

$$\left[\int_{-\infty}^{\infty} du_1 e^{-i\hat{\omega}_1 u_1} \mathcal{O}_{u\dots u}(u_1, v=0, \vec{y}_1), \int_{-\infty}^{\infty} du_2 e^{-i\hat{\omega}_2 u_2} \mathcal{O}_{u\dots u}(u_2, v=0, \vec{y}_2) \right]^{\vec{y}_1 \neq \vec{y}_2} 0. \quad (2.59)$$

One can also try to extend the ω -deformed event shapes as distributions to include the case of coincident points $\vec{y}_1 = \vec{y}_2$. This turns out to be quite subtle and we will discuss it elsewhere [22].

For the same reason, we expect that when expanded around arbitrary $\omega_i \neq 0$ the ω -deformed event shapes (2.30) are real analytic functions. This is indeed what we find in the examples considered below. One interesting aspect of this fact, when interpreted in terms of amplitudes, is that the ω -deformed event shapes are IR finite to any order in perturbation theory for any choice of the detectors. The same argument, however, suggests that the ω -deformed event shapes are not analytic around $\omega_i = 0$.

3 Detector properties: amplitude definition

In this section, we explain how to compute the correlations of the flow operators (2.30) using scattering amplitudes or more precisely matrix elements of local operators with respect to on-shell states. In the context of conformal field theory this can be done if the weak coupling expansion around the free field point exists. In this case we expect that scattering amplitudes can be defined order-by-order in perturbation theory. Computing event shapes using scattering amplitudes may involve IR divergences at the intermediate steps but they cancel in the final answer. In this section we work to leading order in the coupling constant

¹⁷For the precise conditions, see [15].

in a weakly coupled CFT in $d = 4$ dimensions. All the relevant scattering amplitudes, or more precisely form factors, are the tree-level ones and no IR divergences arise.

Using the completeness condition $\sum_X |X\rangle\langle X| = \mathbb{I}$, we can rewrite the Wightman correlation function (2.28) in the following form

$$\sum_{X, X'} \langle 0 | \phi^\dagger(\tilde{q}) | X' \rangle \langle X' | \mathcal{O}_{J_1}(\hat{\omega}_1, n_1) \dots \mathcal{O}_{J_k}(\hat{\omega}_k, n_k) | X \rangle \langle X | \phi(q) | 0 \rangle, \quad (3.1)$$

where the sum runs over the asymptotic states X and X' containing an arbitrary number of on-shell particles. The relation (3.1) has a simple physical meaning. The source $\phi(q)$ excites the vacuum and creates the state X . This state propagates through a collection of detectors located at points n_1, \dots, n_k on the celestial sphere, undergoes a transition to the state X' , which in turn is absorbed by the sink $\phi^\dagger(\tilde{q})$.

To apply (3.1) we have to provide expressions for the on-shell form factors $\langle X | \phi(q) | 0 \rangle$ and $\langle 0 | \phi^\dagger(\tilde{q}) | X' \rangle$ describing the source and sink, respectively, and to evaluate the transition amplitude $\langle X' | \mathcal{O}_{J_1}(\hat{\omega}_1, n_1) \dots \mathcal{O}_{J_k}(\hat{\omega}_k, n_k) | X \rangle$. We recall that the flow operator $\mathcal{O}_{J_i}(\hat{\omega}_i, n_i)$ represents a detector that selects particles propagating in the direction of the null vector n_i and assigns a certain weight to them. For $\hat{\omega} = 0$ the flow operator (2.22) acts on a single-particle state with momentum $p^\mu = (p_0, \vec{p})$ as follows [17],

$$\mathcal{O}_J(\hat{\omega} = 0, n) | p \rangle = | p \rangle \delta^{(2)}(\Omega_{\vec{p}} - \Omega_{\vec{n}}) w_J. \quad (3.2)$$

Here the delta function ensures that the three-momentum of the particle is aligned along the detector direction $n = (1, \vec{n})$ and the function w_J defines the weight. It depends on the type of detector as well as on the energy of the particle. For $\hat{\omega} \neq 0$ the detector transfers the momentum $n\hat{\omega}$ and modifies the particle state to $| p + n\hat{\omega} \rangle$. In addition, for $\hat{\omega} \neq 0$ the detector can either create (for $\hat{\omega} > 0$) or annihilate (for $\hat{\omega} < 0$) particles. This suggests that for $\hat{\omega} \neq 0$ the expression on the right-hand side of (3.2) should contain additional terms describing an inelastic contribution. We compute such terms below, see Eq. (3.10).

Because the detectors are located at different points on the celestial sphere, they are separated by space-time intervals and, therefore, they cannot interact with each other by exchanging on-shell particles with nonzero energy. One might therefore expect that the detectors should work independently. If this were the case, the transition amplitude would factorize into a product of transition amplitudes describing individual detectors, symbolically

$$\langle X', p'_1, \dots, p'_k | \mathcal{O}_{J_1}(\hat{\omega}_1, n_1) \dots \mathcal{O}_{J_k}(\hat{\omega}_k, n_k) | X, p_1, \dots, p_k \rangle \stackrel{?}{=} \langle X' | X \rangle \prod_i \langle p'_i | \mathcal{O}_{J_i}(\hat{\omega}_i, n_i) | p_i \rangle. \quad (3.3)$$

It turns out that this relation is violated already at $\hat{\omega}_i = 0$, see Ref. [17]. The reason for this is that the transition amplitude in (3.3) receives a contribution from particles with zero energy. They generate cross-talk between the detectors, thus invalidating the argument leading to (3.3). We show below that the same phenomenon happens for $\hat{\omega}_i \neq 0$ and identify the missing contribution in (3.3).

3.1 Warm up example: free scalar field

In this subsection, we consider the properties of various detectors (scalar, charge and energy) defined in (2.22). The detectors are located on the celestial sphere where the interaction between the particles is switched off. This allows us to restrict our consideration to free fields.

To start with, we define the conformal operators $O_J = O_{\mu_1 \dots \mu_J} \bar{n}^{\mu_1} \dots \bar{n}^{\mu_J}$ (the same projection appears in (2.22)) with spin $J = 0, 1, 2$ built out of a free complex scalar field,

$$\begin{aligned} O_{J=0} &= \bar{\varphi} \varphi, \\ O_{J=1} &= i(\bar{\varphi} \partial_+ \varphi - \partial_+ \bar{\varphi} \varphi), \\ O_{J=2} &= \frac{1}{6} (\partial_+^2 \bar{\varphi} \varphi - 4 \partial_+ \bar{\varphi} \partial_+ \varphi + \bar{\varphi} \partial_+^2 \varphi), \end{aligned} \quad (3.4)$$

where $\partial_+ = \bar{n}^\mu \partial_\mu$ denotes the projected space-time derivative. The operators $O_{J=1}$ and $O_{J=2}$ coincide with the $U(1)$ current and stress-energy tensor, respectively, projected on the auxiliary null vector \bar{n} .

A free scalar field can be expanded over creation and annihilation operators,

$$\begin{aligned} \varphi(x) &= \int_{-\infty}^{\infty} \frac{d^4 p}{(2\pi)^4} 2\pi \delta_+(p^2) (a_p e^{-ip \cdot x} + b_p^\dagger e^{ip \cdot x}), \\ \bar{\varphi}(x) &= \int_{-\infty}^{\infty} \frac{d^4 p}{(2\pi)^4} 2\pi \delta_+(p^2) (b_p e^{-ip \cdot x} + a_p^\dagger e^{ip \cdot x}), \end{aligned} \quad (3.5)$$

where a_p and b_p are the annihilation operators of the scalars with $U(1)$ charge (+1) and (−1), respectively. They satisfy the canonical commutation relations

$$[a_p, a_{p'}^\dagger] = [b_p, b_{p'}^\dagger] = (2\pi)^3 2|\vec{p}| \delta^{(3)}(\vec{p} - \vec{p}'), \quad (3.6)$$

the remaining commutators vanish. Substituting (3.5) and (3.4) into the definition of the detector (or flow operator) (2.22) we obtain after some algebra (see Appendix D for details)

$$\begin{aligned} \mathcal{O}_{J=0}(\hat{\omega}, n) &= (n\bar{n}) \int_{-\infty}^{\infty} d\alpha e^{-i(n\bar{n})\hat{\omega}\alpha} \lim_{r \rightarrow \infty} r^2 (\bar{\varphi} \varphi)(rn + \alpha \bar{n}) \\ &= \int_0^\infty \frac{ds}{4(2\pi)^3} \left(2a_{(s+\hat{\omega})n}^\dagger a_{sn} - a_{sn}^\dagger b_{(\hat{\omega}-s)n}^\dagger - a_{sn} b_{-(s+\hat{\omega})n} \right) + (a \leftrightarrow b). \end{aligned} \quad (3.7)$$

The last term is obtained by exchanging the operators with opposite values of the $U(1)$ charge. As expected, this relation does not depend on \bar{n}^μ . The integral on the second line contains the annihilation and creation operators of the scalars with their on-shell momenta aligned along the null vector n . The integration variable s , like the deformation parameter $\hat{\omega}$, has the dimension of energy.

The relation (3.7) holds for arbitrary $\hat{\omega}$ and it is tacitly assumed that the annihilation/creation operators with the subscript $s'n$ vanish for $s' < 0$. In particular, for $\hat{\omega} = 0$

the last two terms inside the parentheses in (3.7) vanish. The first term in (3.7) defines the elastic contribution

$$\mathcal{O}^{\text{elastic}}(\hat{\omega}, n) = \int_0^\infty \frac{ds}{2(2\pi)^3} \left(a_{(s+\hat{\omega})n}^\dagger a_{sn} + b_{(s+\hat{\omega})n}^\dagger b_{sn} \right). \quad (3.8)$$

Its action on the single-particle state $|p\rangle = a_p^\dagger|0\rangle$ is given by

$$\mathcal{O}^{\text{elastic}}(\hat{\omega}, n)|p\rangle = |p + n\hat{\omega}\rangle \delta^{(2)}(\Omega_{\vec{p}} - \Omega_{\vec{n}}) \theta(p^0 + \hat{\omega})(p^0)^{-1}. \quad (3.9)$$

For $\hat{\omega} = 0$ this relation is in agreement with (3.2).

An interesting new effect due to $\hat{\omega} \neq 0$ is the inelastic character of the last two terms in the parentheses in (3.7). They create and annihilate a pair of particles, correspondingly. To make this explicit, we rewrite (3.7) as follows

$$\mathcal{O}_{J=0}(\hat{\omega}, n) = \mathcal{O}^{\text{elastic}}(\hat{\omega}, n) - \theta(\hat{\omega})\mathcal{O}^{\text{creation}}(\hat{\omega}, n) - \theta(-\hat{\omega})\mathcal{O}^{\text{annihil.}}(-\hat{\omega}, n), \quad (3.10)$$

where we introduced the notation

$$\begin{aligned} \mathcal{O}^{\text{creation}}(\hat{\omega}, n) &= \int_0^{\hat{\omega}} \frac{ds}{2(2\pi)^3} a_{sn}^\dagger b_{(\hat{\omega}-s)n}^\dagger, \\ \mathcal{O}^{\text{annihil.}}(\hat{\omega}, n) &= \int_0^{\hat{\omega}} \frac{ds}{2(2\pi)^3} a_{sn} b_{(\hat{\omega}-s)n}. \end{aligned} \quad (3.11)$$

Note that these two operators are conjugate to each other. When acting on the vacuum, the operator $\mathcal{O}^{\text{creation}}(\hat{\omega}, n)$ creates a two-particle state that consists of two scalars with opposite $U(1)$ charges. Their on-shell momenta are aligned along the detector direction n and the total momentum is $n\hat{\omega}$. Similarly, $\mathcal{O}^{\text{annihil.}}(\hat{\omega}, n)$ annihilates a pair of scalars.

It is straightforward to repeat the same analysis for the two remaining operators in (3.4). For the charge $\mathcal{Q}(\hat{\omega}, n) = \mathcal{O}_{J=1}$ and energy $\mathcal{E}(\hat{\omega}, n) = \mathcal{O}_{J=2}$ detectors we find

$$\begin{aligned} \mathcal{Q}(\hat{\omega}, n) &= \int_0^\infty \frac{ds}{2(2\pi)^3} \left[w_Q^{(s)}(s, s + \hat{\omega}) (a_{(s+\hat{\omega})n}^\dagger a_{sn} - b_{(s+\hat{\omega})n}^\dagger b_{sn}) \right. \\ &\quad \left. + w_Q^{(s)}(s, s - \hat{\omega}) b_{sn}^\dagger a_{-(s-\hat{\omega})n}^\dagger + w_Q^{(s)}(s, s + \hat{\omega}) b_{sn} a_{-(s+\hat{\omega})n} \right], \end{aligned} \quad (3.12)$$

$$\begin{aligned} \mathcal{E}(\hat{\omega}, n) &= \int_0^\infty \frac{ds}{2(2\pi)^3} \left[w_E^{(s)}(s, s + \hat{\omega}) (a_{(s+\hat{\omega})n}^\dagger a_{sn} + b_{(s+\hat{\omega})n}^\dagger b_{sn}) \right. \\ &\quad + \frac{1}{2} w_E^{(s)}(s, \hat{\omega} - s) (a_{sn}^\dagger a_{-(s-\hat{\omega})n}^\dagger + b_{sn}^\dagger b_{-(s-\hat{\omega})n}^\dagger) \\ &\quad \left. + \frac{1}{2} w_E^{(s)}(s, -s - \hat{\omega}) (a_{sn} a_{-(s+\hat{\omega})n} + b_{sn} b_{-(s+\hat{\omega})n}) \right]. \end{aligned} \quad (3.13)$$

Here $w_Q^{(s)}$ and $w_E^{(s)}$ are the weights assigned to a scalar particle going through the charge and energy detectors, respectively,

$$w_Q^{(s)}(s, s') = s + s', \quad w_E^{(s)}(s, s') = \frac{1}{6}(s^2 + s'^2 + 4ss'). \quad (3.14)$$

For the scalar detector the analogous weight is $w_O^{(s)} = 1$.

We recall that a_{sn}^\dagger and b_{sn}^\dagger are creation operators of scalars with opposite values of the $U(1)$ charge and on-shell momentum $p^\mu = sn^\mu$ with $s \geq 0$. The relations (3.12) and (3.13) have a form similar to the scalar detector (3.10). The first line in the expression for $\mathcal{Q}(\hat{\omega}, n)$ and $\mathcal{E}(\hat{\omega}, n)$ describes the elastic contribution and the remaining terms describe the creation and annihilation of a pair of scalars with aligned momenta.

The weights (3.14) are homogenous polynomials in the energies s and s' of degree equal to the detector spin. We encounter similar polynomials by examining the expression of the twist-two operator $O_J(x)$. This operator is built out of two scalar fields and J derivatives $i(\bar{n}\partial)$ and it takes the following form [33]

$$O_J(x) = \bar{\varphi}(x) P_J \left(i(\bar{n}\partial^\leftarrow), i(\bar{n}\partial^\rightarrow) \right) \varphi(x), \quad (3.15)$$

where P_J is the polynomial defined in (C.5) and the arrows indicate the fields that the derivatives act upon. The close examination shows that the two polynomials coincide up to a normalization factor,

$$w_Q^{(s)}(s, s') = -P_{J=1}(s, -s'), \quad w_E^{(s)}(s, s') = \frac{1}{3}P_{J=2}(s, -s'). \quad (3.16)$$

This relation is not accidental and has the following explanation.

For an arbitrary spin J , the weight can be defined as

$$\langle 0 | O_J(x=0) | s_1, s_2 \rangle = w_J(s_1, -s_2), \quad (3.17)$$

where $|s_1, s_2\rangle = a_{s_1 n}^\dagger b_{s_2 n}^\dagger |0\rangle$ is a two-particle state. Replacing the scalar fields with plane waves (3.5) and evaluating (3.17) we arrive at $w_J^{(s)}(s_1, s_2) \sim P_J(s_1, -s_2)$. This relation is powerful because it allows us to generalize the expressions obtained in (3.12) and (3.13) by including the contribution of the fermions (ψ) and the gauge (g) fields,

$$\begin{aligned} O_{J=1}^{(\psi)} &= \bar{\psi} \gamma_+ \psi, \\ O_{J=2}^{(\psi)+(g)} &= \frac{i}{2} (\bar{\psi} \gamma_+ \partial_+ \psi - \partial_+ \bar{\psi} \gamma_+ \psi) + F_{+\mu} F_{+\mu}. \end{aligned} \quad (3.18)$$

Like in (3.17), we act with these operators on two-particle states built out of fermions and gauge fields and identify the corresponding weights as

$$w_Q^{(\psi)}(s, s') = (ss')^{1/2}, \quad w_E^{(\psi)}(s, s') = \frac{1}{2}(s + s')(ss')^{1/2}, \quad w_E^{(g)}(s, s') = ss', \quad (3.19)$$

where the factor $(ss')^{1/2}$ comes from the wave functions of the fermions.

Comparing these expressions with (3.14) we observe an important difference from the scalar case. The variables s and s' have the meaning of the energy of the particles entering or leaving the detectors. Going to the limit $s \rightarrow 0$ we find that the weights (3.19) corresponding to the fermions and gauge fields vanish, whereas the weights for the scalars, Eq. (3.14), approach a finite value. This implies that scalars with zero energy can give a non-vanishing contribution to the flow operators. As was mentioned above, this leads to cross-talk between the detectors and to the violation of (3.3).

3.2 One-point functions from amplitudes

To illustrate the amplitude approach, we apply (3.1) to computing the one-point function

$$\langle \mathcal{O}_J(\hat{\omega}, n) \rangle_q = \int d^4x e^{-i(qx)} \sum_{X, X'} \langle 0 | \phi(0) | X' \rangle \langle X' | \mathcal{O}_J(\hat{\omega}, n) | X \rangle \langle X | \phi(x) | 0 \rangle. \quad (3.20)$$

For the sake of simplicity we chose the source and sink to be described by an operator $\phi = \bar{\varphi}\varphi$ of dimension $\Delta = 2$.¹⁸ In a free theory the states X and X' contain two scalars with opposite $U(1)$ charges, e.g. $|X\rangle = a_{p_1}^\dagger b_{p_2}^\dagger |0\rangle \equiv |p_1, p_2\rangle$ with $p_i^2 = 0$. The form-factor takes the simple form $\langle X | \phi(x) | 0 \rangle = e^{ix(p_1+p_2)}$ and its substitution into (3.20) yields $(2\pi)^4 \delta^{(4)}(q - p_1 - p_2)$ upon integration over x . In this way, we obtain

$$\langle \mathcal{O}_J(\hat{\omega}, n) \rangle_q = (2\pi)^4 \int \prod_{a=\{1,2,1',2'\}} \frac{d^4 p_a}{(2\pi)^3} \delta_+(p_a^2) \delta^{(4)}(q - p_1 - p_2) \langle p'_1 p'_2 | \mathcal{O}_J(\hat{\omega}, n) | p_1, p_2 \rangle, \quad (3.21)$$

where $\delta_+(p^2) = \theta(p^0) \delta(p^2)$.

As explained in the previous subsection, the flow operator $\mathcal{O}_J(\hat{\omega}, n)$ is a sum of elastic and inelastic terms. The inelastic terms change the number of particles and do not contribute to the matrix element $\langle p'_1 p'_2 | \mathcal{O}_J(\hat{\omega}, n) | p_1, p_2 \rangle$. The elastic contribution factorizes into a product of single-particle matrix elements,

$$\langle p'_1 p'_2 | \mathcal{O}_J(\hat{\omega}, n) | p_1, p_2 \rangle = \langle p'_1 | \mathcal{O}_J^{\text{elastic}}(\hat{\omega}, n) | p_1 \rangle \langle p'_2 | p_2 \rangle + \langle p'_2 | \mathcal{O}_J^{\text{elastic}}(\hat{\omega}, n) | p_2 \rangle \langle p'_1 | p_1 \rangle, \quad (3.22)$$

where $\langle p'_i | p_i \rangle = (2\pi)^3 p_i^0 \delta^{(3)}(\vec{p}'_i - \vec{p}_i)$. The operator $\mathcal{O}_J^{\text{elastic}}(\hat{\omega}, n)$ acts on the single-particle state as

$$\mathcal{O}_J^{\text{elastic}}(\hat{\omega}, n) | p \rangle = | p + n\hat{\omega} \rangle \delta^{(2)}(\Omega_{\vec{p}_1} - \Omega_{\vec{n}}) \theta(p^0 + \hat{\omega}) (p^0)^{-1} w_J, \quad (3.23)$$

where the weight $w_J = w_J(p^0, p^0 + \hat{\omega})$ depends on the energy of the particle entering and leaving the detector. The two terms on the right-hand side of (3.22) give the same contribution to (3.20):

$$\langle \mathcal{O}_J(\hat{\omega}, n) \rangle_q \sim \int \frac{d^4 p_1}{(2\pi)^3} \delta_+(p_1^2) \delta_+((q - p_1)^2) \delta^{(2)}(\Omega_{\vec{p}_1} - \Omega_{\vec{n}}) \theta(p_1^0 + \hat{\omega}) w_J^{(s)}(p_1^0, p_1^0 + \hat{\omega}) (p_1^0)^{-1}. \quad (3.24)$$

Here the product of delta functions $\delta_+(p_1^2) \delta^{(2)}(\Omega_{\vec{p}_1} - \Omega_{\vec{n}})$ aligns the momentum of the scalar with the detector direction, $p_1 = sn$ with $s > 0$. Applying the identity

$$\int_0^\infty ds f(s) \delta^{(4)}(p - ns) = 2f(p^0) (p^0)^{-1} \delta_+(p^2) \delta^{(2)}(\Omega_{\vec{p}} - \Omega_{\vec{n}}), \quad (3.25)$$

¹⁸For operators with arbitrary scaling dimension Δ , the corresponding expression for the one-point function can be found in Appendix C.

with $f(s)$ being a test function, we obtain

$$\begin{aligned}\langle \mathcal{O}_J(\hat{\omega}, n) \rangle_q &\sim \int_0^\infty ds \delta_+((q - ns)^2) w_J^{(s)}(s, s + \hat{\omega}) \theta(s + \hat{\omega}) \\ &= \frac{1}{4\pi} \frac{(q^2)^J}{(qn)^{J+1}} w_J^{(s)}(1, 1 + \omega) \theta(1 + \omega) .\end{aligned}\quad (3.26)$$

Here in the second relation we introduced the dimensionless variable ω defined in (2.34) and took into account that $w_J^{(s)}(s, s + \hat{\omega})$ is a homogenous function of degree J . Replacing the weights w_J by their explicit expressions (3.14), we verify that $\langle \mathcal{O}_J(\hat{\omega}, n) \rangle_q$ has the expected form (2.48), with the function $f_{\mathcal{O}_J}$ given by (2.49) and (2.50) evaluated at $\Delta_\phi = 2$.

3.3 Cross-talk

To demonstrate the phenomenon of cross-talk between the detectors, we consider the two-point functions $\langle \mathcal{O}_{J_1}(\hat{\omega}_1, n_1) \mathcal{O}_{J_2}(\hat{\omega}_2, n_2) \rangle_q$ with the source and sink given by a complex scalar field,

$$\begin{aligned}\langle \mathcal{O}_{J_1}(\hat{\omega}_1, n_1) \mathcal{O}_{J_2}(\hat{\omega}_2, n_2) \rangle_q &\equiv \langle \varphi^\dagger(\tilde{q}) \mathcal{O}_{J_1}(\hat{\omega}_1, n_1) \mathcal{O}_{J_2}(\hat{\omega}_2, n_2) \varphi(q) \rangle \\ &= \langle 0 | a_{\tilde{q}} \mathcal{O}_{J_1}(\hat{\omega}_1, n_1) \mathcal{O}_{J_2}(\hat{\omega}_2, n_2) a_q^\dagger | 0 \rangle ,\end{aligned}\quad (3.27)$$

where $\tilde{q} = q + n_1 \hat{\omega}_1 + n_2 \hat{\omega}_2$ and $q^2 = \tilde{q}^2 = 0$. The expression on the right-hand side coincides with the transition amplitude on the left-hand side of (3.3) with single-particle *in* and *out* states. If the relation (3.3) were correct, the above expression would be proportional to the vacuum expectation value of the flow operator and, therefore, it would vanish. Let us show that this is not the case.

As in the previous case, the inelastic terms in $\mathcal{O}_{J_1}(\hat{\omega}_1, n_1)$ and $\mathcal{O}_{J_2}(\hat{\omega}_2, n_2)$ do not contribute to (3.27) for $n_1 \neq n_2$. The contribution of the elastic terms can be found using (3.23):

$$\begin{aligned}\langle \mathcal{O}_{J_1}(\hat{\omega}_1, n_1) \mathcal{O}_{J_2}(\hat{\omega}_2, n_2) \rangle_q &= \int_0^\infty \frac{ds ds'}{(2(2\pi)^3)^2} w_{J_2}(s, s + \hat{\omega}_2) w_{J_1}(s', s' + \hat{\omega}_1) \\ &\times \langle a_{\tilde{q}} a_{(s' + \hat{\omega}_1)n_1}^\dagger \rangle \langle a_{s'n_1} a_{(s + \hat{\omega}_2)n_2}^\dagger \rangle \langle a_{sn_2} a_q^\dagger \rangle + (\omega_1 \leftrightarrow \omega_2, J_1 \leftrightarrow J_2, n_1 \leftrightarrow n_2) ,\end{aligned}\quad (3.28)$$

where the second term ensures the symmetry under the exchange of the detectors. The first term describes the sequential propagation of a particle through the two detectors, as shown in Figure 1. Since the detectors are located on the celestial sphere at two different directions, we expect that the energy of the particle exchanged between them should vanish.

To show this we examine

$$\begin{aligned}\langle a_{s'n_1} a_{(s + \hat{\omega}_2)n_2}^\dagger \rangle &= (2\pi)^3 2s \delta^{(3)}(s' \vec{n}_1 - (s + \hat{\omega}_2) \vec{n}_2) \\ &= (2\pi)^3 2s \lim_{\epsilon \rightarrow 0} \frac{1}{(\pi\epsilon)^{3/2}} e^{-(s' \vec{n}_1 - (s + \hat{\omega}_2) \vec{n}_2)^2 / \epsilon} = \frac{(2\pi)^2}{(n_1 n_2)} \delta(s') \delta(s + \hat{\omega}_2) ,\end{aligned}\quad (3.29)$$

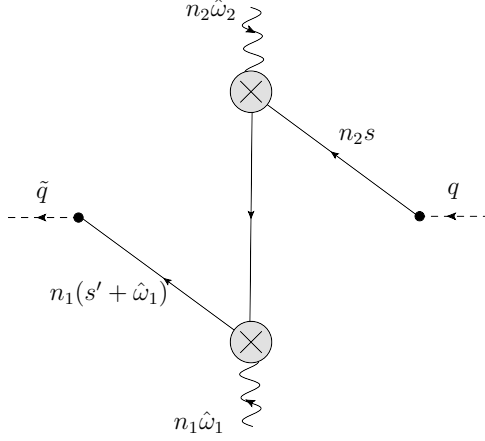


Figure 1. Cross-talk between the detectors. The grey blobs represent the detectors, the solid line depicts the propagator of a scalar particle, the arrows indicate the direction in which it propagates.

where we used (3.6) and replaced $n_1 = (1, \vec{n}_1)$ and $n_2 = (1, \vec{n}_2)$ with $\vec{n}_1^2 = \vec{n}_2^2 = 1$. To check the relation on the second line it is sufficient to integrate both sides against a test function. The expression on the right-hand side of (3.29) is different from zero only for $\hat{\omega}_2 < 0$. Substituting (3.29) into (3.28) and taking into account (3.6) we obtain

$$\begin{aligned} \langle \mathcal{O}_{J_1}(\hat{\omega}_1, n_1) \mathcal{O}_J(\hat{\omega}_2, n_2) \rangle_q &= \frac{(2\pi)^2}{(n_1 n_2)} q^0 \tilde{q}^0 \\ &\times \left[\delta^{(3)}(\vec{q} + \vec{n}_2 \hat{\omega}_2) \delta^{(3)}(\vec{q} - \vec{n}_1 \hat{\omega}_1) w_{J_2}(-\hat{\omega}_2, 0) w_{J_1}(0, \hat{\omega}_1) \theta(-\hat{\omega}_2) \theta(\hat{\omega}_1) \right. \\ &\quad \left. + \delta^{(3)}(\vec{q} + \vec{n}_1 \hat{\omega}_1) \delta^{(3)}(\vec{q} - \vec{n}_2 \hat{\omega}_2) w_{J_2}(0, \hat{\omega}_2) w_{J_1}(-\hat{\omega}_1, 0) \theta(\hat{\omega}_2) \theta(-\hat{\omega}_1) \right]. \end{aligned} \quad (3.30)$$

Notice that this expression is different from zero for $\hat{\omega}_2$ and $\hat{\omega}_1$ of different signs. For instance, for $\hat{\omega}_2 < 0$ and $\hat{\omega}_1 > 0$, a particle with on-shell momentum $q^\mu = (q^0, \vec{q})$ enters the detector $\mathcal{O}_J(\hat{\omega}_2, n_2)$ and leaves it with momentum $q + n_2 \hat{\omega}_2 = 0$, or equivalently $s' = 0$. The second detector $\mathcal{O}_{J_1}(\hat{\omega}_1, n_1)$ transfers the momentum $n_1 \hat{\omega}_1$ and the particle reaches the sink with momentum $\tilde{q} = n_1 \hat{\omega}_1$.

In the above analysis we chose the source and sink to be a scalar field. It is straightforward to show that the relation (3.30) also holds for fermion and gauge fields (up to an overall factor proportional to a power of $q^0 \tilde{q}^0$). However, comparing the relations (3.14) and (3.19), we find that, unlike the scalars, the weights $w_J(0, s)$ and $w_J(s, 0)$ vanish for fermions and gauge fields. Thus, cross-talk can only be generated by the exchange of scalars with zero energy. As follows from (3.30), its contribution is accompanied by a factor of $1/(n_1 n_2)$ that becomes singular for $z \sim (n_1 n_2) \rightarrow 0$. Below we show that an analogous phenomenon occurs in the interacting field theory.

3.4 Two-point functions in $\mathcal{N} = 4$ SYM from amplitudes

In this subsection, we apply the technique described above to compute the two-point function (2.41) in $\mathcal{N} = 4$ SYM at weak coupling. This theory describes a gauge field coupled to four gauginos ψ_i (with $i = 1, \dots, 4$) and six real scalars φ_I ($I = 1, \dots, 6$), all in the adjoint representation of the gauge group $SU(N)$. The index i belongs to the fundamental representation of the R-symmetry group $SU(4)$, while I is an index of the vector representation of $SO(6) \sim SU(4)$.

For the sake of simplicity, we choose the initial and final states, $\phi(q)|0\rangle$ and $\langle 0|\phi^\dagger(\tilde{q})$, respectively, to be defined by the simplest gauge invariant scalar operator of the form

$$\phi = Y^I Y^J \text{tr}(\varphi_I \varphi_J), \quad \phi^\dagger = \bar{Y}^I \bar{Y}^J \text{tr}(\varphi_I \varphi_J), \quad (3.31)$$

where Y are auxiliary (complex) six-dimensional null vectors, $Y^I Y^I = 0$. The operator (3.31) is half-BPS and its scaling dimension $\Delta_\phi = 2$ is protected from quantum corrections. It creates a pair of scalars out of the vacuum, which carries zero total color charge and nonzero R-charge corresponding to the representation $\mathbf{20}'$ of the $SU(4)$.

As mentioned above, we shall consider three different flow operators, scalar (S), charge (Q) and energy (E) operators. They are defined by local twist-two operators of spin $J = 0, 1, 2$, respectively. The stress-energy tensor is given by the spin $J = 2$ operators defined in (3.4) and (3.18) with the only difference that the scalar and fermion fields are replaced by φ_I and ψ_i , respectively. The scalar $J = 0$ operator is defined as

$$O_{J=0}(x, S) = S^{IJ} \text{tr}(\varphi_I \varphi_J(x)), \quad (3.32)$$

where the symmetric traceless ‘polarization’ tensor S^{IJ} determines the orientation of the detector in the isotopic R-space. Like (3.31), the operator (3.32) is protected and lives in the same representation $\mathbf{20}'$ of $SU(4)$. Finally, the spin $J = 1$ operator is given by the R-current

$$O_{J=1}(x, Q) = iQ^{IJ} \text{tr}[\varphi_I \partial_+ \varphi_J] + \dots, \quad (3.33)$$

where the charge polarization matrix Q^{IJ} is an antisymmetric tensor in the adjoint representation $\mathbf{15}$ of $SU(4)$. The dots denote terms involving gauge fields and gauginos, which do not contribute to the two-point correlations $\langle \mathcal{O}_{J_1}(\omega_1, n_1) \mathcal{O}_{J_2}(\omega_2, n_2) \rangle_q$ to one-loop order at weak coupling. The operators (3.32) and (3.33) have scaling dimension $\Delta = 2 + J$ and twist $t = \Delta - J = 2$.

According to (2.52), the two-point correlations are defined by the functions $f_{\mathcal{O}_{J_1} \mathcal{O}_{J_2}}$. At weak coupling, they admit an expansion in the powers of the ’t Hooft coupling $a = g^2 N_c / (4\pi^2)$,

$$f_{\mathcal{O}_{J_1} \mathcal{O}_{J_2}}(\omega_1, \omega_2, z) = f_{\mathcal{O}_{J_1} \mathcal{O}_{J_2}}^{(0)}(\omega_1, \omega_2, z) + \frac{a}{4} f_{\mathcal{O}_{J_1} \mathcal{O}_{J_2}}^{(1)}(\omega_1, \omega_2, z) + \dots, \quad (3.34)$$

where the first and the second terms describe the Born and the one-loop approximations, respectively.

In the Born approximation, the function $\langle \mathcal{O}_{J_1}(\hat{\omega}_1, n_1) \mathcal{O}_{J_2}(\hat{\omega}_2, n_2) \rangle_q^{(0)}$ is given by a sum of two terms describing the two possible propagation channels of the two scalars to the final state: (i) each scalar goes through one of the detectors (see Figure 2(a)) and (ii) one of the scalars goes sequentially through the two detectors and the other one remains undetected (see Figures 2(b) and (c)). The second channel generates cross-talk between the detectors.

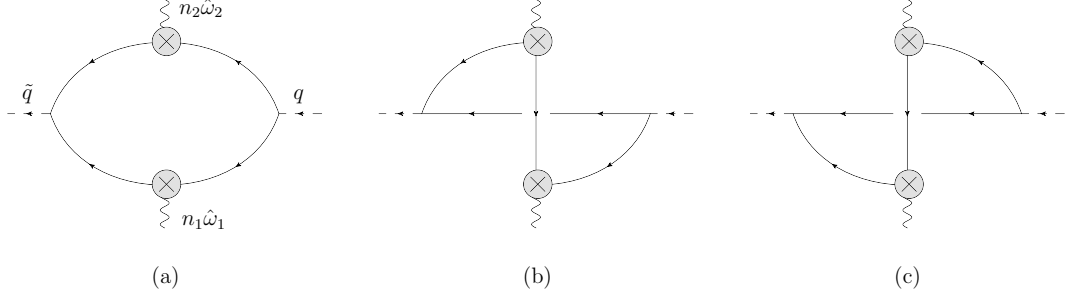


Figure 2. The two-point correlations $\langle \mathcal{O}_{J_1}(\hat{\omega}_1, n_1) \mathcal{O}_{J_2}(\hat{\omega}_2, n_2) \rangle_q$ in the Born approximation.

Each of these contributions is accompanied by a R-symmetry factor arising from the contraction of the indices of the scalar fields in the source and sink with those of the detectors. In particular, for the scalar-scalar and scalar-charge detectors the first contribution comes with a factor of $(\bar{Y}S_1Y)(\bar{Y}S_2Y)$ and $(\bar{Y}S_1Y)(\bar{Y}Q_2Y)$, respectively, where we used a shorthand notation for the contraction of the $SO(6)$ indices, $(\bar{Y}S_1Y) = \bar{Y}^I S^{IJ} Y^J$ and similarly for the charge. For the energy detector, the corresponding isotopic polarization tensor is diagonal in the $SO(6)$ indices, $(E_i)^{IJ} = \delta^{IJ}$ and yields $(\bar{Y}E_iY) = (\bar{Y}Y)$. To simplify the formulae we normalize the $SO(6)$ tensors as follows,

$$(\bar{Y}SY) = (\bar{Y}QY) = 1. \quad (3.35)$$

For the cross-talk contribution the R-symmetry factors look differently. For instance, for the scalar-scalar and scalar-charge correlations they take the form $(\bar{Y}Y)(\bar{Y}S_1S_2Y)$ and $(\bar{Y}Y)(\bar{Y}S_1Q_2Y)$, respectively, plus the same expressions with the detectors exchanged. As mentioned above, the cross-talk between the detectors induces corrections that are singular at $z = 0$. We can eliminate them by imposing additional conditions on the detector polarization tensors,

$$S_1S_2 = S_1S_2 = 0, \quad S_1Q_2 = Q_2S_1 = 0. \quad (3.36)$$

Following Refs. [16, 17], we choose

$$Y = (1, 0, 1, 0, i, i), \quad S_1 = \text{diag}(1, -1, 0, 0, 0, 0), \quad S_2 = \text{diag}(0, 0, 1, -1, 0, 0). \quad (3.37)$$

Notice that a similar condition cannot be imposed on the polarization tensor of the energy detector $(E_i)^{IJ} = \delta^{IJ}$. This means that the correlations involving the energy detector will

necessarily get a cross-talk contribution and, therefore, we expect them to contain additional terms that are singular for $z \rightarrow 0$.

The contribution of the first channel to the two-point correlation is

$$\begin{aligned} & \int \frac{d^4 p_1}{(2\pi)^3} \delta_+(p_1^2) \int \frac{d^4 p_2}{(2\pi)^3} \delta_+(p_2^2) (2\pi)^4 \delta^{(4)}(q - p_1 - p_2) \\ & \times \prod_{i=1,2} w_{J_i}^{(s)}(p_i^0, p_i^0 + \hat{\omega}_i) \delta^{(2)}(\Omega_{\vec{p}_i} - \Omega_{\vec{n}_i}) \theta(p_i^0 + \hat{\omega}_i) (p_i^0)^{-1}, \end{aligned} \quad (3.38)$$

where the first line contains an integral over the Lorentz invariant two-particle phase space and the second line contains the weights (3.14) corresponding to a scalar going through the two detectors. The evaluation of (3.38) can be simplified by going to the rest frame of the source, $q^\mu = (Q, \vec{0})$. Then, $\vec{p}_1 = -\vec{p}_2$ and $p_1^0 = p_2^0 = Q/2$, so that the integral does not vanish only if the detectors are located back-to-back, $\vec{n}_1 = -\vec{n}_2$, or equivalently $z = 1$. The calculation results in

$$f_{\mathcal{O}_{J_1} \mathcal{O}_{J_2}}^{(0)}(\omega_1, \omega_2, z) = \frac{1}{4} \delta(1 - z) \prod_{i=1,2} w_{J_i}^{(s)}(1, 1 + \omega_i). \quad (3.39)$$

This relation holds for all detectors but the energy one. In the latter case, the function $f_{\mathcal{O}_{J_1} \mathcal{O}_{J_2}}^{(0)}$ receives an additional contribution due to the cross-talk between the detectors,

$$\begin{aligned} f_{\mathcal{O}_{J_1} E}^{(0)}(\omega_1, \omega_2, z) &= \frac{1}{4} \delta(1 - z) w_{J_1}^{(s)}(1, 1 + \omega_1) w_E^{(s)}(1, 1 + \omega_2) \\ &+ \frac{1}{z} w_{J_1}^{(s)}(1, 0) w_E^{(s)}(1, 0) [\delta(\omega_1 - 1) \delta(\omega_2 + 1) + \delta(\omega_1 + 1) \delta(\omega_2 - 1)], \\ f_{E \mathcal{O}_{J_1}}^{(0)}(\omega_1, \omega_2, z) &= f_{\mathcal{O}_{J_1} E}^{(0)}(\omega_2, \omega_1, z). \end{aligned} \quad (3.40)$$

where the product of delta functions originates from (3.30). Namely, in the Born approximation the source creates a pair of scalar particles each having energy $Q/2$ in the rest frame $q^\mu = (Q, \vec{0})$. The energy of one of the particles is absorbed by the detector and, therefore, the two-point correlation should be localized at $\omega_i = -1$. The second delta function arises because the other detector has to transfer the energy $Q/2$ to the same scalar particle before it reaches the sink. To avoid such contributions we tacitly assumed elsewhere that $\omega_i > -1$.

The relation (3.40) holds for $0 < z \leq 1$ and it does not take into account the contact terms proportional to $\delta(z)$. Such contact terms have interesting properties and we shall discuss them elsewhere [22].

Turning on the interaction, we find that to order $O(a)$ the two-point correlation (3.1) receives contributions from the states X and X' containing up to four particles. Following the discussion in the previous subsection, we split $\langle \mathcal{O}_{\hat{\omega}_1, J_1}(n_1) \mathcal{O}_{\hat{\omega}_2, J_2}(n_2) \rangle_q$ into a sum of elastic and inelastic contributions. The former is given by (3.1) with X and X' containing the same number of particles. For $z \neq 1$, or equivalently $\vec{n}_1 \neq -\vec{n}_2$ in the rest frame of the source, there are only three particles. The inelastic contribution takes into account the possibility for the detector to create or annihilate a pair of particles. As a result, the states X and X' can have 2 or 4 particles.

Elastic contribution

In this case, the states X and X' in (3.1) contain three particles, either two scalars and a gluon, or a scalar and a pair of gauginos. Two of these particles with on-shell momenta p_i , $i = 1, 2$, go through the detectors which transfer to them the energy $\hat{\omega}_i$ and modify their momenta to $p'_i = p_i + n_i \hat{\omega}_i$. The remaining undetected particle propagates from the source to the sink and has momentum $p_3 = q - p_1 - p_2$. This results in the contribution

$$\begin{aligned} \langle \mathcal{O}_{J_1}(\omega_1, n_1) \mathcal{O}_{J_2}(\omega_2, n_2) \rangle_q^{\text{elastic}} &= 2 \int \frac{d^4 p_1}{(2\pi)^3} \delta_+(p_1^2) \int \frac{d^4 p_2}{(2\pi)^3} \delta_+(p_2^2) 2\pi \delta_+((q - p_1 - p_2)^2) \\ &\times \prod_{i=1,2} w_{J_i}(p_i^0, p_i^0 + \hat{\omega}_i) \delta^{(2)}(\Omega_{\vec{p}_i} - \Omega_{\vec{n}_i}) \theta(p_i^0 + \hat{\omega}_i) (p_i^0)^{-1} \\ &\times A_{q \rightarrow p_1 + p_2 + p_3} (A_{\bar{q} \rightarrow p'_1 + p'_2 + p_3})^*, \end{aligned} \quad (3.41)$$

where the first two lines contain the integral over the phase space of the three particles with on-shell momenta p_1 , p_2 and $p_3 = q - p_1 - p_2$. The particles p_1 and p_2 enter the detectors located in the direction \vec{n}_1 and \vec{n}_2 , respectively. The two factors in the last line of (3.41) describe the transition amplitudes $|\text{source}\rangle \rightarrow |p_1, p_2, p_3\rangle$ and $|p'_1, p'_2, p_3\rangle \rightarrow |\text{sink}\rangle$. They coincide with the on-shell form factors of the operators (3.31),

$$A_{q \rightarrow p_1 + p_2 + p_3} = \langle p_1, p_2, p_3 | \phi(0) | 0 \rangle, \quad (3.42)$$

and similarly for the sink.

The evaluation of (3.41) can be simplified by making use of the identity (3.25),

$$\begin{aligned} \langle \mathcal{O}_{J_1}(\omega_1, n_1) \mathcal{O}_{J_2}(\omega_2, n_2) \rangle_q^{\text{elastic}} &= \frac{1}{2} \int_0^\infty ds_1 ds_2 \int \frac{d^4 p_1}{(2\pi)^3} \int \frac{d^4 p_2}{(2\pi)^3} 2\pi \delta_+((q - p_1 - p_2)^2) \\ &\times A_{q \rightarrow p_1 + p_2 + p_3} (A_{\bar{q} \rightarrow p'_1 + p'_2 + p_3})^* \prod_{i=1,2} w_{J_i}(p_i^0, p_i^0 + \hat{\omega}_i) \theta(p_i^0 + \hat{\omega}_i) \delta^{(4)}(p_i - n_i s_i). \end{aligned} \quad (3.43)$$

In this representation, it is manifest that the particle momenta $p_i = n_i s_i$ are aligned with the null directions of the detectors and s_i play the role of their energy. Switching to the dimensionless integration variables $s_i \rightarrow s_i q^2 / (2(qn_i))$ and taking into account the homogeneity of the weights w_{J_i} we obtain from (3.43)

$$\begin{aligned} &\langle \mathcal{O}_{J_1}(\omega_1, n_1) \mathcal{O}_{J_2}(\omega_2, n_2) \rangle_q^{\text{elastic}} \\ &\sim \int_0^\infty ds_1 ds_2 \delta_+(1 - s_1 - s_2 + s_1 s_2 z) \theta(s_1 + \omega_1) \theta(s_2 + \omega_2) \mathcal{M}(s_1, s_2). \end{aligned} \quad (3.44)$$

Here the dimensionless parameters z and ω_i are defined in (2.42) and (2.34), respectively, and we denote

$$\mathcal{M}(s_1, s_2) = A_{q \rightarrow p_1 + p_2 + p_3} (A_{\bar{q} \rightarrow p'_1 + p'_2 + p_3})^* \prod_{i=1,2} w_{J_i}(s_i, s_i + \omega_i). \quad (3.45)$$

The product of on-shell form factors is evaluated at $p_i^\mu = n_i^\mu s_i q^2 / (2(qn_i))$ and $p_i' = p_i + n_i \omega_i$.

As was already mentioned, to order $O(a)$ we have to consider two form factors (3.42) describing the transitions $\text{source} \rightarrow s + s + g$ and $\text{source} \rightarrow s + \psi + \psi$, where s , ψ and g denote the scalar, gaugino and gluon on-shell states. These form factors are given by (up to overall normalization factors)

$$\begin{aligned} A(s(1)s(2)g^\lambda(3)) &= \epsilon_\mu^\lambda(p_3) \left[\frac{p_1^\mu}{(p_1 p_3)} - \frac{p_2^\mu}{(p_2 p_3)} \right], \\ A(\psi(1)\psi(2)s(3)) &= \sqrt{2} \frac{\langle p_1 p_2 \rangle}{(p_1 p_2)} = \frac{2\sqrt{2}}{[p_2 p_1]}, \end{aligned} \quad (3.46)$$

where $s(i)$ denotes the scalar state with momentum k_i and similarly for the gaugino and the gluon. Here $\epsilon_\mu^\lambda(p_3)$ is the polarization vector of the gluon with helicity $\lambda = \pm 1$ and in the second relation we employed the spinor-helicity representation of the on-shell momenta, $2(p_1 p_2) = \langle p_1 p_2 \rangle [p_2 p_1]$.

Replacing the transition amplitudes $A_{q \rightarrow p_1 + p_2 + p_3}$ in (3.45) with their expressions (3.46), we have to specify which particles (scalars, gauginos or gluons) enter the detectors and replace the weights w_{J_i} with the corresponding expressions (3.14) and (3.19). As an example, consider the scalar-scalar correlation

$$\langle \mathcal{O}_{J_1=0}(\omega_1, n_1) \mathcal{O}_{J_2=0}(\omega_2, n_2) \rangle_q = \frac{1}{8\pi^2(qn_1)(qn_2)} \text{SSC}(\omega_1, \omega_2, z). \quad (3.47)$$

In this case, the detector only selects the scalar particles and the second amplitude in (3.46) does not contribute. The corresponding expression for the function (3.45) looks as

$$\begin{aligned} \mathcal{M}_{\text{SSC}}(s_1, s_2) &= w_S^{(s)}(s_1, s_1') w_S^{(s)}(s_2, s_2') \sum_{\lambda=\pm 1} A(s(1)s(2)g^\lambda(3)) \overline{A(s(1')s(2')g^\lambda(3))} \\ &= \frac{4}{q^2} \frac{s_1 + s_2 - 1}{(1 - s_1)(1 - s_2)}. \end{aligned} \quad (3.48)$$

Here we replaced $w_S^{(s)} = 1$ and substituted the momenta $p_i = s_i n_i q^2 / (2(qn_i))$ and $p_i' = s_i' n_i q^2 / (2(qn_i))$ with $s_i' = s_i + \omega_i$.

For the energy-scalar correlation

$$\langle \mathcal{O}_{J_1=2}(\omega_1, n_1) \mathcal{O}_{J_2=0}(\omega_2, n_2) \rangle_q = \frac{(q^2)^2}{8\pi^2(qn_1)^3(qn_2)} \text{ESC}(\omega_1, \omega_2, z), \quad (3.49)$$

the energy detector sees all the particles and the function (3.45) takes the form

$$\begin{aligned} \mathcal{M}_{\text{ESC}} &= w_E^{(s)}(s_1, s_1') w_S^{(s)}(s_2, s_2') \sum_{\lambda=\pm 1} A(s(1)s(2)g^\lambda(3)) \overline{A(s(1')s(2')g^\lambda(3))} \\ &\quad + w_E^{(g)}(s_1, s_1') w_S^{(s)}(s_2, s_2') \sum_{\lambda=\pm 1} A(s(3)s(2)g^\lambda(1)) \overline{A(s(3)s(2')g^\lambda(1'))} \\ &\quad + w_E^{(\psi)}(s_1, s_1') w_S^{(s)}(s_2, s_2') A(\psi(1)\psi(3)s(2)) \overline{A(\psi(1')\psi(3)s(2'))}, \end{aligned} \quad (3.50)$$

where we changed the indices i and i' in the arguments of A to specify the particles that go through the detectors. Using the expressions for the energy weights, Eqs. (3.14) and (3.19), and going through the calculation we find from (3.50), term-for-term,

$$\mathcal{M}_{\text{ESC}} = \frac{z(6s_1\omega_1 + 6s_1^2 + \omega_1^2)}{6(1-z)} + \frac{(1-s_1z)^2}{(1-z)z} + \frac{(2s_1 + \omega_1)(1-s_1z)}{1-z}, \quad (3.51)$$

where we used the delta function in (3.44) to replace $s_2 = (1-s_1)/(1-s_1z)$.

Substituting (3.48) and (3.51) into (3.44) we obtain the elastic contribution to the two-point functions (3.47) and (3.49),

$$\begin{aligned} \text{SSC}_{\text{elastic}}^{(1)} &= \frac{1}{1-z} I_{\omega_1, \omega_2}(z), \\ \text{ESC}_{\text{elastic}}^{(1)} &= \frac{1 + z\omega_1 + \frac{1}{6}(z\omega_1)^2}{z^2(1-z)} I_{\omega_1, \omega_2}(z), \end{aligned} \quad (3.52)$$

where the superscript refers to the perturbative order in (3.34). The function

$$I_{\omega_1, \omega_2}(z) = \int_0^1 \frac{z ds_1}{1-zs_1} \theta(s_1 + \omega_1) \theta\left(\frac{1+\omega_2}{1+z\omega_2} - s_1\right) \quad (3.53)$$

depends on the angle variable z and on the energies ω_1 and ω_2 transferred by the detectors. It takes different forms depending on the signs of ω_i :

$$I_{\omega_1, \omega_2}(z) = \begin{cases} -\log(1-z), & \omega_1 > 0, \omega_2 > 0, \\ -\log\left(\frac{1-z}{1-z|\omega_2|}\right), & \omega_1 > 0, \omega_2 < 0, \\ -\log\left(\frac{1-z}{(1-z|\omega_1|)(1-z|\omega_2|)}\right), & \omega_1 < 0, \omega_2 < 0, \end{cases} \quad (3.54)$$

and satisfies the relation $I_{\omega_1, \omega_2}(z) = I_{\omega_2, \omega_1}(z)$. The following comments are in order.

It is straightforward to verify that the obtained expressions (3.52) verify the crossing symmetry relations (2.55) and (2.56). For $\omega_1 = \omega_2 = 0$ the inelastic contribution to the detectors vanishes and the relations (3.52) match the one-loop result for the two-point correlations previously found in Ref. [17].

The elastic contributions to the correlations (3.52) are proportional to the same function $I_{\omega_1, \omega_2}(z)$ and they only differ by a rational prefactor. The same is true for all the remaining two-point correlations of flow operators that can be evaluated in a similar manner. To save space, we do not present their explicit expressions here. We shall encounter these expressions later in the paper when we compute the correlations using another approach based on the correlation functions.

We observed previously that the one-point correlations of the flow operators have different dependence on the detector energies for positive and negative ω . It follows from (3.52) and (3.54) that the same is true for the two-point correlations.

Inelastic contribution

In this subsection we compute the additional contribution to the correlations due to the possibility for the detectors $\mathcal{O}_J(\omega, n)$ to create (for $\omega > 0$) and annihilate (for $\omega < 0$) particles.

We start with the scalar correlation (3.47). As was already mentioned, depending on the signs of ω_1 and ω_2 , we can distinguish between four different functions $\text{SSC}_{\pm, \pm}$ and $\text{SSC}_{\pm, \mp}$, with SSC_{++} corresponding to $\omega_1 > 0$ and $\omega_2 > 0$, etc. The crossing symmetry relations (2.55) allow us to limit the discussion to the two functions SSC_{++} and SSC_{+-} . The elastic contribution to these functions is given by (3.52) and (3.54).

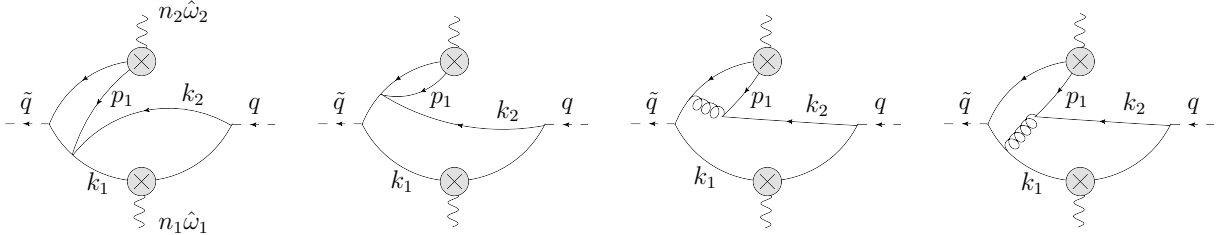


Figure 3. Creation of particles by the scalar detector $\mathcal{O}_{J=0}(\hat{\omega}_2, n_2)$.

To one-loop order, the creation of particles by the scalar detector $\mathcal{O}_{J=0}(\hat{\omega}_2, n_2)$ is described by the diagrams shown in Figure 3. The annihilation of particles is described by similar diagrams in which the initial and final states are swapped. These diagrams contain interaction vertices describing the quartic scalar coupling and the interaction of scalars with gluons in $\mathcal{N} = 4$ SYM. The creation and annihilation of particles by the detector $\mathcal{O}_{J=0}(\hat{\omega}_1, n_1)$ is described by analogous diagrams.

It is clear from Figure 3 that to order $O(a)$ only one of the detectors can create/annihilate particles. This leads to the following expressions for the correlations:

$$\begin{aligned} \text{SSC}_{++}^{\text{inelastic}} &= \langle \tilde{q} | sss \rangle \langle sss | \mathcal{O}^{\text{elastic}}(\hat{\omega}_1, n_1) \mathcal{O}^{\text{creation}}(\hat{\omega}_2, n_2) | ss \rangle \langle ss | q \rangle \\ &\quad + \langle \tilde{q} | sss \rangle \langle sss | \mathcal{O}^{\text{creation}}(\hat{\omega}_1, n_1) \mathcal{O}^{\text{elastic}}(\hat{\omega}_2, n_2) | ss \rangle \langle ss | q \rangle, \end{aligned} \quad (3.55)$$

$$\begin{aligned} \text{SSC}_{+-}^{\text{inelastic}} &= \langle \tilde{q} | ss \rangle \langle ss | \mathcal{O}^{\text{elastic}}(\hat{\omega}_1, n_1) \mathcal{O}^{\text{annihil.}}(\hat{\omega}_2, n_2) | ssss \rangle \langle ssss | q \rangle \\ &\quad + \langle \tilde{q} | ssss \rangle \langle ssss | \mathcal{O}^{\text{creation}}(\hat{\omega}_1, n_1) \mathcal{O}^{\text{elastic}}(\hat{\omega}_2, n_2) | ss \rangle \langle ss | q \rangle, \end{aligned} \quad (3.56)$$

where $\langle ssss | q \rangle$ and $\langle ss | q \rangle$ are the transition amplitudes for the source going to two- and four-scalar states and the detector operators were defined in Eqs. (3.9) – (3.11).

Let us consider the first term in the expression for SSC_{++} , Eq. (3.55). According to (3.11), the operator $\mathcal{O}^{\text{creation}}(\hat{\omega}_2, n_2)$ creates a pair of scalars with momenta $p_1 = sn_2$ and $p_2 = (\omega_2 - s)n_2$, so that the four-particle state looks as $|s(p_1)s(p_2)s(k_1)s(k_2)\rangle$. Here k_1 is the momentum of the scalar that leaves the detector $\mathcal{O}^{\text{elastic}}(\hat{\omega}_1, n_1)$. The incoming two-particle state is $|s(k'_1)s(k_2)\rangle$ where k'_1 is the momentum of the scalar that enters the detector

$\mathcal{O}^{\text{elastic}}(\hat{\omega}_1, n_1)$. The momenta k_1 and k'_1 should be aligned with the null vectors of the detectors, $k_1 = En_1$ and $k'_1 = (E - \omega_1)n_1$. This leads to

$$\begin{aligned} & \langle \tilde{q} | sss s \rangle \langle sss s | \mathcal{O}^{\text{elastic}}(\hat{\omega}_1, n_1) \mathcal{O}^{\text{creation}}(\hat{\omega}_2, n_2) | ss \rangle \langle ss | q \rangle \\ &= \int_0^{\omega_2} ds \int dE \left(A_{\tilde{q} \rightarrow s(p_1)s(p_2)s(k_1)s(k_2)} \right)^* A_{q \rightarrow s(k'_1)s(k_2)} 2\pi \delta_+((q - k'_1)^2), \end{aligned} \quad (3.57)$$

where the integration goes over the energy of the scalars $s(p_1)$ and $s(k_1)$. Here we took into account that the scalar detector assigns a trivial weight to the scalar particles, $w_S^{(s)} = 1$. The delta function in (3.57) comes from the on-shell propagator of the scalar $s(k_2)$ with momentum $k_2 = q - k'_1$. Replacing $k'_1 = (E - \omega_1)n_1$ we find that the on-shell condition $(q - k'_1)^2 = 0$ leads to $E = (\omega_1 + 1)q^2/(2(qn_1))$ and fixes $k_1 = En_1$ unambiguously.

The transition amplitudes entering (3.57) are given by $A_{q \rightarrow s(k'_1)s(k_2)} = 1$ and

$$\begin{aligned} A_{\tilde{q} \rightarrow s(p_1)s(p_2)s(k_1)s(k_2)} &= \frac{1}{(p_1 + k_1 + k_2)^2} - \frac{1}{(p_1 + p_2 + k_2)^2} \\ &+ \frac{1}{2(p_1 k_2)} \left[\frac{2(p_2(p_1 - k_2))}{(p_1 + p_2 + k_2)^2} - \frac{2(k_1(p_1 - k_2))}{(p_1 + k_1 + k_2)^2} \right]. \end{aligned} \quad (3.58)$$

This relation takes into account the contribution of the diagrams shown in Figure 3. Substituting the particle momenta $p_1 = sn_2$, $p_2 = (\omega_2 - s)n_2$, $k_1 = n_1(\omega_1 + 1)q^2/(2(qn_1))$ and $k_2 = q - k_1 + n_1\hat{\omega}_1$, and performing the integration in (3.57) we obtain

$$\begin{aligned} & \langle \tilde{q} | sss s \rangle \langle sss s | \mathcal{O}^{\text{elastic}}(\hat{\omega}_1, n_1) \mathcal{O}^{\text{creation}}(\hat{\omega}_2, n_2) | ss \rangle \langle ss | q \rangle \\ & \sim -\frac{(\omega_1 + 1)z}{(1 - z)(\omega_1 z + 1)} \log \left(\frac{1 + \omega_1 + \omega_2 + \omega_2 \omega_1 z}{\omega_1 + 1} \right) \theta(\omega_2) \theta(1 + \omega_1). \end{aligned} \quad (3.59)$$

The calculation of the first term in the expression for SSC_{+-} , Eq. (3.56), goes along the same lines. We have

$$\begin{aligned} & \langle \tilde{q} | ss \rangle \langle ss | \mathcal{O}^{\text{elastic}}(\hat{\omega}_1, n_1) \mathcal{O}^{\text{annihil.}}(\hat{\omega}_2, n_2) | sss s \rangle \langle sss s | q \rangle \\ &= \int_0^{-\omega_2} ds \int dE \left(A_{\tilde{q} \rightarrow s(k'_1)s(k_2)} \right)^* A_{q \rightarrow s(p_1)s(p_2)s(k_1)s(k_2)} 2\pi \delta_+((\tilde{q} - k'_1)^2), \end{aligned} \quad (3.60)$$

where $p_1 = sn_1$ and $p_2 = -\omega_2 n_2 - p_1$ are the momenta of the scalars absorbed by the detector $\mathcal{O}^{\text{annihil.}}(\hat{\omega}_2, n_2)$. The momenta of the two remaining scalars are $k_1 = En_1$, $k'_1 = n_1(E + \omega_1)$ and $k_2 = \tilde{q} - k'_1$. As in the previous case, the relation $(\tilde{q} - k'_1)^2 = 0$ fixes the energy $E = (1 + \omega_2)/(1 + z\omega_2)q^2/(2(qn_1))$. Going through the calculation of (3.60) we find

$$\begin{aligned} & \langle \tilde{q} | ss \rangle \langle ss | \mathcal{O}^{\text{elastic}}(\hat{\omega}_1, n_1) \mathcal{O}^{\text{annihil.}}(\hat{\omega}_2, n_2) | sss s \rangle \langle sss s | q \rangle \\ & \sim -\frac{(\omega_2 + 1)z}{(1 - z)(\omega_2 z + 1)} \log \left(\frac{1}{\omega_2 + 1} \right) \theta(-\omega_2) \theta(1 + \omega_2). \end{aligned} \quad (3.61)$$

Note that this relation is independent of ω_1 .

Substituting the relations (3.59) and (3.61) into (3.55) and (3.56), we obtain the inelastic contribution to the scalar-scalar correlations. Combining it with the elastic contribution (3.52) we finally arrive at

$$\begin{aligned} \text{SSC}_{++}^{(1)}(\omega_1, \omega_2, z) &= \frac{1}{1-z} \log \left(\frac{1}{1-z} \right) \\ &+ \frac{(\omega_1 + 1)z}{2(1-z)(\omega_1 z + 1)} \log \left(\frac{\omega_1 + \omega_2 + \omega_1 \omega_2 z + 1}{\omega_1 + 1} \right) \\ &+ \frac{(\omega_2 + 1)z}{2(1-z)(\omega_2 z + 1)} \log \left(\frac{\omega_1 + \omega_2 + \omega_1 \omega_2 z + 1}{\omega_2 + 1} \right), \end{aligned} \quad (3.62)$$

$$\text{SSC}_{+-}^{(1)}(\omega_1, \omega_2, z) = \frac{\log \left(\frac{1+\omega_2 z}{1-z} \right)}{1-z} + \frac{(\omega_2 + 1)z}{2(1-z)(\omega_2 z + 1)} \log \left(\frac{\omega_1 + \omega_2 + \omega_2 \omega_1 z + 1}{(\omega_2 + 1)^2} \right). \quad (3.63)$$

Here the first terms in both relations correspond to the elastic contribution and the remaining terms describe the inelastic contribution. The relations (3.62) and (3.63) are valid for $0 < z < 1$ and they do not take into account contact terms of the types $\delta(z)$ and $\delta(1-z)$.

For $\omega_1 = \omega_2 = 0$ the inelastic contribution to (3.62) and (3.63) vanishes and one recovers the known result for the SSC derived in Ref. [17]. We observe that the above relations are given by a linear combination of logarithms with rational coefficients. To make this property manifest, it is convenient to assign weight 1 to the logarithm and weight 0 to the rational functions. Then, all the terms in the expressions for the correlations have the same weight 1. This is yet another manifestation of the uniform weight property previously observed for various quantities in $\mathcal{N} = 4$ SYM.

Applying the crossing symmetry relations (2.55) we can find from (3.62) and (3.63) the two remaining scalar-scalar correlations,

$$\begin{aligned} \text{SSC}_{--}^{(1)}(\omega_1, \omega_2, z) &= \frac{1}{1-z} \log \left(\frac{(1 + \omega_1 z)(1 + \omega_2 z)}{1-z} \right) \\ &+ \frac{(\omega_1 + 1)z}{2(1-z)(\omega_1 z + 1)} \log \left(\frac{1}{\omega_1 + 1} \right) + \frac{(\omega_2 + 1)z}{2(1-z)(\omega_2 z + 1)} \log \left(\frac{1}{\omega_2 + 1} \right), \end{aligned} \quad (3.64)$$

$$\text{SSC}_{-+}^{(1)}(\omega_1, \omega_2, z) = \text{SSC}_{+-}^{(1)}(\omega_2, \omega_1, z). \quad (3.65)$$

Here the last relation can be obtained by taking into account the symmetry of the SSC under the exchange of the detectors.

Comparing the above expressions we observe an interesting relation,

$$\text{SSC}_{++}^{(1)}(\omega_1, \omega_2, z) + \text{SSC}_{--}^{(1)}(\omega_1, \omega_2, z) = \text{SSC}_{+-}^{(1)}(\omega_1, \omega_2, z) + \text{SSC}_{-+}^{(1)}(\omega_1, \omega_2, z), \quad (3.66)$$

where it is tacitly assumed that the functions are continued from the domain of their validity (positive or negative ω 's) to arbitrary real ω_1 and ω_2 . We elucidate the origin of this relation in Section 4.4 below. We will show that it is rather general and holds for the various correlations both at weak and strong coupling.

It is straightforward to extend the above analysis to the correlations involving charge and energy detectors. These detectors receive contributions from all the particles (scalars, gauginos and gluons). Due to the growing number of relevant diagrams, the calculation is more involved. To save space we do not present it here. In the next section, we introduce a more efficient approach to computing the various correlations based on correlation functions. We have checked that the two approaches yield the same expressions for the correlations.

4 Generalized event shapes with scalar detectors

In this section, we consider the four-point Wightman function of scalar primaries. We introduce the Mellin representation for the connected part of this function and use it to compute the ω -deformed event shapes (2.30). This section generalizes the analysis of [16, 17] to $\omega_i \neq 0$.

Following [17], we consider the four-point function of $\mathbf{20}'$ operators in $\mathcal{N} = 4$ SYM

$$\langle \phi^\dagger(x_4) O(x_1, S_1) O(x_2, S_2) \phi(x_3) \rangle = \frac{G^{(\mathbf{105})}(u, v)}{x_{12}^4 x_{34}^4}, \quad (4.1)$$

where the explicit expressions for the operators can be found in (3.31), (3.32) and (3.37), and the two conformal cross-ratios are defined as

$$u = \frac{x_{12}^2 x_{34}^2}{x_{13}^2 x_{24}^2}, \quad v = \frac{x_{14}^2 x_{23}^2}{x_{13}^2 x_{24}^2}. \quad (4.2)$$

In (4.1) the notation $G^{(\mathbf{105})}(u, v)$ emphasizes that with the choice of R-symmetry polarizations (3.37) only the $\mathbf{105}$ representation of $SU(4)$ appears in the OPE of the detector operators $O(x_1, S_1) O(x_2, S_2)$. This particular representation played a privileged role in [16] because for $\hat{\omega}_i = 0$ it is very simply related to the energy-energy correlation, which is the observable of our prime interest.

It is convenient to write $G^{(\mathbf{105})}(u, v)$ as follows

$$G^{(\mathbf{105})}(u, v) = \frac{c_T}{2(2\pi)^4} \left(u^2 + \frac{u^2}{v^2} \right) + \frac{1}{(2\pi)^4} \frac{u^2}{v} \left(\frac{1}{2} + u\Phi(u, v) \right), \quad (4.3)$$

where the central charge c_T is given by

$$c_T = \frac{N_c^2 - 1}{4}. \quad (4.4)$$

Let us briefly comment on the structure of (4.3). The rational term $\frac{c_T}{2(2\pi)^4} \left(u^2 + \frac{u^2}{v^2} \right)$ is the disconnected part of the correlation function. It does not contribute to the generalized event shapes at separated points ($z \neq 0$) and can be safely discarded. The other rational term $\frac{1}{(2\pi)^4} \frac{u^2}{2v}$ is the connected correlator at zero coupling (i.e. Born level or free theory). Finally, the most important for our purposes part of (4.3) is the function $\Phi(u, v)$. At weak coupling

it encodes the perturbative corrections, i.e. it is proportional the 't Hooft coupling constant $a \equiv g_{\text{YM}}^2 N_c / (4\pi^2)$. This function satisfies the crossing symmetry relations

$$\Phi(u, v) = \Phi(v, u) = \frac{1}{v} \Phi\left(\frac{u}{v}, \frac{1}{v}\right). \quad (4.5)$$

The starting point of our discussion is the Mellin representation of the function $\Phi(u, v)$ in the form used in [16, 17]

$$\Phi(u, v) = \int_{\mathcal{C}_0} \frac{dj_1 dj_2}{(2\pi i)^2} [\Gamma(1 - j_1) \Gamma(1 - j_2) \Gamma(j_1 + j_2)]^2 M(j_1, j_2) u^{j_1} v^{j_2}, \quad (4.6)$$

where the integration contour \mathcal{C}_0 runs parallel to the imaginary axis and satisfies $\text{Re}(j_1 + j_2) > -1$ and $\text{Re}(j_1), \text{Re}(j_2) < 0$. The crossing symmetry (4.5) implies that

$$M(j_1, j_2) = M(j_2, j_1) = \frac{(j_1 + j_2)^2 (j_1 + j_2 + 1)^2}{j_1^2 (1 + j_1)^2} M(-1 - j_1 - j_2, j_2). \quad (4.7)$$

Equivalently, if we write

$$M(j_1, j_2) = (j_1 + j_2)^2 (j_1 + j_2 + 1)^2 \tilde{M}(j_1, j_2) \quad (4.8)$$

then $\tilde{M}(j_1, j_2)$ is fully crossing-symmetric $\tilde{M}(j_1, j_2) = \tilde{M}(j_2, j_1) = \tilde{M}(-1 - j_1 - j_2, j_2)$.

The leading weak and strong coupling results take the form

$$\begin{aligned} M^{\text{weak}}(j_1, j_2) &= -\frac{a}{4} \frac{(j_1 + j_2)^2}{j_1^2 j_2^2}, \\ M^{\text{strong}}(j_1, j_2) &= -\frac{1}{2} \frac{(j_1 + j_2)^2 (1 + j_1 + j_2)}{j_1 j_2}. \end{aligned} \quad (4.9)$$

Using the $\mathcal{N} = 4$ supersymmetry Ward identities, similar but more complicated expressions can be written for other four-point functions, in particular those with the insertions of the R-symmetry current and the stress-energy tensor at the detector points 1 and 2 (see Section 5).

Our next task is to go from the Mellin representation of the correlator to the Mellin representation of generalized event shapes. This amounts to three steps:

1. Take the detector limit (2.22).
2. Fourier transform with respect to the detector working time.
3. Fourier transform with respect to the position of the sink.

In the Mellin representation of the correlator (4.6) all the dependence on the positions of the operators is encoded in the factor $u^{j_1} v^{j_2}$, to which we apply the steps above. All the dynamical information (i.e., the coupling dependence) on the other hand is contained in the Mellin amplitude $M(j_1, j_2)$ which factors out. This computation is a straightforward

generalization of the one done in [16] and we refer the reader to appendix E for the details. The result takes the following form

$$\langle \mathcal{O}(\omega_1, n_1) \mathcal{O}(\omega_2, n_2) \rangle_q = \frac{1}{8\pi^2} \frac{\text{SSC}(\omega_1, \omega_2, z)}{(qn_1)(qn_2)}, \quad (4.10)$$

where $\text{SSC}(\omega_1, \omega_2, z)$ is the convolution of the Mellin amplitude of the four-point correlation function $M(j_1, j_2)$ and the detector kernel K_{SS}

$$\text{SSC}(\omega_1, \omega_2, z) = \int_{\mathcal{C}_0} \frac{dj_1 dj_2}{(2\pi i)^2} M(j_1, j_2) K_{\text{SS}}(j_1, j_2 | \omega_1, \omega_2, z). \quad (4.11)$$

In the undeformed case $\omega_i = 0$ the detector kernel K_{SS} is very simple [17]:

$$K_{\text{SS}}(j_1, j_2 | 0, 0, z) = \frac{2\pi}{\sin \pi(j_1 + j_2)} z^{-j_1 - j_2} (1 - z)^{j_1 + j_2 - 1}. \quad (4.12)$$

Let us now see how this simple result changes when $\omega_i \neq 0$.

We start by quoting the result for the detector kernel in the most compact form. As discussed earlier we consider separately the cases where the detector frequencies have the same sign $\omega_i \geq 0$ (we denote this case by $++$), and the case when they have opposite signs $\omega_1 \geq 0, \omega_2 \leq 0$ (we denote this case by $+-$). The result takes the form (see Appendix E for details)

$$\begin{aligned} K_{\text{SS}}^{+-}(j_1, j_2 | \omega_1, \omega_2, z) &= \frac{1}{2(1-z)} \left(-\frac{z\omega_1\omega_2}{1+\omega_2} \right)^{-j_2} \left(\frac{z(1+\omega_2)}{1-z} \right)^{-j_1} \frac{\Gamma(1-j_1)^2 \Gamma(j_1+j_2)}{\Gamma(1+j_2-j_1)} \\ &\times {}_2F_1 \left(j_2, 1-j_1, 1+j_2-j_1, \frac{(1+\omega_1)(1+\omega_2)}{\omega_1\omega_2(1-z)} \right), \end{aligned} \quad (4.13)$$

$$\begin{aligned} K_{\text{SS}}^{++}(j_1, j_2 | \omega_1, \omega_2, z) &= \frac{1}{2(1-z)} \left(\frac{z\omega_1\omega_2}{1+\omega_2} \right)^{-j_2} \left(\frac{z(1+\omega_2)}{1-z} \right)^{-j_1} \Gamma(1-j_1) \Gamma(1-j_2) \Gamma(j_1+j_2) \\ &\times {}_2F_1 \left(j_2, 1-j_1, 1, 1 - \frac{(1+\omega_1)(1+\omega_2)}{\omega_1\omega_2(1-z)} \right). \end{aligned} \quad (4.14)$$

If one of the frequencies vanishes, the kernels become simply related to the undeformed one in (4.12), e.g.

$$K_{\text{SS}}^{+-}(j_1, j_2 | 0, \omega_2, z) = K_{\text{SS}}^{++}(j_1, j_2 | 0, \omega_2, z) = K_{\text{SS}}(j_1, j_2 | 0, 0, z) (1 + \omega_2)^{-j_1}. \quad (4.15)$$

While the above formulas are rather compact, they obscure some of the properties of the kernels which are useful in the subsequent computation of the Mellin integral in (4.11). Below we present another representation of the kernels which makes these properties manifest.

4.1 SSC kernel: opposite signs

Let us first consider the case where the frequencies of the detectors have opposite signs, namely $\omega_1\omega_2 < 0$. This covers the cases $+-$ and $-+$. The kernel (4.13) can be recast in the

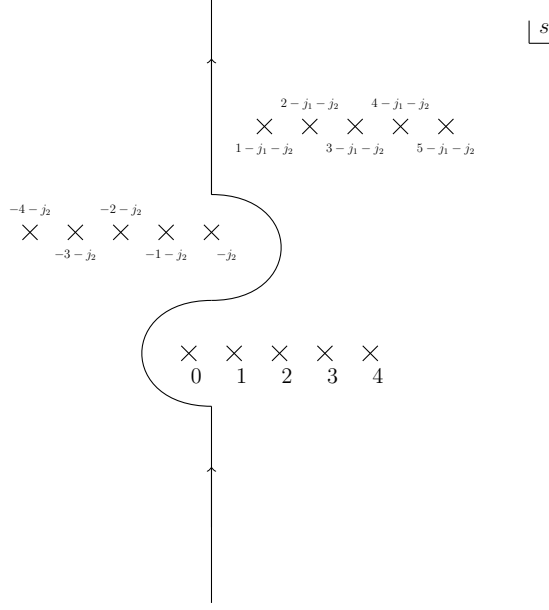


Figure 4. Integration contour \mathcal{C}_K in the s -plane for the kernel in (4.16). The poles come from $\Gamma(-s)\Gamma(1 - j_1 - j_2 - s)\Gamma(j_2 + s)$. In drawing the plot we used the fact that $\text{Re}[j_2] < 0$ and $-1 < \text{Re}[j_1 + j_2] < 0$ as in (4.6).

following convenient form (see appendix E for the derivation)

$$\begin{aligned} \frac{K_{\text{SS}}^{+-}(j_1, j_2 | \omega_1, \omega_2, z)}{K_{\text{SS}}(j_1, j_2 | 0, 0, z)} &= (1 + \omega_1)^{-j_2} (1 + \omega_2)^{-j_1} \\ &\times \int_{\mathcal{C}_K} \frac{ds}{2\pi i} \Gamma(-s) \frac{\Gamma(1 - j_1 - j_2 - s) \Gamma(j_2 + s) \Gamma(1 - j_1)}{\Gamma(1 - j_1 - j_2) \Gamma(j_2) \Gamma(1 - j_1 - s)} \left(-\frac{(1 - z) \omega_1 \omega_2}{(1 + \omega_1)(1 + \omega_2)} \right)^s. \end{aligned} \quad (4.16)$$

The integration contour \mathcal{C}_K runs parallel to the imaginary axis and separates the poles generated by the product of gamma functions in the numerator, i.e. ascending poles coming from $\Gamma(\dots - s)$ from the left and descending poles coming from $\Gamma(\dots + s)$ from the right, see Figure 4.

For SSC_{-+} we define

$$K_{\text{SS}}^{-+}(j_1, j_2 | \omega_1, \omega_2, z) \equiv K_{\text{SS}}^{+-}(j_2, j_1 | \omega_2, \omega_1, z), \quad (4.17)$$

where on the right-hand side we permuted both $\omega_1 \leftrightarrow \omega_2$ and $j_1 \leftrightarrow j_2$ using the symmetry of the Mellin amplitude $M(j_1, j_2) = M(j_2, j_1)$.

The Mellin integral in (4.16) can be done explicitly resulting in (4.13). The representation (4.16) makes many of the properties of the kernel manifest, so we can equally use it instead. Let us discuss these properties one by one.

Firstly, consider the small $\omega_i \rightarrow 0$ limit of the kernel. This corresponds to closing the s -contour in (4.16) to the right with the contribution from $s = 0$ producing 1 and thus correctly reproducing (4.12). Similarly, if we are interested in the small ω_i expansion of our

event shapes, we can consistently do it by keeping more and more residues from the poles at $s = n$ and $s = 1 - j_1 - j_2 + n$, $n \in \mathbb{Z}_+$. The poles at $s = n$ correspond to the analytic part $(\omega_1 \omega_2)^n$ of the expansion of the kernel around $\omega_i = 0$. The poles at $s = 1 - j_1 - j_2 + n$ result in the non-analytic part $(\omega_1 \omega_2)^{1-j_1-j_2+n}$.

Secondly, the ratio of kernels (4.16) is analytic for $\text{Re}(j_2) > 0$, $\text{Re}(j_1) < 0$ and fixed $j_1 + j_2$. This is clear from the fact that no pinch in the s integration contour arises in this case. This is particularly useful if we take into account that $K_{\text{SS}}(j_2, j_1|z, 0, 0)$ is analytic for fixed $j_1 + j_2$ as well. We find this property very helpful in the perturbative computations.

For $\omega_1 > 0$, $\omega_2 < 0$ and $j_1 + j_2$ fixed the kernel decays if we deform the j_1 contour to the left. The fact that the kernel is analytic means that we only pick the contribution from the poles of $M(j_1, j_2)$. As can be seen from (4.9), both at weak and at strong coupling only a single pole at $j_2 = 0$ contributes. This dramatically simplifies the calculation.

Thirdly, note that SSC_{+-} should go into itself under the combination of the crossing symmetry transformation (2.55) and the permutation of the detectors. This is indeed reflected in the following property of the kernel,

$$K_{\text{SS}}^{+-}(j_2, j_1|\omega_2, \omega_1, z) = \frac{1}{(1 + \omega_1 z)(1 + \omega_2 z)} K_{\text{SS}}^{+-}(j_2, j_1|\omega'_1, \omega'_2, z'). \quad (4.18)$$

To check this property note that the argument of the s -integral in (4.16) is invariant under this transformation, namely

$$-\frac{\omega_1 \omega_2 (1 - z)}{1 + \omega_1 + \omega_2 + \omega_1 \omega_2 z} = -\frac{\omega'_1 \omega'_2 (1 - z')}{1 + \omega'_1 + \omega'_2 + \omega'_1 \omega'_2 z'}, \quad (4.19)$$

which makes checking (4.18) trivial.

Using the properties of the kernel described above and the explicit expressions (4.9) for the Mellin amplitudes it is easy to compute

$$\text{SSC}_{+-}^{\text{weak}} = \frac{a}{4} \left[\frac{\log\left(\frac{1+\omega_2 z}{1-z}\right)}{1-z} + \frac{(1+\omega_2)z}{2(1-z)(1+z\omega_2)} \log\left(\frac{\omega_1 + \omega_2 + \omega_1 \omega_2 z + 1}{(\omega_2 + 1)^2}\right) \right], \quad (4.20)$$

$$\text{SSC}_{+-}^{\text{strong}} = \frac{z^2}{2} \frac{(\omega_2 + 1)^2}{(\omega_2 z + 1)^3}. \quad (4.21)$$

Let us reiterate that only the $j_2 = 0$ pole of the Mellin amplitude contributes to the above computations. The expressions for SSC_{-+} can be obtained from SSC_{+-} by permuting $\omega_1 \leftrightarrow \omega_2$. We have also checked our calculation by performing the Mellin integrals numerically and found perfect agreement with the formulas above.

4.2 SSC kernel: same sign

Consider next the case when the frequencies of the detectors have the same sign, $\omega_1 \omega_2 > 0$. This covers both cases $++$ and $--$. The convenient representation of the kernel (4.14) takes the form (see appendix E for the derivation)

$$\frac{K_{\text{SS}}^{++}(j_1, j_2|\omega_1, \omega_2, z)}{K_{\text{SS}}(j_1, j_2|0, 0, z)} = (1 + \omega_1)^{-j_2} (1 + \omega_2)^{-j_1}$$

$$\times \int_{\mathcal{C}_K} \frac{ds}{2\pi i} \Gamma(-s) \frac{\Gamma(1-j_1-j_2-s)\Gamma(j_2+s)\Gamma(j_1+s)}{\Gamma(1-j_1-j_2)\Gamma(j_2)\Gamma(j_1)} \left(\frac{\omega_1\omega_2(1-z)}{(1+\omega_1)(1+\omega_2)} \right)^s, \quad (4.22)$$

where the contour of integration \mathcal{C}_K is defined in the same way as in (4.16).

Let us comment on the relevant properties of (4.22). Firstly, as expected, the kernel is invariant under the permutation of the detectors $\omega_1 \leftrightarrow \omega_2$ combined with $j_1 \leftrightarrow j_2$. The latter exchange does not affect the event shape since $M(j_1, j_2) = M(j_2, j_1)$. Due to the relation (which one can explicitly check using (4.22))

$$K_{\text{SS}}^{++}(j_1, j_2 | \omega_1, \omega_2, z) = \frac{1}{(1+\omega_1 z)(1+\omega_2 z)} K_{\text{SS}}^{++}(j_2, j_1 | \omega'_1, \omega'_2, z'), \quad (4.23)$$

where $\omega'_i < 0$, and the crossing symmetry relations (2.55), the right-hand side of (4.22) defines the kernel for the $--$ case as well.

Secondly, as before it is trivial to extract the $\omega_i \rightarrow 0$ limit from (4.22) by closing the Mellin contour in (4.22) to the right and picking the contributions from the poles at $s = n$ and $s = 1 - j_1 - j_2 + n$, $n \in \mathbb{Z}_+$. For example, the case $\omega_i = 0$ is simply given by the residue at $s = 0$, which produces 1 for the ratio (4.22). These two series of poles can be resummed into a pair of hypergeometric functions (E.17).

Thirdly, there is an important difference in the analytic properties of the kernel (4.22) compared to the $+-$ case. Namely, for fixed $j_1 + j_2$ the kernel has an infinite number of singularities both to the left and to the right of the j_1 contour. This means that in evaluating the Mellin integrals we have to deal with infinitely many poles in both Mellin variables, even though the Mellin amplitudes of interest (4.9) are relatively simple. We will see that the result can still be computed analytically.

Because of the complicated properties of the Mellin kernel, the computation of SSC_{++} is more difficult than in the $+-$ case. The result agrees with the amplitude computation and takes the following form (the details of the computation can be found in Appendix F)

$$\begin{aligned} \text{SSC}_{++}^{\text{weak}} &= \frac{a}{4} \left[\frac{1}{1-z} \log \left(\frac{1}{1-z} \right) \right. \\ &\quad + \frac{(\omega_1 + 1)z}{2(1-z)(\omega_1 z + 1)} \log \left(\frac{\omega_1 + \omega_2 + \omega_1 \omega_2 z + 1}{\omega_1 + 1} \right) \\ &\quad \left. + \frac{(\omega_2 + 1)z}{2(1-z)(\omega_2 z + 1)} \log \left(\frac{\omega_1 + \omega_2 + \omega_1 \omega_2 z + 1}{\omega_2 + 1} \right) \right], \end{aligned} \quad (4.24)$$

$$\begin{aligned} \text{SSC}_{++}^{\text{strong}} &= \frac{z^2}{2} \left[\frac{6\omega_1^2 \omega_2^2 (\omega_1 + \omega_2)}{(\omega_1 + \omega_2 + \omega_2 \omega_1 z)^5} + \frac{3\omega_1 (2\omega_2 \omega_1^2 + 2\omega_2^2 \omega_1 + \omega_1^2 + \omega_2^2) \omega_2}{(\omega_1 + \omega_2 + \omega_2 \omega_1 z)^4} \right. \\ &\quad \left. + \frac{\omega_2^2 \omega_1^3 + \omega_2^3 \omega_1^2 + 2\omega_2 \omega_1^3 + 2\omega_2^3 \omega_1 + \omega_1^3 + \omega_2^3}{(\omega_1 + \omega_2 + \omega_2 \omega_1 z)^3} \right]. \end{aligned} \quad (4.25)$$

As a consistency check, we verify that the relations (4.20) and (4.24) coincide for $\omega_2 = 0$. The singularities at $\omega_1 + \omega_2 + \omega_2 \omega_1 z = 0$ are related to the bulk point singularities of the correlator. They only appear at strong coupling and we discuss them in more details in Section 4.5.

For the $--$ case, we use the transformation (2.55) to get

$$\begin{aligned}
\text{SSC}_{--}^{\text{weak}} &= \frac{a}{4} \left[\frac{1}{1-z} \log \left(\frac{(\omega_1 z + 1)(\omega_2 z + 1)}{1-z} \right) \right. \\
&\quad \left. + \frac{(\omega_1 + 1)z}{2(1-z)(\omega_1 z + 1)} \log \left(\frac{1}{\omega_1 + 1} \right) + \frac{(\omega_2 + 1)z}{2(1-z)(\omega_2 z + 1)} \log \left(\frac{1}{\omega_2 + 1} \right) \right], \quad (4.26) \\
\text{SSC}_{--}^{\text{strong}} &= \frac{z^2}{2} \left[\frac{(\omega_1 + 1)^2}{(\omega_1 z + 1)^3} + \frac{(\omega_2 + 1)^2}{(\omega_2 z + 1)^3} \right. \\
&\quad - \frac{6\omega_1^2 \omega_2^2 (\omega_1 + \omega_2)}{(\omega_1 + \omega_2 + \omega_2 \omega_1 z)^5} - \frac{3\omega_1 (2\omega_2 \omega_1^2 + 2\omega_2^2 \omega_1 + \omega_1^2 + \omega_2^2) \omega_2}{(\omega_1 + \omega_2 + \omega_2 \omega_1 z)^4} \\
&\quad \left. - \frac{\omega_2^2 \omega_1^3 + \omega_2^3 \omega_1^2 + 2\omega_2 \omega_1^3 + 2\omega_2^3 \omega_1 + \omega_1^3 + \omega_2^3}{(\omega_1 + \omega_2 + \omega_2 \omega_1 z)^3} \right]. \quad (4.27)
\end{aligned}$$

We recall that the above relations are valid for $0 < z < 1$ and $\omega_i > -1$.

4.3 Closing the contour

The reader might have noted something puzzling about our result above: if the kernel does not depend on the choice $++$ versus $--$, as explained around (4.23), how is it possible that the expressions for SSC_{++} and SSC_{--} are different?

To understand the reason, it is instructive to consider the following simple integral

$$\int_{-\epsilon-i\infty}^{-\epsilon+i\infty} \frac{dj}{2\pi i} \frac{(1+\omega)^{-j}}{j} = -\theta(\omega). \quad (4.28)$$

For negative ω we evaluate the integral by closing the contour to the left and get zero. For positive ω we are allowed to close the contour to the right. Picking up the residue of the pole at $j = 0$ we arrive at (4.28).

The same mechanism is at work for our observables. Consider first the simpler case $\omega_1 = 0$ with the kernel given by (4.15). Switching to the integration variables j_1 and $j = j_1 + j_2$ in the Mellin integral, we see that the dependence on j_1 enters only through the factor $(1 + \omega_2)^{-j_1}$. Therefore, as in the simple example (4.28) above, the allowed direction of closing the j_1 contour depends on the sign of ω_2 . For $\omega_2 \geq 0$ we can close the contour to the right, whereas for $\omega_2 \leq 0$ we can close the contour to the left. This can lead to different results and it explains the difference between $\text{SSC}(0, \omega_2, z)$ for positive and negative ω_2 , even though the Mellin kernel does not depend on the sign of ω_2 .

For $\omega_1, \omega_2 \neq 0$, the kernels become much more complicated. Nevertheless, one can identify by inspection the allowed directions of closing the j_1, j_2 contours, depending on the parameters of the problem. We found that the representations of the kernel (E.17) and (E.20) are particularly useful for this purpose. The result is, as expected, that the generalized event shapes are not analytic around $\omega_1, \omega_2 = 0$.

4.4 Detector identity

We observe that both at weak and strong coupling the scalar-scalar correlations satisfy the identity (cf. (3.66))

$$\text{SSC}_{--} + \text{SSC}_{++} - \text{SSC}_{+-} - \text{SSC}_{-+} = 0. \quad (4.29)$$

It is understood as an *analytic continuation* from the region where each function has been originally computed to some common values of ω_i . In Section 6 we check that this relation also holds for the other detectors except for the energy one. In the latter case, the identity is violated at weak coupling due to the contribution from the cross-talk between the detectors. Here we derive a general formula for the left-hand side of (4.29) which is valid at finite coupling and from which its vanishing at weak and strong coupling follows immediately.

In order to proceed we have to specify the analytic continuation in ω of the event shapes in (4.29). Consider for example SSC_{++} written for the detector operators defined in the null plane conformal frame (2.17). We have schematically

$$\text{SSC}_{++} = \int_{-\infty}^{\infty} du_1 du_2 e^{-i \sum_{k=1}^2 \hat{\omega}_k u_k} \langle O_4 O_1(u_1) O_2(u_2) O_3 \rangle, \quad (4.30)$$

where we suppressed the dependence on the positions of the source and the sink, as well as the transverse coordinates of the detector operators. Such details will not be relevant for what follows.

Since the light-ray operators with $\hat{\omega}_i \geq 0$ annihilate the left vacuum (see Eq. (2.25)), we can rewrite (4.30) in the following equivalent way

$$\text{SSC}_{++} = \int_{-\infty}^{\infty} du_1 du_2 e^{-i \sum_{k=1}^2 \hat{\omega}_k u_k} \langle [[O_4, O_1(u_1)], O_2(u_2)] O_3 \rangle. \quad (4.31)$$

Now we can ‘analytically continue’ SSC_{++} to any sign of $\hat{\omega}_i$ by using Eq. (4.31) instead of (4.30) for any signs of $\hat{\omega}_i$. Let us emphasize again that (4.31) is equivalent to (4.30) only for $\hat{\omega}_i > 0$ but they differ otherwise. Similarly, we get the following relations for other choices of the signs of ω_i

$$\begin{aligned} \text{SSC}_{--} &= \int_{-\infty}^{\infty} du_1 du_2 e^{-i \sum_{k=1}^2 \hat{\omega}_k u_k} \langle O_4 [O_1(u_1), [O_2(u_2), O_3]] \rangle, \\ \text{SSC}_{+-} &= \int_{-\infty}^{\infty} du_1 du_2 e^{-i \sum_{k=1}^2 \hat{\omega}_k u_k} \langle [O_4, O_1(u_1)] [O_2(u_2), O_3] \rangle, \\ \text{SSC}_{-+} &= \int_{-\infty}^{\infty} du_1 du_2 e^{-i \sum_{k=1}^2 \hat{\omega}_k u_k} \langle [O_4, O_2(u_2)] [O_1(u_1), O_3] \rangle, \end{aligned} \quad (4.32)$$

where we used again Eq. (2.25). Switching to commutators does not produce any effect in the region where each of the event shapes was originally defined. However, as we go away from this region (by flipping some of the signs of ω_i), formulas (4.31) and (4.32) define the analytic continuation needed to check the identity (4.29).

Now we can evaluate the formulas above for any sign of $\hat{\omega}_i$. We get the following result (where we also use the fact that the detectors commute with each other for $z \neq 0$)

$$\begin{aligned} \text{SSC}_{--} + \text{SSC}_{++} - \text{SSC}_{+-} - \text{SSC}_{-+} &= \int_{-\infty}^{\infty} du_1 du_2 e^{-i \sum_{k=1}^2 \hat{\omega}_k u_k} \left[\langle O_1(u_1) O_2(u_2) O_4 O_3 \rangle \right. \\ &\quad \left. + \langle O_4 O_3 O_1(u_1) O_2(u_2) \rangle - \langle O_1(u_1) O_4 O_3 O_2(u_2) \rangle - \langle O_2(u_2) O_4 O_3 O_1(u_1) \rangle \right]. \end{aligned} \quad (4.33)$$

Let us now specify the signs of $\hat{\omega}_i$ and choose, for example, $\hat{\omega}_i > 0$. Since the positive frequency detectors annihilate the left vacuum (see Eq. (2.25)), we find that only one term survives,

$$\text{SSC}_{--} + \text{SSC}_{++} - \text{SSC}_{+-} - \text{SSC}_{-+} \stackrel{\hat{\omega}_i > 0}{=} \int du_1 du_2 e^{-i \sum_{k=1}^2 \hat{\omega}_k u_k} \langle O_4 O_3 O(u_1) O(u_2) \rangle. \quad (4.34)$$

This formula is completely general and it should hold for any choice of the detectors.

Compared to (4.30), the Wightman function on the right-hand side of (4.34) has different operator ordering. In a close analogy with (4.11), the integral over u_i in (4.34) can be expressed as the convolution of the Mellin amplitude $M(j_1, j_2)$ and the kernel $\tilde{K}_{SS}(j_1, j_2 | \omega_1, \omega_2, z)$. Going through the same steps as in Appendix E, we find that this kernel takes the form

$$\begin{aligned} \tilde{K}_{SS}(j_1, j_2 | \omega_1, \omega_2, z) &= \frac{(j_1 + j_2 - 1)(qn_1)(qn_2)}{2^{j_1+j_2-1}(n_1 n_2)^{j_1+j_2}} \int_0^{\hat{\omega}_1} ds_1 \int_0^{\hat{\omega}_2} ds_2 \\ &\quad \times [(\hat{\omega}_1 - s_1)s_2]^{-j_1} [s_1(\hat{\omega}_2 - s_2)]^{-j_2} [(q + n_1 s_1 + n_2 s_2)^2]^{j_1+j_2-2}. \end{aligned} \quad (4.35)$$

When integrated against the Mellin amplitudes (4.9) it gives zero both at weak and strong coupling. Indeed, from the integral representation (4.35) it follows that \tilde{K}_{SS} is an analytic function of j_2 for $\text{Re } j_2 < 0$. The same is true for the Mellin amplitudes (4.9). Closing the integration contour for $\text{Re } j_2 < 0$ we get that the integral on the right-hand side of (4.34) is zero. For more complicated Mellin amplitudes with extra poles at negative j_2 the integral in (4.34) will not vanish. This happens in particular for the correlations involving the energy detector. We checked that (4.34) correctly reproduces our results in these cases as well.

4.5 Bulk point singularity

The reader might have noticed something peculiar about the expressions for SSC at strong coupling, Eqs. (4.21) and (4.25). We see that there is a new type of singularity that appears in $\text{SSC}_{++}^{\text{strong}}$ at

$$\omega_1 + \omega_2 + \omega_2 \omega_1 z = 0, \quad (4.36)$$

but is absent in $\text{SSC}_{+-}^{\text{strong}}$. This locus cannot be reached for $\omega_{1,2} > 0$ and $0 < z < 1$ but a singularity appears if we analytically continue ω_2 to negative values. Using (4.31) and (4.32) we get

$$\text{SSC}_{++} \stackrel{\hat{\omega}_2 \leq 0}{=} \text{SSC}_{+-} - \int du_1 du_2 e^{-i \sum_{k=1}^2 \hat{\omega}_k u_k} \langle O_2(u_2) O_4 O_1(u_1) O_3 \rangle. \quad (4.37)$$

Given that $\text{SSC}_{+-}^{\text{strong}}$ is regular at (4.36), we deduce that the singular contribution is generated by the second term in (4.37).

Coming back to the four-point correlation function (4.1), it is a well-known fact that there are certain Lorentzian singularities which are present at strong coupling but are absent at weak coupling [34], namely the bulk point limit singularities [35]. It is therefore natural to conjecture that the singularity at (4.36) is nothing but an avatar of the bulk point singularity in the ω -deformed event shape. We will now demonstrate that this is indeed the case.

Recall that the emergence of the bulk point singularity in Mellin space is related to the behavior of the Mellin amplitude (4.6) in the limit $j_i \rightarrow \infty$ with j_1/j_2 fixed, see [36]. We see from (4.9) that

$$M^{\text{weak}}(\lambda j_1, \lambda j_2) = O(\lambda^{-2}), \quad M^{\text{strong}}(\lambda j_1, \lambda j_2) = O(\lambda), \quad (4.38)$$

and indeed at strong coupling the Mellin amplitude grows as $\lambda \rightarrow \infty$.

To make the connection between the bulk point singularity and the structure of the ω -deformed event shapes more direct, let us consider the following toy model

$$M_p(j_1, j_2) = (j_1 + j_2)^2 (1 + j_1 + j_2)^2 [j_1 j_2 (1 + j_1 + j_2)]^{p-2}, \quad (4.39)$$

where p is positive integer. This Mellin amplitude is polynomial for $p \geq 2$ and thus corresponds to a contact quartic interaction in the AdS dual theory [36]. In the large j limit we have $M_p(\lambda j_1, \lambda j_2) = O(\lambda^{3p-2})$.

We now want to compute the ω -deformed event shapes (4.11) for the toy Mellin amplitude (4.39). First, one can readily see that

$$\text{SSC}_{p,+-} = 0. \quad (4.40)$$

This immediately follows from the analytic properties of the kernel described in the previous sections. A more interesting case is $\text{SSC}_{p,++}$ for which we get

$$\text{SSC}_{p,++} = z^2 \frac{f_p(\omega_1, \omega_2)}{(\omega_1 + \omega_2 + \omega_1 \omega_2 z)^{6p-1}} + \dots \quad (4.41)$$

The details of the computation are given in Appendix G. For the first few values of p we find

$$\begin{aligned} f_1(\omega_1, \omega_2) &= -12(\omega_1 \omega_2)^2 (\omega_1 + \omega_2), \\ f_2(\omega_1, \omega_2) &= 6 \times 7! \times (\omega_1 \omega_2)^3 (\omega_1 + \omega_2)^2. \end{aligned} \quad (4.42)$$

As expected, the maximal power of the singularity in (4.41) is linked to the growth of the amplitude in the large λ limit.

Let us also write down the complete answer for $p = 2$

$$\text{SSC}_{p=2,++} = \frac{12\omega_1^3 \omega_2^3}{(\omega_1 + \omega_2 + \omega_1 \omega_2 z)^{11}} \sum_{k=0}^7 c_k(\omega_1, \omega_2) (\omega_1 + \omega_2 + \omega_1 \omega_2 z)^k, \quad (4.43)$$

where the explicit form of the coefficients $c_k(\omega_1, \omega_2)$ can be found in appendix G.

The function $\text{SSC}_{p=2,++}$ has interesting properties in the zero frequency limit $\omega_i \rightarrow 0$. If we consider $\omega_1 \rightarrow 0$ with ω_2 fixed the result vanishes as $O(\omega_1^3)$. If on the other hand we take both $\omega_i \rightarrow 0$ at the same rate, the result diverges as $\text{SSC}_{p=2,++}(z, \lambda\omega_1, \lambda\omega_2) \sim 1/\lambda$.

Another interesting subtlety related to polynomial Mellin amplitudes of the type (4.39) is that they lead to nontrivial distributional terms in the generalized event shapes which are supported at $\omega_i = 0$. Let us consider for simplicity $\omega_1 = 0$ and $p = 2$ (this example will also be relevant in section 7 when we discuss one-loop supergravity and stringy corrections). In this case we apply (4.11), (4.12) and (4.15) to get the following expression for the scalar-scalar correlation

$$\begin{aligned} \text{SSC}_{p=2}(0, \omega_2, z) &= \int \frac{dj dj_1}{(2\pi i)^2} \frac{\pi}{2 \sin \pi j} z^{-j} (1-z)^{j-1} j^2 (1+j)^2 (1+\omega_2)^{-j_1} \\ &= 2z^2(1-6z+6z^2)\delta(\omega_2). \end{aligned} \quad (4.44)$$

Here the j_1 integral was obtained by differentiating (4.28) with respect to ω .

5 $\mathcal{N} = 4$ supersymmetry Ward identities for the kernels

In the previous sections we used the known results for the four-point correlation functions of scalar half-BPS operators in $\mathcal{N} = 4$ SYM to compute the correlation between the scalar detectors SSC. In this section, we extend the consideration to more complicated correlations that involve charge and energy flow operators. According to their definition (2.22), they are light-ray operators built out of the R -current J_μ^R and the stress-energy tensor $T_{\mu\nu}$. As a consequence, their correlations can be expressed in terms of the four-point correlation functions of these operators.

We start in Section 5.1 with a brief review of the $\mathcal{N} = 4$ supersymmetry Ward identities for the four-point correlation functions and for the undeformed flow correlations, i.e. for $\omega_i = 0$. Then in Section 5.2 we give a summary of the new relationships between the Mellin kernels of the various flow correlations with the frequencies ω_i turned on. The detailed derivation is presented in Appendix H.

5.1 Stress-energy tensor multiplet in $\mathcal{N} = 4$ SYM

In what follows, we assume that the source and sink are given by scalar operators $\phi(3) \equiv O_{20'}(x_3, Y)$ and $\phi^\dagger(4) \equiv O_{20'}(x_4, \bar{Y})$ (see (3.31)) and consider the following correlation functions¹⁹

$$G_{J_1 J_2} = \langle \phi^\dagger(4) O_{J_1}(1) O_{J_2}(2) \phi(3) \rangle, \quad (5.1)$$

where $O_J(i) \equiv O_J(x_i)$ denotes an operator with spin J whose Lorentz indices are projected on the light cone,

$$O_{J=1}(i) = \bar{n}_i^\mu J_\mu^R(x_i), \quad O_{J=2}(i) = \bar{n}_i^\mu \bar{n}_i^\nu T_{\mu\nu}(x_i), \quad (5.2)$$

¹⁹For definiteness we always assume that $J_1 \geq J_2$.

and $O_{J=0}$ was defined in (3.32). In a generic CFT, the correlation functions (5.1) are very complicated and are not related to each other.

A unique feature of $\mathcal{N} = 4$ SYM is that the operators (5.2) belong to the same stress-tensor supermultiplet. As a result, their correlation functions are related to each other by $\mathcal{N} = 4$ superconformal Ward identities. Solving them one can express (5.1) in terms of the simplest four-point function involving scalar operators only [20, 21]. The correlation functions (5.1) have a rather complicated R-symmetry structure. It corresponds to the overlap of the tensor product of two real $SO(6) \sim SU(4)$ representations $\mathbf{20}' \times \mathbf{20}' = \mathbf{1} + \mathbf{15} + \mathbf{20}' + \mathbf{84} + \mathbf{105} + \mathbf{175}$ for the scalar source (ϕ) and sink (ϕ^\dagger), and that for the detectors O_J , for example for two R-symmetry currents $\mathbf{15} \times \mathbf{15} = \mathbf{1} + \mathbf{15}_s + \mathbf{15}_a + \mathbf{20}' + \mathbf{45} + \overline{\mathbf{45}} + \mathbf{84}$. We are not going to study this rich structure in full generality. Instead, we will concentrate on a single R-symmetry channel in each correlation function, namely the one corresponding to the top value of the $SU(4)$ quadratic Casimir. In the example above this is the channel **84**. The reason for this choice is the remarkably simple relation between the various flow correlations in this channel for vanishing ω_i discovered in [17, 20] (see (5.12) below).

We wish to find out to what extent these relations are preserved in the case of interest $\omega_i \neq 0$. So, we concentrate on the preferred channel and show only the space-time dependence of the correlation functions, dropping the isotopic variables Y and S of Section 3.4. For instance, the all-scalar correlation function in the top Casimir channel **105** (denoted by $G^{(\mathbf{105})}$ in (4.1)) is

$$G_{00} = (x_{12}^2 x_{34}^2)^2 F(x). \quad (5.3)$$

Here the dependence on the coupling resides in the function $F(x)$ given by

$$F(x) = \frac{1}{(2\pi)^4} \frac{\Phi(u, v)}{uv(x_{12}^2 x_{34}^2)^4}, \quad u = \frac{x_{12}^2 x_{34}^2}{x_{13}^2 x_{24}^2}, \quad v = \frac{x_{23}^2 x_{14}^2}{x_{13}^2 x_{24}^2}, \quad (5.4)$$

where $\Phi(u, v)$ is a function of the conformal cross-ratios u, v that admits the Mellin representation (4.6).²⁰

Following [21], in order to present explicit expressions for the higher-spin correlator components $G_{J_1 J_2}$, it is convenient to introduce a pair of auxiliary commuting Weyl spinors, $\lambda_{i,\alpha}$ and $\bar{\lambda}_{i,\dot{\alpha}}$, for each spinning operator in (5.1). They form the null vectors \bar{n}_i in (5.2),

$$\bar{n}_{i,\mu} \sigma_{\alpha\dot{\alpha}}^\mu = \lambda_{i,\alpha} \bar{\lambda}_{i,\dot{\alpha}}, \quad i = 1, 2, \quad (5.5)$$

where $\sigma^\mu = (1, \vec{\sigma})$ is the four-vector of Pauli matrices. The general form of the correlation function (5.1) is (up to normalization and only for the top Casimir channel), see Ref. [21],

$$G_{J_1 J_2} = \mathcal{D}_1^{J_1} \mathcal{D}_2^{J_2} \left[\mathcal{M}_{J_1, J_2} F(x) \right], \quad (5.6)$$

²⁰Note that in this section we do not consider the explicit rational (Born-level) terms in (4.3).

where \mathcal{M}_{J_1, J_2} is a homogenous polynomial in λ_1^α and λ_2^α of degree $2J_1$ and $2J_2$, respectively. \mathcal{D}_i is a differential operator acting both on the coordinates of the operator x_i and the spinors λ_i ,

$$\mathcal{D}_i = \bar{\lambda}_{i\dot{\alpha}}(\sigma^\mu)^{\dot{\alpha}\alpha} \frac{\partial}{\partial \lambda_i^\alpha} \frac{\partial}{\partial x_i^\mu}. \quad (5.7)$$

The functions \mathcal{M}_{J_1, J_2} are expressed in terms of three building blocks,

$$\begin{aligned} \mathcal{X}_{1[234]} &= \lambda_1^\alpha (x_{12})_{\alpha\dot{\alpha}} (\tilde{x}_{23})^{\dot{\alpha}\beta} (x_{34})_{\beta\dot{\gamma}} (\tilde{x}_{41})^{\dot{\gamma}\delta} \lambda_{1,\delta} \equiv \langle 1 | x_{12} \tilde{x}_{23} x_{34} \tilde{x}_{41} | 1 \rangle, \\ \mathcal{X}_{[12]i} &= \lambda_1^\alpha (x_{1i})_{\alpha\dot{\alpha}} (\tilde{x}_{i2})^{\dot{\alpha}\beta} \lambda_{2,\beta} \equiv \langle 1 | x_{1i} \tilde{x}_{i2} | 2 \rangle, \quad (i = 3, 4), \end{aligned} \quad (5.8)$$

as follows:

$$\begin{aligned} \mathcal{M}_{0,0} &= 1, & \mathcal{M}_{1,0} &= x_{12}^2 x_{34}^2 \mathcal{X}_{1[234]}, \\ \mathcal{M}_{2,0} &= (\mathcal{X}_{1[234]})^2, & \mathcal{M}_{1,1} &= x_{12}^2 x_{34}^2 \mathcal{X}_{[12]3} \mathcal{X}_{[12]4}, \\ \mathcal{M}_{2,1} &= \mathcal{X}_{1[234]} \mathcal{X}_{[12]3} \mathcal{X}_{[12]4}, & \mathcal{M}_{2,2} &= (\mathcal{X}_{[12]3} \mathcal{X}_{[12]4})^2. \end{aligned} \quad (5.9)$$

As explained in Section 4, we can use the correlation functions $G_{J_1 J_2}$ to obtain the various flow correlations. To this end, we have to apply the transformations specified in (2.22) to the operators at points 1 and 2. This amounts to sending both operators to the celestial sphere in the direction of the null vectors n_i , that is $x_i = r_i n_i + \alpha_i \bar{n}_i$ with $r_i \rightarrow \infty$, and integrating along the light-rays \bar{n}_i with the exponential weight $e^{-i(n_i \bar{n}_i) \hat{\omega}_i \alpha_i}$. As a result the operators at points 1 and 2 in the four-point function (5.1) are converted into flow operators and the correlator becomes a function of the two sets of detector variables $(n_i, \hat{\omega}_i)$ and of the separation between the source and sink x_{34} . This is followed by a Fourier transform to momentum space, $x_{34} \rightarrow q$. In the simplest case of SSC, i.e. $J_1 = J_2 = 0$, the result is the convolution of the Mellin amplitude $M(j_1, j_2)$ and the detector kernel $K_{\text{SS}}(j_1, j_2 | z, \omega_1, \omega_2)$ (see Eq. (4.11)). It is important to remember that the dynamical information (i.e. the coupling dependence) resides in the Mellin amplitude while the kernel is universal, so it applies to both weak and strong coupling.

Because the various correlation functions (5.6) are determined by the same function $\Phi(u, v)$, we expect that the same Mellin representation (4.11) should hold for the two-point correlations of flow operators with arbitrary spin, schematically

$$\text{XYC}(\omega_1, \omega_2, z) = \int \frac{dj_1 dj_2}{(2\pi i)^2} K_{\text{XY}}(j_1, j_2 | z, \omega_1, \omega_2) M(j_1, j_2). \quad (5.10)$$

Here X and Y stand for the scalar (S), charge (Q) or energy (E) flow operators. The kernels K_{XY} are coupling-independent and have a fixed form for each pair of detectors. They are functions of the scaling variable z (the angle between the detectors) and the energies ω_i transferred by the detectors.

The special form of the correlation functions (5.6) is dictated by $\mathcal{N} = 4$ superconformal symmetry. It is natural to ask whether analogous relations exist between the correlations (5.10). Indeed, in Ref. [20] it was shown that for $\omega_i = 0$ the correlation of two flow operators of spins J_1, J_2 in the top $SU(4)$ Casimir channel, before the final Fourier transform $x \rightarrow q$,²¹ is a *total space-time derivative* of the fundamental scalar-scalar one (for $J_1 \geq J_2$):

$$\frac{(\square_x)^{J_2} (n_2 \partial_x)^{J_1 - J_2}}{2^{J_1 - 1} (n_1 n_2)^{J_1 + 1}} \left(\frac{\mathcal{G}(\gamma)}{x^2} \right) = \frac{2^{J_2 + 1} (x n_2)^{J_1 - J_2}}{(n_1 n_2)^{J_1 + 1} (x^2)^{J_1 + 1}} \frac{d^{J_1}}{d\gamma^{J_1}} [(1 - \gamma)^{J_1} \gamma^{J_2} \mathcal{G}^{(J_2)}(\gamma)] . \quad (5.11)$$

Here $\gamma = 2(xn_1)(xn_2)/(x^2(n_1n_2))$ is the Lorentz-invariant and dimensionless angle variable. The function $\mathcal{G}(\gamma)$ contains the coupling constant dependence. After the Fourier transform $x \rightarrow q$ the left-hand side of (5.11) gives rise to a very simple relation between the corresponding kernels K_{XY} in (5.10). Stripping off the kinematic prefactor $\sim (q^2)^{J_2} (qn_2)^{J_1 - J_2} / (n_1 n_2)^{J_1 + 1}$ (i.e., the Fourier transform of the derivatives on the left-hand side of (5.11)), and replacing it with the factor $\sim (q^2)^{J_1 + J_2} / ((qn_1)^{J_1 + 1} (qn_2)^{J_2 + 1})$ from the definition (2.52), one finds

$$K_{XY}(j_1, j_2|z, 0, 0) = z^{-J_X} K_{SS}(j_1, j_2|z, 0, 0) , \quad (5.12)$$

where $J_X \geq J_Y$. In application to (5.10) this implies that for $\omega_i = 0$ all the flow correlations are given by the same universal function of z , up to an overall power of z .

5.2 Summary of the relationships between the kernels for $\omega_i \neq 0$

Below we show that for $\omega_i \neq 0$ the relation (5.12) is generalized in the form of differential operators expressing each K_{XY} in terms of the basic scalar one K_{SS} :

$$K_{XY}(j_1, j_2|z, \omega_1, \omega_2) = z^{-J_X} \sum_{p,q=0}^2 C_{XY}^{p,q}(j_1, j_2|z, \omega_1, \omega_2) \partial_{\omega_1}^p \partial_{\omega_2}^q K_{SS}(j_1, j_2|z, \omega_1, \omega_2) , \quad (5.13)$$

where $J_X \geq J_Y$ and the coefficients C_{XY} are polynomials in z and ω_i and rational functions of the Mellin parameters j_1 and j_2 . The order of the differential operator is at most 2 in each variable, depending on the choice of the detectors.

Here we list some of these non-vanishing coefficients:

(i) Charge-scalar correlation:

$$C_{QS}^{0,0} = 1 + \frac{j_2 \omega_1 z}{j_1 + j_2} , \quad C_{QS}^{1,0} = \frac{\omega_1 (\omega_1 z + 1)}{2(j_1 + j_2)} , \quad C_{QS}^{0,1} = -\frac{\omega_1 (\omega_2 z + 1)}{2(j_1 + j_2)} ; \quad (5.14)$$

(ii) Charge-charge correlation:

$$C_{QQ}^{0,0} = 1 + \frac{(j_1 + j_2)^2 (\omega_1 + \omega_2 + z\omega_1\omega_2) + j_1 j_2 (\omega_1 + \omega_2)}{2(j_1 + j_2)^2} ,$$

$$C_{QQ}^{1,0} = \frac{\omega_1 (2j_1 (\omega_1 + 1) + (j_1 + j_2) \omega_2 (\omega_1 z + 1))}{4(j_1 + j_2)^2} ,$$

²¹Without loss of generality we can set $x_3 \equiv x$ and $x_4 = 0$.

$$C_{\text{QQ}}^{0,1} = \frac{\omega_2 (2j_2 (\omega_2 + 1) + (j_1 + j_2) \omega_1 (\omega_2 z + 1))}{4 (j_1 + j_2)^2}; \quad (5.15)$$

(i) Energy-scalar correlation:

$$\begin{aligned} C_{\text{ES}}^{0,0} &= 1 + \frac{z\omega_1 [j_2 ((j_1 + j_2)^2 + j_1 - 1) \omega_1 z + ((j_1 + j_2)^2 - 1) (j_1 + 2j_2)]}{(j_1 + j_2 - 1) (j_1 + j_2) (j_1 + j_2 + 1)}, \\ C_{\text{ES}}^{1,0} &= \frac{\omega_1 (\omega_1 z + 1) [(\omega_1 z + 1) ((j_1 + j_2)^2 - 1) + 2j_1 j_2 \omega_1 z]}{(j_1 + j_2 - 1) (j_1 + j_2) (j_1 + j_2 + 1)}, \\ C_{\text{ES}}^{0,1} &= \frac{\omega_1 [j_2 \omega_1 z (\omega_2 z + 1) + ((j_1 + j_2)^2 - 1)(z - 1)]}{(j_1 + j_2 - 1) (j_1 + j_2) (j_1 + j_2 + 1)}, \\ C_{\text{ES}}^{1,1} &= \frac{\omega_1^2 [(j_1 + j_2 + 2) (1 + z\omega_1 + z\omega_2 + z^2 \omega_1 \omega_2) + (j_1 + j_2)(2z - 1) + z + 1]}{3 (j_1 + j_2 - 1) (j_1 + j_2) (j_1 + j_2 + 1)}, \\ C_{\text{ES}}^{2,0} &= \frac{\omega_1^2 (z\omega_1 + 1)^2}{6 (j_1 + j_2) (j_1 + j_2 + 1)}, \quad C_{\text{ES}}^{0,2} = \frac{\omega_1^2 (z\omega_2 + 1)^2}{6 (j_1 + j_2) (j_1 + j_2 + 1)}. \end{aligned} \quad (5.16)$$

We see that setting $\omega_i = 0$ reproduces the relations (5.12). The differential operators (5.13) for EQC and EEC are presented in the ancillary file. The detailed derivation of the various differential operators from the $\mathcal{N} = 4$ supersymmetry Ward identity (5.6) is explained in Appendix H.

Another interesting result of the above analysis is the observation that the basic kernel K_{SS} satisfies a simple homogeneous partial differential equation:

$$\begin{aligned} &\left[j_1 j_2 (j_1 (\omega_1 + \omega_2 + \omega_2 \omega_1 z) + j_2 (\omega_1 + \omega_2 + \omega_2 \omega_1 z) - \omega_1 - \omega_2) \right. \\ &+ j_1 \omega_1 ((j_1 + j_2 - 1) (\omega_1 + 1) + (j_1 + j_2) \omega_2 (\omega_1 z + 1)) \partial_{\omega_1} \\ &+ j_2 \omega_2 ((j_1 + j_2 - 1) (\omega_2 + 1) + (j_1 + j_2) \omega_1 (\omega_2 z + 1)) \partial_{\omega_2} \\ &\left. + (j_1 + j_2) \omega_1 \omega_2 (\omega_1 + \omega_2 + \omega_2 \omega_1 z + 1) \partial_{\omega_1} \partial_{\omega_2} \right] K_{\text{SS}}(j_1, j_2 | z, \omega_1, \omega_2) = 0. \end{aligned} \quad (5.17)$$

Its solutions are discussed in Appendix H.

We remark that the differential operators that relate the various kernels depend on the Mellin parameters j_1, j_2 , so they do not commute with the Mellin integral (5.10). Consequently, the event shapes (5.10) are not related to each other in a simple way, except for two special cases discussed in the next subsection.

5.3 Relationship between generalized event shapes in special cases

We might ask the question what happens if we switch off one of the frequencies? It turns out that the relations between the kernels described above simplify dramatically. The differential operators (5.13) are reduced to simple factors *independent of the Mellin parameters j_1, j_2* . Consequently, we can establish very simple relations between the Mellin integrals (5.10), i.e. between the flow correlations, and not only between the kernels.

Vanishing frequency $\omega_1 = 0$

Let us start with the asymmetric correlations QSC, ESC and EQC. From (5.14) and (5.16) it is obvious that setting $\omega_1 = 0$ trivializes the differential operators, reducing them to 1. The situation is similar for EQC. Denoting the ratio

$$r_{XY}(z, \omega_2) = \frac{K_{XY}(j_1, j_2|z, 0, \omega_2)}{K_{SS}(j_1, j_2|z, 0, \omega_2)}, \quad (5.18)$$

we find

$$r_{QS} = \frac{1}{z}, \quad r_{ES} = \frac{1}{z^2}, \quad r_{EQ} = \frac{1}{z^2} \left(1 + \frac{\omega_2}{2}\right). \quad (5.19)$$

At the same time, setting $\omega_2 = 0$ in (5.14) leaves the derivative $\partial_{\omega_2} K_{SS}|_{\omega_2=0}$ in place, and we do not observe any substantial simplification of the differential operator. The same applies to the other two asymmetric correlations ESC and EQC.

The two symmetric correlations QQC and EEC also undergo drastic simplifications if we set $\omega_1 = 0$ (or similarly $\omega_2 = 0$, due to the symmetry). Take for example QQC: putting $\omega_1 = 0$ in (5.15) we get

$$C_{QQ}^{0,0} = 1 + \frac{(j_1^2 + 3j_2j_1 + j_2^2)\omega_2}{2(j_1 + j_2)^2}, \quad C_{QQ}^{0,1} = \frac{j_2\omega_2(\omega_2 + 1)}{2(j_1 + j_2)^2}, \quad C_{QQ}^{1,0} = 0. \quad (5.20)$$

This is not all, we still have to explore the consequences of the differential equation (5.17), which now reads simply

$$[(\omega_2 + 1)\partial_{\omega_2} + j_1]K_{SS}(z, \omega_1 = 0, \omega_2) = 0. \quad (5.21)$$

This equation allows us to eliminate the term with ∂_{ω_2} in (5.13),

$$C_{QQ}^{0,0} - \frac{j_1}{\omega_2 + 1}C_{QQ}^{0,1} = 1 + \frac{\omega_2}{2}, \quad (5.22)$$

so that the differential operator (5.13) collapses to (compare with the third relation in (5.19))

$$r_{QQ} = \frac{1}{z} \left(1 + \frac{\omega_2}{2}\right). \quad (5.23)$$

The analysis of the differential operator for EEC yields an equally simple relation,

$$r_{EE} = \frac{1}{z^2} \left(1 + \omega_2 + \frac{\omega_2^2}{6}\right). \quad (5.24)$$

As mentioned earlier, the remarkable feature of the relations (5.19), (5.23) and (5.24) is that they do not depend on the Mellin parameters j_i . Inserting them in (5.10) yields equivalent relations between the various event shapes,

$$\frac{XYC(0, \omega_2, z)}{SSC(0, \omega_2, z)} = r_{XY}, \quad J_X \geq J_Y. \quad (5.25)$$

Most importantly, these relations hold both perturbatively (at weak and at strong coupling) and nonperturbatively (at finite coupling).

Event shapes XYC_{+-} at strong coupling

As explained in Section 4.1, the computation of the event shape $\text{SSC}_{+-}^{\text{strong}}$ is drastically simplified by using the integral representation (4.16) of the kernel K_{SS}^{+-} . The expression in (4.16) is analytic in j_1, j_2 , while the Mellin amplitude M^{strong} from (4.9) has simple poles. Consequently, the Mellin integral over j_2 with $j_1 + j_2$ fixed amounts to evaluating (4.16) at $j_2 = 0$. To this end we have to analyze the behavior of the factors $\Gamma(-s)\Gamma(j_2 + s)/\Gamma(j_2)$ under the s -integral, when $s, j_2 \rightarrow 0$. The pole in $\Gamma(j_2 + s)$ at $s = -j_2 \rightarrow 0$ lies outside the contour whereas the pole in $\Gamma(-s)$ at $s = 0$ has the trivial residue -1 . After setting $j_2 = 0$, the only remaining ω dependence is in the factor $(1 + \omega_2)^{-j_1}$ in front of the integral. The Mellin integral over j_1 is easily done by residues resulting in the simple expression (4.21).

The same scenario applies when we act with the differential operators (5.13). We observe another drastic simplification, namely the Mellin integral over j_2 turns the differential operators into simple factors *independent of j_1* . They go through the j_1 -integral and the resulting event shapes $\text{XYC}_{+-}^{\text{strong}}$ are obtained by multiplying $\text{SSC}_{+-}^{\text{strong}}$ by these factors.

Let us illustrate the mechanism on the simplest example of $\text{QSC}_{+-}^{\text{strong}}$. When the differential operator (5.13) with coefficients from (5.14) acts under the integral in (4.16), it produces terms $\sim s \rightarrow 0$. Similarly, its action on the factor $(1 + \omega_1)^{-j_2}$ in front of the integral produces terms $\sim j_2 \rightarrow 0$. So, we just need to evaluate

$$\begin{aligned} & \frac{1}{(1 + \omega_2)^{-j_1}} \left[\frac{1}{z} \sum_{q=0}^2 C_{\text{QS}}^{0,q}(j_1, 0 | \omega_1, \omega_2) \partial_{\omega_2}^q (1 + \omega_2)^{-j_1} \right] \\ &= \frac{1}{(1 + \omega_2)^{-j_1}} \left[\frac{1}{z} \left(1 - \frac{1}{2j_1} \omega_1 (\omega_2 z + 1) \partial_{\omega_2} \right) (1 + \omega_2)^{-j_1} \right] = \frac{\omega_1 + 2\omega_2 + \omega_2 \omega_1 z + 2}{2z(\omega_2 + 1)}. \end{aligned} \quad (5.26)$$

As explained above, this result is independent of j_1 , so it immediately gives the ratio of the event shapes $\text{QSC}_{+-}^{\text{strong}}/\text{SSC}_{+-}^{\text{strong}}$ listed in (6.22) and (6.20), respectively. The calculation with all the other differential operators (5.13) is equally simple and we obtain all the event shapes $\text{XYC}_{+-}^{\text{strong}}$ from Section 6.2. The non-trivial feature of the operators (5.13) is that their action on $(1 + \omega_2)^{-j_1}$ gives a result independent of j_1 .

Note that the situation is different if we employ the Mellin amplitude M^{weak} from (4.9). In order to evaluate the residue at the double pole $j_2 = 0$, we need to consider the complete sequence of poles of the integrand in (4.16) at $s = 0, 1, 2, \dots$. This results in an infinite sum which, together with that originating from the poles at $j_1 = -1, -2, -3, \dots$ gives rise to the logs in (4.20). Further, the action of the differential operators (5.13) on the kernel (4.16) modifies the residue at the double pole $j_2 = 0$, so the result is not as simple as in (5.26).

6 Summary of the generalized event shapes in $\mathcal{N} = 4$ SYM

In this section, we present the explicit expressions for the two-point correlations (2.41) in $\mathcal{N} = 4$ SYM at weak and strong coupling.²² Following (2.53) we distinguish six different functions XYC with $X, Y = \{S, Q, E\}$.

6.1 Weak coupling

At weak coupling, the correlations take the form

$$\text{XYC}(\omega_1, \omega_2, z) = \text{XYC}^{(0)} + \frac{a}{4} \text{XYC}^{(1)} + O(a^2), \quad (6.1)$$

where $a = g^2 N / (4\pi^2)$. In the Born approximation, the correlations are given by (3.39) and (3.40). The functions $\text{XYC}^{(0)}$ vanish for $0 < z < 1$ and $\omega_i > -1$. To one-loop order, depending on the signs of ω_1 and ω_2 we find the following expressions:

Scalar-scalar correlation

$$\text{SSC}_{+-}^{(1)} = \frac{\log\left(\frac{\omega_2 z + 1}{1 - z}\right)}{1 - z} + \frac{(\omega_2 + 1) z \log\left(\frac{\omega_1 + \omega_2 + \omega_2 \omega_1 z + 1}{(\omega_2 + 1)^2}\right)}{2(1 - z)(\omega_2 z + 1)} \quad (6.2)$$

$$\text{SSC}_{++}^{(1)} = \frac{\log\left(\frac{1}{1 - z}\right)}{1 - z} + \frac{(\omega_1 + 1) z \log\left(\frac{\omega_1 + \omega_2 + \omega_1 \omega_2 z + 1}{\omega_1 + 1}\right)}{2(1 - z)(\omega_1 z + 1)} + \frac{(\omega_2 + 1) z \log\left(\frac{\omega_1 + \omega_2 + \omega_1 \omega_2 z + 1}{\omega_2 + 1}\right)}{2(1 - z)(\omega_2 z + 1)} \quad (6.3)$$

Charge-scalar correlation

$$\text{QSC}_{+-}^{(1)} = \frac{\left(\frac{\omega_1 z}{2} + 1\right) \log\left(\frac{\omega_2 z + 1}{1 - z}\right)}{(1 - z)z} + \frac{(\omega_1 + 2\omega_2 + \omega_2 \omega_1 z + 2) \log\left(\frac{\omega_1 + \omega_2 + \omega_2 \omega_1 z + 1}{(\omega_2 + 1)^2}\right)}{4(1 - z)(\omega_2 z + 1)} \quad (6.4)$$

$$\text{QSC}_{-+}^{(1)} = \frac{\left(\frac{\omega_1 z}{2} + 1\right) \log\left(\frac{\omega_1 z + 1}{1 - z}\right)}{(1 - z)z} + \frac{(\omega_1 + 2) \log\left(\frac{\omega_1 + \omega_2 + \omega_2 \omega_1 z + 1}{(\omega_1 + 1)^2}\right)}{4(1 - z)} \quad (6.5)$$

$$\begin{aligned} \text{QSC}_{++}^{(1)} &= \frac{\left(1 + \frac{\omega_1 z}{2}\right) \log\left(\frac{1}{1 - z}\right)}{(1 - z)z} + \frac{(\omega_1 + 2) \log\left(\frac{\omega_1 + \omega_2 + \omega_2 \omega_1 z + 1}{\omega_1 + 1}\right)}{4(1 - z)} \\ &+ \frac{(\omega_1(1 + \omega_2 z) + 2(\omega_2 + 1)) \log\left(\frac{\omega_1 + \omega_2 + \omega_2 \omega_1 z + 1}{\omega_2 + 1}\right)}{4(1 - z)(\omega_2 z + 1)} \end{aligned} \quad (6.6)$$

Charge-charge correlation

$$\text{QQC}_{+-}^{(1)} = \frac{(\omega_1 \omega_2 z + 2(\omega_1 + \omega_2 + 2)) \log\left(\frac{\omega_2 z + 1}{1 - z}\right)}{4(1 - z)z}$$

²²For the reader's convenience, we presented the expressions for all two-point correlations in a Mathematica readable format in the ancillary file included with an arXiv submission.

$$+ \frac{(\omega_2 + 2)(\omega_2(\omega_1 z + 2) + \omega_1 + 2) \log \left(\frac{\omega_1 \omega_2 z + \omega_1 + \omega_2 + 1}{(\omega_2 + 1)^2} \right)}{8(1 - z)(\omega_2 z + 1)} \quad (6.7)$$

$$\begin{aligned} \text{QQC}_{++}^{(1)} &= \frac{(2\omega_1 + 2\omega_2 + \omega_2 \omega_1 z + 4) \log \left(\frac{1}{1-z} \right)}{4(1 - z)z} \\ &+ \frac{(\omega_1 + 2)(\omega_2(1 + \omega_1 z) + 2(\omega_1 + 1)) \log \left(\frac{\omega_1 + \omega_2 + \omega_2 \omega_1 z + 1}{\omega_1 + 1} \right)}{8(1 - z)(\omega_1 z + 1)} \\ &+ \frac{(\omega_2 + 2)(\omega_1(1 + \omega_2 z) + 2(\omega_2 + 1)) \log \left(\frac{\omega_1 + \omega_2 + \omega_2 \omega_1 z + 1}{\omega_2 + 1} \right)}{8(1 - z)(\omega_2 z + 1)} \end{aligned} \quad (6.8)$$

Energy-scalar correlation

$$\begin{aligned} \text{ESC}_{+-}^{(1)} &= \frac{(\omega_1^2 z^2 + 6\omega_1 z + 6) \log \left(\frac{\omega_2 z + 1}{1-z} \right)}{6(1 - z)z^2} - \frac{\omega_1^2 \log \left(\frac{(\omega_2 + 1)z}{\omega_2 z + 1} \right)}{6(\omega_2 + 1)z} \\ &+ \frac{(6(\omega_2 + 1)^2 + 6\omega_1(\omega_2 + 1)(\omega_2 z + 1) + (\omega_1 + \omega_2 \omega_1 z)^2) \log \left(\frac{\omega_1 + \omega_2 + \omega_2 \omega_1 z + 1}{(\omega_2 + 1)^2} \right)}{12(\omega_2 + 1)(1 - z)z(\omega_2 z + 1)} \end{aligned} \quad (6.9)$$

$$\begin{aligned} \text{ESC}_{-+}^{(1)} &= \frac{(\omega_1^2 z^2 + 6\omega_1 z + 6) \log \left(\frac{\omega_1 z + 1}{1-z} \right)}{6(1 - z)z^2} - \frac{\omega_1^2 \log \left(\frac{(\omega_1 + 1)z}{\omega_1 z + 1} \right)}{6(\omega_1 + 1)z} \\ &+ \frac{(\omega_1^2 + 6\omega_1 + 6)(\omega_1 z + 1) \log \left(\frac{\omega_1 + \omega_2 + \omega_2 \omega_1 z + 1}{(\omega_1 + 1)^2} \right)}{12(\omega_1 + 1)(1 - z)z} \end{aligned} \quad (6.10)$$

$$\begin{aligned} \text{ESC}_{++}^{(1)} &= \frac{(\omega_1^2 z^2 + 6\omega_1 z + 6) \log \left(\frac{1}{1-z} \right)}{6(1 - z)z^2} \\ &+ \frac{(\omega_1^2 + 6\omega_1 + 6)(\omega_1 z + 1) \log \left(\frac{\omega_1 + \omega_2 + \omega_2 \omega_1 z + 1}{\omega_1 + 1} \right)}{12(\omega_1 + 1)(1 - z)z} \\ &+ \frac{(6(\omega_2 + 1)^2 + 6\omega_1(\omega_2 + 1)(\omega_2 z + 1) + \omega_1^2(\omega_2 z + 1)^2) \log \left(\frac{\omega_1 + \omega_2 + \omega_2 \omega_1 z + 1}{\omega_2 + 1} \right)}{12(\omega_2 + 1)(1 - z)z(\omega_2 z + 1)} \\ &- \omega_1^2 \left(\frac{\log \left(\frac{(\omega_1 + 1)^2 \omega_2 z}{\omega_1(\omega_1 + \omega_2 + \omega_2 \omega_1 z + 1)} \right)}{12(\omega_1 + 1)z} + \frac{\log \left(\frac{\omega_1(\omega_2 + 1)^2 z}{\omega_2(\omega_1 + \omega_2 + \omega_2 \omega_1 z + 1)} \right)}{12(\omega_2 + 1)z} \right) \end{aligned} \quad (6.11)$$

Energy-charge correlation

$$\begin{aligned} \text{EQC}_{+-}^{(1)} &= \frac{(6(\omega_2 + 2) + \omega_1(z(2\omega_1 + 6\omega_2 + \omega_2 \omega_1 z + 6) + 6)) \log \left(\frac{\omega_2 z + 1}{1-z} \right)}{12(1 - z)z^2} \\ &+ \frac{(\omega_2 + 2)(\omega_2 + 1) \left(6 + 6 \frac{\omega_1(\omega_2 z + 1)}{(\omega_2 + 1)} + \frac{\omega_1^2(1 + \omega_2 z)^2}{(\omega_2 + 1)^2} \right) \log \left(\frac{\omega_1 + \omega_2 + \omega_2 \omega_1 z + 1}{(\omega_2 + 1)^2} \right)}{24(1 - z)z(\omega_2 z + 1)} \end{aligned}$$

$$+ \frac{\omega_2 \omega_1^2 \log \left(\frac{z(\omega_2+1)}{\omega_2 z+1} \right)}{12z(\omega_2+1)} \quad (6.12)$$

$$\begin{aligned} \text{EQC}_{-+}^{(1)} &= \frac{(6(\omega_2+2) + \omega_1(z(2\omega_1+6\omega_2+\omega_2\omega_1 z+6)+6)) \log \left(\frac{\omega_1 z+1}{1-z} \right)}{12(1-z)z^2} \\ &+ \frac{(\omega_1^2+6\omega_1+6)(\omega_2+\omega_1(\omega_2 z+2)+2) \log \left(\frac{\omega_1+\omega_2+\omega_2\omega_1 z+1}{(\omega_1+1)^2} \right)}{24(\omega_1+1)(1-z)z} \\ &- \frac{\omega_2 \omega_1^2 \log \left(\frac{z(\omega_1+1)}{\omega_1 z+1} \right)}{12z(\omega_1+1)} \end{aligned} \quad (6.13)$$

$$\begin{aligned} \text{EQC}_{++}^{(1)} &= \frac{(6(\omega_2+2) + \omega_1(z(2\omega_1+6\omega_2+\omega_2\omega_1 z+6)+6)) \log \left(\frac{1}{1-z} \right)}{12(1-z)z^2} \\ &+ \frac{(\omega_1^2+6\omega_1+6)(\omega_2+\omega_1(\omega_2 z+2)+2) \log \left(\frac{\omega_1+\omega_2+\omega_2\omega_1 z+1}{\omega_1+1} \right)}{24(\omega_1+1)(1-z)z} \\ &+ \frac{(\omega_2+2)(6(\omega_2+1)^2+6\omega_1(\omega_2+1)(\omega_2 z+1)+\omega_1^2(\omega_2 z+1)^2) \log \left(\frac{\omega_1+\omega_2+\omega_2\omega_1 z+1}{\omega_2+1} \right)}{24(\omega_2+1)(1-z)z(\omega_2 z+1)} \\ &- \omega_2 \omega_1^2 \left(\frac{\log \left(\frac{(\omega_1+1)^2 \omega_2 z}{\omega_1(\omega_1+\omega_2+\omega_2\omega_1 z+1)} \right)}{24(\omega_1+1)z} - \frac{\log \left(\frac{\omega_1(\omega_2+1)^2 z}{\omega_2(\omega_1+\omega_2+\omega_2\omega_1 z+1)} \right)}{24(\omega_2+1)z} \right) \end{aligned} \quad (6.14)$$

Energy-energy correlation

$$\begin{aligned} \text{EEC}_{+-}^{(1)} &= \frac{(\omega_1^2(\omega_2 z(\omega_2 z+6)+6) + 6\omega_1(\omega_2((\omega_2+3)z+3)+6) + 6(\omega_2(\omega_2+6)+6)) \log \left(\frac{\omega_2 z+1}{1-z} \right)}{36(1-z)z^2} \\ &+ \frac{(\omega_2+1)(\omega_2^2+6\omega_2+6) \left(\frac{\omega_1^2(\omega_2 z+1)^2}{(\omega_2+1)^2} + \frac{6\omega_1(\omega_2 z+1)}{\omega_2+1} + 6 \right) \log \left(\frac{\omega_1 \omega_2 z + \omega_1 + \omega_2 + 1}{(\omega_2+1)^2} \right)}{72(1-z)z(\omega_2 z+1)} \\ &- \frac{\omega_1^2 \omega_2^2}{36(\omega_2+1)z} \log \left(\frac{z(\omega_2+1)}{\omega_2 z+1} \right) \end{aligned} \quad (6.15)$$

$$\begin{aligned} \text{EEC}_{++}^{(1)} &= \frac{(6(\omega_1^2+6\omega_1+6) + \omega_2^2(\omega_1^2 z^2+6\omega_1 z+6) + 6\omega_2(\omega_1^2 z+3\omega_1(z+1)+6)) \log \left(\frac{1}{1-z} \right)}{36(1-z)z^2} \\ &+ \frac{(\omega_1+1)(\omega_1^2+6\omega_1+6) \left(\frac{\omega_2^2(\omega_1 z+1)^2}{(\omega_1+1)^2} + \frac{6\omega_2(\omega_1 z+1)}{\omega_1+1} + 6 \right) \log \left(\frac{\omega_1+\omega_2+\omega_2\omega_1 z+1}{\omega_1+1} \right)}{72(1-z)z(\omega_1 z+1)} \\ &+ \frac{(\omega_2+1)(\omega_2^2+6\omega_2+6) \left(\frac{\omega_1^2(\omega_2 z+1)^2}{(\omega_2+1)^2} + \frac{6\omega_1(\omega_2 z+1)}{\omega_2+1} + 6 \right) \log \left(\frac{\omega_1+\omega_2+\omega_2\omega_1 z+1}{\omega_2+1} \right)}{72(1-z)z(\omega_2 z+1)} \\ &- \omega_1^2 \omega_2^2 \left(\frac{\log \left(\frac{(\omega_1+1)^2 \omega_2 z}{\omega_1(\omega_1+\omega_2+\omega_2\omega_1 z+1)} \right)}{72(\omega_1+1)z} + \frac{\log \left(\frac{(\omega_2+1)^2 \omega_1 z}{\omega_2(\omega_1+\omega_2+\omega_2\omega_1 z+1)} \right)}{72(\omega_2+1)z} \right) \end{aligned}$$

$$- \omega_1^2 \omega_2^2 \frac{\log \left(\frac{z \left(\omega_1 \omega_2 z + \frac{1}{2} (\omega_1 + \omega_2 + \sqrt{(\omega_1 + \omega_2)^2 - 4\omega_1 \omega_2 z}) \right)^2}{\omega_1 \omega_2 (\omega_1 + \omega_2 + \omega_2 \omega_1 z + 1)} \right)}{12z \sqrt{(\omega_1 + \omega_2)^2 - 4\omega_1 \omega_2 z}} \quad (6.16)$$

The following comments are in order.

The above relations are valid for $0 < z < 1$ and $\omega_i > -1$. We verify that for $\omega_1 = \omega_2 = 0$ they simplify to

$$\text{XYC}^{(1)}(0, 0, z) = \frac{1}{(1-z)z^{J_X}} \log \left(\frac{1}{1-z} \right), \quad (6.17)$$

where $J_X \geq J_Y$. This relation is in agreement with the findings of Ref. [17].

For $\omega_1 = 0$ and nonzero ω_2 it is possible to show that the above expressions verify the relation (5.25). For nonzero ω_i , the first term in the above expressions for the correlations describes the elastic contribution discussed in Section 3.4. For the correlations SSC, QSC and QQC, the remaining terms describe the annihilation and production of particles by the detectors, depending on the sign of ω_i (see Section 3.4). In addition to such terms, the correlations ESC, EQC and EEC also contain terms that scale at small z as $(\log z)/z$. They are accompanied by powers of ω_1 and ω_2 and take the form

$$\text{EXC}^{(1)}(\omega_1, \omega_2, z) \stackrel{z \rightarrow 0}{\sim} \omega_1^2 \omega_2^{J_X} \times \frac{\log z}{z}, \quad (6.18)$$

where J_X is the spin of the detector $X = \{S, Q, E\}$. These additional terms come from the cross-talk between the detectors. For the energy-energy correlation (6.16), such terms are accompanied by a square-root $\sqrt{(\omega_1 + \omega_2)^2 - 4\omega_1 \omega_2 z}$. Its origin and physical interpretation are discussed in Appendix I.

We did not display the expressions for XYC_{--} and XXC_{-+} . They can be obtained by applying the crossing relation (2.56) to XYC_{++} and XXC_{+-} , respectively. Doing so, we examined the relation

$$\text{XYC}_{--} + \text{XYC}_{++} \stackrel{?}{=} \text{XXC}_{+-} + \text{XXC}_{-+}, \quad (6.19)$$

which was previously observed to hold for the scalar-scalar correlation (3.66). We found that it is satisfied for the correlations SSC, QSC and QQC, which do not receive contributions from the cross-talk between the detectors. At the same time, it is violated for the correlations involving the energy detector. As explained in Section 4.4, this can be understood using the general formula (4.34) and the properties of the corresponding kernels.

6.2 Strong coupling

At strong coupling, in the leading supergravity approximation, we find the correlations:

Scalar-scalar correlation

$$\text{SSC}_{+-} = \frac{z^2 (\omega_2 + 1)^2}{2 (\omega_2 z + 1)^3} \quad (6.20)$$

$$\begin{aligned} \text{SSC}_{++} = & \frac{z^2}{2} \left[\frac{(\omega_1 + 1)^2}{(\omega_1 z + 1)^3} + \frac{(\omega_2 + 1)^2}{(\omega_2 z + 1)^3} \right. \\ & - \frac{6\omega_1^2 \omega_2^2 (\omega_1 + \omega_2)}{(\omega_1 + \omega_2 + \omega_2 \omega_1 z)^5} - \frac{3\omega_1 (2\omega_2 \omega_1^2 + 2\omega_2^2 \omega_1 + \omega_1^2 + \omega_2^2) \omega_2}{(\omega_1 + \omega_2 + \omega_2 \omega_1 z)^4} \\ & \left. - \frac{\omega_2^2 \omega_1^3 + \omega_2^3 \omega_1^2 + 2\omega_2 \omega_1^3 + 2\omega_2^3 \omega_1 + \omega_1^3 + \omega_2^3}{(\omega_1 + \omega_2 + \omega_2 \omega_1 z)^3} \right] \end{aligned} \quad (6.21)$$

Charge-scalar correlation

$$\text{QSC}_{+-} = \frac{z (\omega_2 + 1) (\omega_1 + 2\omega_2 + \omega_2 \omega_1 z + 2)}{4 (\omega_2 z + 1)^3} \quad (6.22)$$

$$\text{QSC}_{-+} = \frac{z (\omega_1 + 1) (\omega_1 + 2)}{4 (\omega_1 z + 1)^2} \quad (6.23)$$

$$\begin{aligned} \text{QSC}_{++} = & \frac{z}{4} \left[\frac{(\omega_1 + 1) (\omega_1 + 2)}{(\omega_1 z + 1)^2} + \frac{(\omega_2 + 1) (\omega_1 + 2\omega_2 + \omega_2 \omega_1 z + 2)}{(\omega_2 z + 1)^3} \right. \\ & - \frac{6\omega_1^2 \omega_2 (\omega_1 + \omega_2)}{(\omega_1 + \omega_2 + \omega_2 \omega_1 z)^4} - \frac{2 (3\omega_2 \omega_1^2 + 3\omega_2^2 \omega_1 + \omega_1^2 + 2\omega_2^2) \omega_1}{(\omega_1 + \omega_2 + \omega_2 \omega_1 z)^3} \\ & \left. - \frac{\omega_2 \omega_1^3 + \omega_2^2 \omega_1^2 + 3\omega_2^2 \omega_1 + \omega_1^3 + 2\omega_2^2}{(\omega_1 + \omega_2 + \omega_2 \omega_1 z)^2} \right] \end{aligned} \quad (6.24)$$

Charge-charge correlation

$$\text{QQC}_{+-} = \frac{z (\omega_2 + 1) (\omega_2 + 2) (\omega_1 \omega_2 z + \omega_1 + 2\omega_2 + 2)}{8 (\omega_2 z + 1)^3} \quad (6.25)$$

$$\begin{aligned} \text{QQC}_{++} = & \frac{z}{16} \left[\frac{2 (\omega_1 + 1) (\omega_1 + 2) (2\omega_1 + \omega_2 + \omega_2 \omega_1 z + 2)}{(\omega_1 z + 1)^3} \right. \\ & + \frac{2 (\omega_2 + 1) (\omega_2 + 2) (\omega_1 + 2\omega_2 + \omega_2 \omega_1 z + 2)}{(\omega_2 z + 1)^3} \\ & - \frac{2 (\omega_2 \omega_1 + \omega_1 + \omega_2) (\omega_2 \omega_1^2 + \omega_2^2 \omega_1 - 2\omega_2 \omega_1 + 2\omega_1^2 + 2\omega_2^2)}{(\omega_1 + \omega_2 + \omega_2 \omega_1 z)^2} \\ & - \frac{4 (\omega_2^3 \omega_1^3 + 7\omega_2^2 \omega_1^3 + 7\omega_2 \omega_1^3 + 7\omega_2^3 \omega_1^2 + 7\omega_2^3 \omega_1 + 2\omega_1^3 + 2\omega_2^3)}{(\omega_1 + \omega_2 + \omega_2 \omega_1 z)^3} \\ & - \frac{24\omega_1 \omega_2 (\omega_2^2 \omega_1^2 + 3\omega_2 \omega_1^2 + 3\omega_2^2 \omega_1 + \omega_1^2 + \omega_2^2)}{(\omega_1 + \omega_2 + \omega_2 \omega_1 z)^4} \\ & \left. - \frac{24\omega_1^2 \omega_2^2 (\omega_1 \omega_2 + 2(\omega_1 + \omega_2))}{(\omega_1 + \omega_2 + \omega_2 \omega_1 z)^5} \right] \end{aligned} \quad (6.26)$$

Energy-scalar correlation

$$\text{ESC}_{+-} = \frac{(\omega_2 + 1)^2 \left(\frac{\omega_1^2 (\omega_2 z + 1)^2}{(\omega_2 + 1)^2} + \frac{6\omega_1 (\omega_2 z + 1)}{\omega_2 + 1} + 6 \right)}{12 (\omega_2 z + 1)^3} \quad (6.27)$$

$$\text{ESC}_{-+} = \frac{(\omega_1^2 + 6\omega_1 + 6)}{12(\omega_1 z + 1)} \quad (6.28)$$

$$\begin{aligned} \text{ESC}_{++} = & \frac{1}{12} \left[\frac{(\omega_1^2 + 6\omega_1 + 6)}{(\omega_1 z + 1)} + \frac{(\omega_2 + 1)^2}{(\omega_2 z + 1)^3} \left(\frac{\omega_1^2 (\omega_2 z + 1)^2}{(\omega_2 + 1)^2} + \frac{6\omega_1 (\omega_2 z + 1)}{\omega_2 + 1} + 6 \right) \right. \\ & - \frac{\omega_1^2}{z(\omega_1 + \omega_2 + \omega_2 \omega_1 z)} - \frac{(\omega_1^3 + (\omega_1^2 + 6\omega_1 + 6)\omega_2)}{(\omega_1 + \omega_2 + \omega_2 \omega_1 z)} \\ & \left. - \frac{(6\omega_1^2 + (\omega_1^2 + 6\omega_1 + 6)\omega_2) \omega_1}{(\omega_1 + \omega_2 + \omega_2 \omega_1 z)^2} - \frac{2(\omega_2 \omega_1 + 3(\omega_1 + \omega_2)) \omega_1^2}{(\omega_1 + \omega_2 + \omega_2 \omega_1 z)^3} \right] \end{aligned} \quad (6.29)$$

Energy-charge correlation

$$\text{EQC}_{+-} = \frac{(\omega_2 + 2) (\omega_2 + 1)^2 \left(\frac{\omega_1^2 (\omega_2 z + 1)^2}{(\omega_2 + 1)^2} + \frac{6\omega_1 (\omega_2 z + 1)}{\omega_2 + 1} + 6 \right)}{24 (\omega_2 z + 1)^3} \quad (6.30)$$

$$\text{EQC}_{-+} = \frac{(\omega_1^2 + 6\omega_1 + 6) (2 + 2\omega_1 + \omega_2 + \omega_1 \omega_2 z)}{24 (\omega_1 z + 1)^2} \quad (6.31)$$

$$\begin{aligned} \text{EQC}_{++} = & \frac{1}{24} \left[\frac{4(\omega_2 + 2) (\omega_2 + 1)^2}{(\omega_2 z + 1)^3} \left(\frac{\omega_1^2 (\omega_2 z + 1)^2}{(\omega_2 + 1)^2} + \frac{6\omega_1 (\omega_2 z + 1)}{\omega_2 + 1} + 6 \right) \right. \\ & + \frac{(\omega_1^2 + 6\omega_1 + 6) (2 + 2\omega_1 + \omega_2 + \omega_1 \omega_2 z)}{(\omega_1 z + 1)^2} \\ & - \frac{\omega_1^2 \omega_2 (\omega_1 - \omega_2) (2 + \omega_1 + \omega_2)}{z(\omega_1 + \omega_2 + \omega_1 \omega_2 z)^3} - \frac{12\omega_1^2 \omega_2 (2\omega_1 \omega_2 + 3(\omega_1 + \omega_2))}{(\omega_1 + \omega_2 + \omega_2 \omega_1 z)^4} \\ & + \frac{(\omega_2^2 \omega_1^3 - (\omega_2 (\omega_2 (\omega_2 + 24) + 54) + 12) \omega_1^2 - 54\omega_2^2 \omega_1 - 24\omega_2^2) \omega_1}{(\omega_1 + \omega_2 + \omega_2 \omega_1 z)^3} \\ & - \frac{20\omega_2 \omega_1^3 + 12\omega_1^3 + 2(\omega_1 + 2) (2\omega_1 (\omega_1 + 3) + 3) \omega_2^2}{(\omega_1 + \omega_2 + \omega_2 \omega_1 z)^2} \\ & \left. - \frac{(\omega_2 + 2) \omega_1^3 + (\omega_1^2 + 6\omega_1 + 6) \omega_2^2}{\omega_1 + \omega_2 + \omega_2 \omega_1 z} \right] \end{aligned} \quad (6.32)$$

Energy-energy correlation

$$\text{EEC}_{+-} = \frac{(\omega_2 + 1)^2 (\omega_2^2 + 6\omega_2 + 6) \left(\frac{\omega_1^2 (\omega_2 z + 1)^2}{(\omega_2 + 1)^2} + \frac{6\omega_1 (\omega_2 z + 1)}{\omega_2 + 1} + 6 \right)}{72 (\omega_2 z + 1)^3} \quad (6.33)$$

$$\text{EEC}_{++} = \frac{1}{72} \left[\frac{(\omega_2 + 1)^2}{(\omega_2 z + 1)^3} (\omega_2^2 + 6\omega_2 + 6) \left(\frac{\omega_1^2 (\omega_2 z + 1)^2}{(\omega_2 + 1)^2} + \frac{6\omega_1 (\omega_2 z + 1)}{\omega_2 + 1} + 6 \right) \right]$$

$$\begin{aligned}
& + \frac{(\omega_1 + 1)^2}{(\omega_1 z + 1)^3} (\omega_1^2 + 6\omega_1 + 6) \left(\frac{\omega_2^2 (\omega_1 z + 1)^2}{(\omega_1 + 1)^2} + \frac{6\omega_2 (\omega_1 z + 1)}{\omega_1 + 1} + 6 \right) \\
& - \frac{\omega_1^2 \omega_2^2 (\omega_1^2 - 4\omega_1 \omega_2 + \omega_2^2)}{z(\omega_1 + \omega_2 + \omega_1 \omega_2 z)^5} ((\omega_1 + \omega_2)^2 + 6(\omega_1 + \omega_2) + 6) \\
& - \frac{\omega_1^3 (\omega_2^2 + 6\omega_2 + 6) + \omega_2^3 (\omega_1^2 + 6\omega_1 + 6)}{(\omega_1 + \omega_2 + \omega_1 \omega_2 z)} \\
& - \frac{2(4\omega_1^3 \omega_2^2 + 24\omega_1^2 \omega_2^2 (\omega_1 + \omega_2) + 39\omega_1 \omega_2 (\omega_1^2 + \omega_2^2) + 18(\omega_1 + \omega_2)(\omega_1^2 - \omega_2 \omega_1 + \omega_2^2))}{(\omega_1 + \omega_2 + \omega_1 \omega_2 z)^2} \\
& - \frac{116\omega_1^3 \omega_2^2 + \omega_1^3 \omega_2^2 (\omega_1 + \omega_2) + 264\omega_1^2 \omega_2^2 (\omega_1 + \omega_2) + 180\omega_1 \omega_2 (\omega_1^2 + \omega_2^2)}{(\omega_1 + \omega_2 + \omega_1 \omega_2 z)^3} \\
& - \frac{36(\omega_1 + \omega_2)(\omega_1^2 - \omega_2 \omega_1 + \omega_2^2)}{(\omega_1 + \omega_2 + \omega_1 \omega_2 z)^3} - \frac{\omega_1^3 \omega_2^3 (312 + 6(\omega_1 + \omega_2))}{(\omega_1 + \omega_2 + \omega_1 \omega_2 z)^4} \\
& - \frac{\omega_1 \omega_2 (\omega_1^2 \omega_2^2 (\omega_1^2 - 4\omega_2 \omega_1 + \omega_2^2) + 432\omega_1 \omega_2 (\omega_1 + \omega_2) + 108(\omega_1^2 + \omega_2^2))}{(\omega_1 + \omega_2 + \omega_1 \omega_2 z)^4} \\
& - \frac{\omega_1^2 \omega_2^2 (6\omega_1 \omega_2 (\omega_1 + \omega_2) + \omega_1 \omega_2 (6 + \omega_1 + \omega_2)(\omega_1^2 - 4\omega_2 \omega_1 + \omega_2^2) + 216(\omega_1 \omega_2 + \omega_1 + \omega_2))}{(\omega_1 + \omega_2 + \omega_1 \omega_2 z)^5} \Big]
\end{aligned} \tag{6.34}$$

Let us summarize the properties of the above results.

We verify that for $\omega_1 = \omega_2 = 0$ they are in agreement with the findings of Ref. [17, 20],

$$\text{XYC}(0, 0, z) = \frac{1}{2} z^{2-J_X}, \tag{6.35}$$

where $J_X \geq J_Y$. For $\omega_1 = 0$ and $\omega_2 \neq 0$ they satisfy the relation (5.25).

We observe that the expressions for the correlations XYC_{++} are more complicated compared to XYC_{+-} and XYC_{-+} . They contain additional terms involving inverse powers of $\tilde{q}^2/q^2 - 1 = \omega_1 + \omega_2 + \omega_1 \omega_2 z$. As we explained in Section 4.5, such terms are generated by a bulk point singularity.

As at weak coupling, the remaining correlations XYC_{--} can be found using the crossing relation (2.56). They have a form similar to XYC_{++} . Then, examining the sum $\text{XYC}_{--} + \text{XYC}_{++}$ we observe that all the terms with the bulk singularity induced scale $\omega_1 + \omega_2 + \omega_1 \omega_2 z$ cancel against each other and the resulting expression exactly matches the sum $\text{XYC}_{-+} + \text{XYC}_{+-}$. We therefore conclude that the relation (6.19) holds at strong coupling. We recall that at weak coupling this relation is broken for the correlations that receive a contribution from the detector cross-talk. In terms of the OPE, the cross-talk is associated with the contribution of the leading, twist-two operators in the product of the detector operators. At weak coupling, these operators develop anomalous dimensions that manifest themselves through $\log z$ terms in the small z limit. At strong coupling, these operators become infinitely heavy and do not contribute. This explains why the cross-talk contribution is not present at strong coupling.

7 Quantum gravity corrections to event shapes

In this section we analyze $1/c_T \sim 1/N_c^2$ corrections to the generalized energy-energy correlations at strong coupling. Such corrections come from gravitational loops in the bulk theory. Here we only consider the case $\omega_1 = 0$ which simplifies the analysis dramatically. We use the Mellin amplitude recently computed in [26] to study the structure of the generalized event shapes at one loop in supergravity. As expected on general grounds [15], we find that the result is divergent when $\omega_i \rightarrow 0$. To understand the nature of this divergence we derive a dispersive representation of the generalized event shapes using CFT dispersion relations in Mellin space [27]. We then discuss the expected structure of the undeformed ($\omega_i = 0$) event shapes at finite λ and c_T .

7.1 One-loop supergravity

Conventional event shapes, like the energy-energy correlation, cannot be computed perturbatively in $1/c_T$ at strong coupling. The reason is that the correlation function becomes more and more singular in the Regge limit at higher loops which renders the event shape of interest divergent. This divergence is an artifact of perturbation theory and, based on general grounds, it is absent at finite c_T , see [15]. Since the correlation functions at finite c_T are not accessible, we can alternatively deform the observable in a way that makes it finite order by order in $1/c_T$. We can then try to understand what happens as we take the deformation parameter to zero. Introducing non-zero ω_i is one natural way to do it.

The divergence of the undeformed event shape manifests itself in the appearance of divergences in the $\omega_i \rightarrow 0$ limit. In other words, the $c_T \rightarrow \infty$ and $\omega_i \rightarrow 0$ limits do not commute. Here we compute the ω -deformed event shapes using the one-loop Mellin amplitude in supergravity. The relevant one-loop supergravity correlation function was recently found in [23–25].

The starting point of our analysis is the one-loop Mellin amplitude [26]

$$M^{\text{1-loop sugra}}(j_1, j_2) = \frac{1}{4c_T} (j_1 + j_2)^2 (j_1 + j_2 + 1)^2 \sum_{m,n=0}^{\infty} c_{m,n} \left[\frac{1}{(j_1 - m - 1)(j_2 - n - 1)} - \frac{1}{(j_1 - m - 1)(j_1 + j_2 + 2 + n)} - \frac{1}{(j_2 - m - 1)(j_1 + j_2 + 2 + n)} \right]. \quad (7.1)$$

The expression inside the brackets is fully crossing symmetric. The expansion coefficients are given by

$$c_{m,n} = c_{n,m} = \frac{1}{5(m+n-1)_5} \left(15m^4n^2 + 25m^4n + 12m^4 + 30m^3n^3 + 120m^3n^2 + 114m^3n + 36m^3 + 15m^2n^4 + 120m^2n^3 + 216m^2n^2 + 77m^2n - 8m^2 + 25mn^4 + 114mn^3 + 77mn^2 - 76mn - 40m + 12n^4 + 36n^3 - 8n^2 - 40n \right). \quad (7.2)$$

The double sum in (7.1) is divergent. This is a reflection of the UV divergence in the bulk theory at one loop which needs to be renormalized. The divergence does not depend on j_i and leads to an ambiguity in the renormalized one-loop supergravity amplitude which we denote by c_∞ .

We introduce a crossing-symmetric regulator in the sum, $\sum_{m,n} c_{m,n} \rightarrow \sum_{m,n} c_{m,n} \frac{x^m + x^n}{2}$. To recover the original sum we take $x \rightarrow 1$. The divergent part of the sum is given by $\propto 1/(1-x)$ and is indeed j_i independent. We then arrive at

$$M^{\text{1-loop sugra}}(j_1, j_2) = (j_1 + j_2)^2 (j_1 + j_2 + 1)^2 \left(c_\infty + \hat{M}^{\text{reg}}(j_1, j_2) \right), \quad (7.3)$$

where $\hat{M}^{\text{reg}}(j_1, j_2)$ can be easily computed explicitly using the regulator above and dropping the divergent $1/(1-x)$ part. It takes a relatively simple form of a sum of various polygamma functions with rational coefficients, and we do not present it here to save space.²³ After this step, the Mellin integral representation for the the generalized event shapes becomes well defined and it can be studied both analytically and numerically. The result takes the following form

$$\text{SSC}_{++}^{\text{1-loop sugra}}(\omega_1, \omega_2, z) = c_\infty \text{SSC}_{++}^{p=2}(\omega_1, \omega_2, z) + \text{SSC}_{++}^{\text{reg}}(\omega_1, \omega_2, z), \quad (7.4)$$

where $\text{SSC}_{++}^{p=2}$ is given in (4.43) and c_∞ is fixed in the nonperturbative theory. It is known explicitly using the power of supersymmetric localization [38]

$$c_\infty = \frac{1}{c_T} \left(\frac{5\sqrt{\lambda}}{16} + 18\zeta(3) - \frac{3\pi^2}{2} - \frac{2141}{192} + O(\lambda^{-\frac{3}{2}}) \right). \quad (7.5)$$

Instead of keeping ω_i general, here we focus our attention on understanding the small ω_i limit. Setting $\omega_1 = 0$ does not spoil the finiteness of the result but dramatically simplifies the kernel, see (4.15). According to (4.44), $\text{SSC}_{++}^{p=2}(0, \omega_2, z) \sim \delta(\omega_2)$ and, therefore, the $\text{SSC}_{++}^{\text{1-loop sugra}}(0, \omega_2, z)$ does not depend on the coefficient c_∞ for $\omega_2 \neq 0$. In fact, any four-point contact interaction in AdS does not contribute to the generalized event shape for $\omega_1 = 0$ and $\omega_2 \neq 0$.²⁴

The result for the generalized energy-energy correlation at one loop in supergravity takes the form

$$\begin{aligned} \text{EEC}^{\text{1-loop sugra}}(0, \omega_2, z) &= \frac{5}{4c_T} \left[\frac{1 - 6z + 6z^2}{\omega_2^2} + \frac{3}{2} \frac{2 - 15z + 24z^2 - 10z^3}{\omega_2} \right. \\ &\quad \left. + \frac{12}{25} (1 - 36z + 216z^2 - 400z^3 + 225z^4) \log |\omega_2| \log(z^2 |\omega_2|) \right] \end{aligned}$$

²³It can be found in the ancillary file that we provided together with the submission. In fact, the explicit expression for the one-loop Mellin amplitude was recently found in [37]. We checked that our results agree. We thank Francesco Aprile for pointing this out to us.

²⁴Microscopically this is related to the extra suppression of the double trace operators familiar from studies of undeformed event shapes.

$$+ \left(\frac{716 - 20496z + 111396z^2}{125} - 1560z^3 + 846z^4 \right) \log |\omega_2| + O(\omega_2^0) \Big], \quad (7.6)$$

where we only presented the terms that are singular in the $\omega_2 \rightarrow 0$ limit and did not include the contact term $\delta(\omega_2)$.²⁵ One can also check that the expression above correctly implements the transformation property (2.56) which relates the cases $\omega_2 > 0$ and $\omega_2 < 0$.

As an immediate consistency check, we verified that the stress-tensor Ward identities (2.54) continue to hold when we include the one-loop correction, because (7.6) satisfies

$$\int_0^1 dz \text{EEC}^{\text{1-loop sugra}}(z, 0, \omega_2) = \int_0^1 dz z \text{EEC}^{\text{1-loop sugra}}(z, 0, \omega_2) = 0. \quad (7.7)$$

7.2 Dispersive representation of the energy-energy correlator

To elucidate the origin of the $1/\omega_2$ divergences in (7.6) and to understand what happens to them at finite coupling, it is useful to consider the dispersive representation for the Mellin amplitude [27].²⁶

To make as many symmetries as possible manifest, we find it convenient to write down dispersion relations for the Mellin amplitude $\tilde{M}(j_1, j_2) \equiv M(j_1, j_2)/((j_1 + j_2)^2(j_1 + j_2 + 1)^2)$ introduced in (4.8). The advantage of using $\tilde{M}(j_1, j_2)$ is that it is fully crossing-symmetric function of j_1 and j_2

$$\tilde{M}(j_1, j_2) = \tilde{M}(j_2, j_1) = \tilde{M}(j_1, -1 - j_1 - j_2). \quad (7.8)$$

Consistency with the OPE implies that $M(j_1, j_2)$ has simple poles at the positions dictated by the quantum numbers of the exchanged operators [42, 43]. Let us start by recalling the structure of these poles in variable j defined as

$$j = j_1 + j_2. \quad (7.9)$$

Poles in j correspond to the detector \times detector OPE channel which due to our choice of detectors is the same as the **105** R-symmetry channel. The residues at the poles are fixed in terms of the three-point functions of the exchanged operator, see e.g. [44] for the detailed derivation,

$$M(j - j_2, j_2) = -\frac{1}{2} \frac{C_{\tau, J}^2 \mathcal{Q}_{J, m}^\tau(2(1 - j_2))}{j + \frac{\tau}{2} + m - 2} + O\left(j + \frac{\tau}{2} + m - 2\right). \quad (7.10)$$

Here τ and $J \in 2\mathbb{Z}_+$ are the twist and spin of the exchanged operator correspondingly. At finite c_T and λ these include all operators present in the theory. Below, when analyzing the one-loop supergravity, only double trace operators will contribute. Descendants are labeled

²⁵The leading contact term contribution can be read off from (4.44) and (7.5) and it is given by $\frac{5\sqrt{\lambda}}{8c_T} \delta(\omega_2)(1 - 6z + 6z^2)$.

²⁶It would be very interesting to generalize this analysis to the coordinate space as well using the coordinate space CFT dispersion relations [39–41].

by integer $m \geq 0$, and $\mathcal{Q}_{J,m}^\tau(2(1-j_2))$ are the so-called Mack polynomials known explicitly, see e.g. [45] for an explicit formula. $C_{\tau,J}^2$ is the square of the three-point function of the external operators and the operator that appears in the OPE. Only even spin operators appear in the formula above due to the crossing symmetry $M(j_1, j_2) = M(j_2, j_1)$.

Let us now translate the relation (7.10) to the statement about the singularities of the crossing-symmetric modified Mellin amplitude $\tilde{M}(j_1, j_2)$. The relation (7.10) implies that it has simple poles in $j = j_1 + j_2$ with the following residues

$$\tilde{M}(j - j_2, j_2) = -\frac{1}{2} \frac{C_{\tau,J}^2 \mathcal{Q}_{J,m}^\tau(2(1-j_2))}{j + \frac{\tau}{2} + m - 2} \frac{1}{(\frac{\tau}{2} + m - 2)^2 (\frac{\tau}{2} + m - 3)^2} + O\left(j + \frac{\tau}{2} + m - 2\right), \quad (7.11)$$

where $J \in 2\mathbb{Z}_+$. Of course, in addition it could have singularities at $j = 0$ and $j = -1$ since $\tilde{M}(j - j_2, j_2) \equiv M(j - j_2, j_2)/(j^2(j+1)^2)$.

Since $\tilde{M}(j_1, j_2)$ is fully crossing-symmetric, see (7.8), by replacing $j_2 \rightarrow -(1+j)$ and $j \rightarrow -(1+j_2)$ in (7.11) we find that $\tilde{M}(j - j_2, j_2)$ has additional poles in j_2 . They correspond to the OPE channel detector \times source. The residues at these poles can be found by applying the crossing to (7.11)

$$\tilde{M}(j - j_2, j_2) = \frac{1}{2} \frac{C_{\tau,J}^2 \mathcal{Q}_{J,m}^\tau(-2(2+j))}{j_2 - \frac{\tau}{2} - m + 3} \frac{1}{(\frac{\tau}{2} + m - 2)^2 (\frac{\tau}{2} + m - 3)^2} + O(j_2 - \frac{\tau}{2} - m + 3). \quad (7.12)$$

The additional singularities at $j = -1, 0$ are mapped to $j_2 = 0, -1$ under the crossing.

We now write down the dispersive representation for $\hat{M}(j_1, j_2)$ for fixed $j = j_1 + j_2$

$$\begin{aligned} \tilde{M}(j - j_2, j_2) &= \oint \frac{dj'_2}{2\pi i} \frac{\tilde{M}(j - j'_2, j'_2)}{j'_2 - j_2} = - \sum_{\alpha=\{0,-1,j,j-1\}} \text{Res}_{j'_2=\alpha} \frac{\tilde{M}(j - j'_2, j'_2)}{j'_2 - j_2} \\ &\quad - \frac{1}{2} \sum_{\tau,J-\text{even},m} \frac{C_{\tau,J}^2 \mathcal{Q}_{J,m}^\tau(-2(2+j))}{(\frac{\tau}{2} + m - 2)^2 (\frac{\tau}{2} + m - 3)^2} \left(\frac{1}{\frac{\tau}{2} + m - 3 - j_2} + \frac{1}{\frac{\tau}{2} + m - 3 - (j - j_2)} \right). \end{aligned} \quad (7.13)$$

In deriving this relation we used the non-perturbative bound on the Mellin amplitude $|M(j_1, j_2)| \leq |j_2|$ as $|j_2| \rightarrow \infty$, see [27], which translates to $|\tilde{M}(j_1, j_2)| \leq |j_2|^{-3}$ as $|j_2| \rightarrow \infty$. Using the crossing symmetry this also implies that $|\tilde{M}(j - j_2, j_2)| \leq |j_2|^{-3}$ for fixed j , therefore the arc at infinity does not contribute to (7.13). The sum on the first line of (7.13) comes from the contribution of protected twist-two operators and it is fixed by the OPE.²⁷

As a result we get the following representation for the nonperturbative Mellin amplitude

$$M(j_1, j_2) = -\frac{1}{2} \frac{(j_1 + j_2)^2 (1 + j_1 + j_2)}{j_1 j_2} - \frac{(j_1 + j_2)^2 (j_1 + j_2 + 1)^2}{2}$$

²⁷Here we assume that the coupling is finite and there are no higher spin conserved currents in the spectrum.

$$\times \sum_{\tau, J-\text{even}, m} \frac{C_{\tau, J}^2 \mathcal{Q}_{J, m}^\tau(-2(2+j_1+j_2))}{(\frac{\tau}{2}+m-2)^2(\frac{\tau}{2}+m-3)^2} \left(\frac{1}{\frac{\tau}{2}+m-3-j_2} + \frac{1}{\frac{\tau}{2}+m-3-j_1} \right). \quad (7.14)$$

Let us emphasize that this formula is exact. The first term comes from the protected twist two operators and it coincides with the leading result at strong coupling (4.9). The infinite sum encodes corrections to this result.

For the one loop supergravity Mellin amplitude, the only operators that appear in the sum in (7.14) are the double trace operators which have twist $\tau_{n, J} = 8 + 2n + \gamma(n, J)$ with $\gamma(n, J) \sim 1/c_T$.²⁸ The Mack polynomials $\mathcal{Q}_{J, m}^\tau$ that enter (7.14) are importantly proportional to

$$\mathcal{Q}_{J, m}^\tau \sim \sin^2 \left(\frac{\pi \tau}{2} \right). \quad (7.15)$$

For the double trace operators this becomes

$$\sin^2 \left(\frac{\pi \tau_{n, J}}{2} \right) = \sin^2 \left(\frac{\pi \gamma_{n, J}}{2} \right) \sim \frac{1}{c_T^2} \quad (7.16)$$

Double trace operators have three-point functions that scale as $C_{\tau, J}^2 \sim c_T$ which can be seen from form of the disconnected part of the correlator in (4.3). Combining this fact with (7.16) we correctly recover the $1/c_T$ scaling of the leading correction to (7.14) in supergravity.

Next we can use the dispersive representation (7.14) to compute the ω -deformed event shapes at finite coupling in terms of the OPE data. For simplicity we consider $\omega_1 = 0$ and $\omega_2 > 0$. Using relations (5.24), (5.25), and (4.15), we get the following representation for the event shape

$$\text{EEC}_+(0, \omega_2, z) = \left(1 + \omega_2 + \frac{\omega_2^2}{6} \right) \left[\frac{1}{2} + \sum_{\tau, J-\text{even}} 2 \sin^2 \left(\frac{\pi \tau}{2} \right) C_{\tau, J}^2 (1 + \omega_2)^{-(\frac{\tau}{2}-1)} \widetilde{\text{EEC}}_{\tau, J}(z, 0, \omega_2) \right], \quad (7.17)$$

where we have defined a function

$$\begin{aligned} \widetilde{\text{EEC}}_{\tau, J}(z, 0, \omega_2) &\equiv -\frac{1}{2} \int \frac{dj}{2\pi i} \frac{\pi}{2 \sin \pi j} z^{-j-2} (1-z)^{j-1} j^2 (1+j)^2 \\ &\times \sum_{m=0}^{\infty} (1+\omega_2)^{-m} \frac{\mathcal{Q}_{J, m}^\tau(-2(j+2))}{2 \sin^2 \left(\frac{\pi \tau}{2} \right)} \frac{1}{(\frac{\tau}{2}+m-2)^2(\frac{\tau}{2}+m-3)^2}. \end{aligned} \quad (7.18)$$

It encodes the contribution to the energy-energy correlation of a set of poles in (7.14) associated to a given primary operator.²⁹ In writing the formula above we used the fact that

²⁸The shift of the twist τ by $(+4)$ is a consequence of superconformal symmetry, see e.g. Eqs. (2.5) and (2.6) in [25]. In the language of [24], we have $\tau = 4 + 2t$, where $t \geq 2$.

²⁹For correlation functions these are known as Polyakov blocks, see e.g. [39–41] for details. Therefore $\widetilde{\text{EEC}}_{\tau, J}(z, 0, \omega_2)$ encodes the contribution of a given Polyakov block to the energy-energy correlation.

for $\omega_2 > 0$ we can close the j_1 contour to the right half-plane since this is the direction in which $(1 + \omega_2)^{-j_1}$ decays.

It is possible to compute $\widetilde{\text{EEC}}_{\tau,J}(z, 0, \omega_2)$ explicitly for the first few values of J . For $J = 0$ we get

$$\widetilde{\text{EEC}}_{\tau,J=0}(z, 0, \omega_2) = -(1 - 6z + 6z^2) \frac{\Gamma\left(\frac{\tau-6}{2}\right)^2 \Gamma(\tau)}{\pi^2 \Gamma\left(\frac{\tau}{2}\right)^4} {}_2F_1\left(\frac{\tau-6}{2}, \frac{\tau-6}{2}, \tau-1, \frac{1}{1+\omega_2}\right). \quad (7.19)$$

For $J > 0$ we similarly get polynomials in z , $\widetilde{\text{EEC}}_{\tau,J}(z, 0, \omega_2) = \sum_{i=0}^{J+2} c_i(\tau, \omega_2) z^i$. Curiously, we also observed the relation

$$\lim_{\tau \rightarrow \infty} \widetilde{\text{EEC}}_{\tau,J}(z, 0, \omega_2) \sim (1 - 6z + 6z^2) \left(1 + O(\tau^{-1})\right), \quad (7.20)$$

which will be useful for our discussion below. Note that the dependence of (7.20) on z matches the leading $1/\omega_2^2$ term in (7.6).

It is now easy to understand how the terms singular for $\omega_2 \rightarrow 0$ are generated in (7.6). The underlying mechanism has already been discussed in the literature, see for example [35], and it is related to the contribution of double trace operators to the sum (7.17). In this case the factor $\sin^2(\pi\tau/2)$ becomes $\sin^2(\pi\gamma_{n,J,i}/2)$ where n is related to the twist, J is spin, and i accounts for the degeneracies of the double trace operators in question. We now see that

$$\sin^2\left(\frac{\pi\gamma_{n,J,i}}{2}\right) \leq 1, \quad c_T - \text{finite}. \quad (7.21)$$

If on the other hand we first expand at large c_T using the fact that $\gamma_{n,J,i} \sim 1/c_T \ll 1$ we get

$$\sin^2\left(\frac{\pi\gamma_{n,J,i}}{2}\right) = \frac{\pi^2}{4} \gamma_{n,J,i}^2 + O(1/c_T^4). \quad (7.22)$$

To compute the contribution of double trace operators to (7.17) we need to sum both over spin J and twists of the operators labeled by n . Because the anomalous dimensions $\gamma_{n,J,i}$ are growing functions of n , it is the sum over twists of the operators in (7.17) that produces terms that diverge in the limit $\omega_2 \rightarrow 0$. Non-perturbatively we know that an infinite series of $1/c_T$ corrections turn $\gamma_{n,J,i}^2$ into (7.21) in this way regulating the sum. This mechanism of regulating the divergences in perturbation theory is sometimes called “eikonalization” [46]. To summarize, we see that the large twist operators can generate divergences in $1/c_T$ perturbation theory but they are absent at finite c_T .

Let us next work out the form of the $1/\omega_2^2$ term in (7.6) in more detail. In order to do it we replace $C_{\tau,J}^2$ in (7.17) with its leading asymptotic behaviour in mean field theory at tree level

$$\lim_{\tau \rightarrow \infty} \langle C_{\tau,J}^2 \rangle = c_T 2^5 \pi (J+1) 4^{-J} 4^{-\tau} \tau^2. \quad (7.23)$$

For the anomalous dimensions we use the results of [24] to get

$$\lim_{c_T \rightarrow \infty} \frac{\langle 2 \sin^2 \left(\frac{\pi\tau}{2} \right) C_{\tau,J}^2 \rangle}{\langle C_{\tau,J}^2 \rangle} \sim \frac{\pi^2 \langle \gamma_{\tau,J}^2 C_{\tau,J}^2 \rangle}{2 \langle C_{\tau,J}^2 \rangle} \sim \frac{\tau^{11}}{c_T^2}. \quad (7.24)$$

Substituting these relations into (7.17) and taking into account (7.19) we find that the contribution of the operators with large twist and $J = 0$ involves the following integral

$$\begin{aligned} & \int_{\tau_0}^{\infty} d\tau \langle C_{\tau,J}^2 \rangle \frac{\langle 2 \sin^2 \left(\frac{\pi\tau}{2} \right) C_{\tau,J}^2 \rangle}{\langle C_{\tau,J}^2 \rangle} \widetilde{\text{EEC}}_{\tau,J=0}(z, 0, \omega_2) (1 + \omega_2)^{-\frac{\tau}{2}} \\ & \sim \frac{1}{c_T} \int_{\tau_0}^{\infty} d\tau 2^{-\tau} \tau^{\frac{15}{2}} {}_2F_1 \left(\frac{\tau-6}{2}, \frac{\tau-6}{2}, \tau-1, \frac{1}{1+\omega_2} \right) (1 + \omega_2)^{-\frac{\tau}{2}}, \end{aligned} \quad (7.25)$$

where we replaced the sum over twist by an integral over $\tau > \tau_0$. To understand its behaviour for $\omega_2 \rightarrow 0$ it is convenient to use the integral representation of the hypergeometric function. The result then takes the following form at large τ

$$\frac{1}{c_T} \int_0^1 dt \int_{\tau_0}^{\infty} d\tau \tau^8 \frac{(1-t)(1-t+\omega_2)^3}{t^4} \left(\frac{1-t+\omega_2}{t(1-t)} \right)^{-\frac{\tau}{2}} \sim \frac{1}{c_T \omega_2^2}. \quad (7.26)$$

The integral over τ is trivial to do. The integral over t can be easily analyzed numerically or by the saddle point method, with the expected result that it behaves as $1/\omega_2^2$. In this way we have also correctly reproduced the dependence on ω_2 of the first term in (7.6). We have not tried to reproduce the $1/\omega_2$ term using the formulas above. It would be interesting to do it by analyzing the $1/\tau$ corrections as well as to generalize the above analysis to higher loops.

Let us also comment on how contact terms $\delta(\omega_2)$ originate from the finite coupling formulas above in the perturbative expansion. Consider an exchange by a heavy operator ($\tau \gg 1$), which could be for example a stringy mode, in the dispersion representation (7.13) of the Mellin amplitude $\tilde{M}(j - j_2, j_2)$. Expanding the right-hand side of (7.13) in $1/\tau$, we get polynomial in j and j_2 corrections to the Mellin amplitude. As we explained, these yield contact terms in the generalized event shape $\text{EEC}(0, \omega_2, z)$ localized at $\omega_2 = 0$. Let us now see how this comes about directly from (7.17). In this case we can write the following distributional identity

$$\lim_{\tau \rightarrow \infty} (1 + \omega_2)^{-\frac{\tau}{2}} = \frac{2}{\tau} \delta(\omega_2) + \frac{4}{\tau^2} \left(\delta(\omega_2) + \delta'(\omega_2) \right) + O(1/\tau^3). \quad (7.27)$$

These are terms that will appear in the generalized event shapes in string perturbation theory, with the 't Hooft coupling λ controlling the twist of the stringy modes. On the other hand, by going back to the finite coupling we get

$$\lim_{\tau \rightarrow \infty} \lim_{\omega_2 \rightarrow 0} (1 + \omega_2)^{-\frac{\tau}{2}} = 1, \quad (7.28)$$

so that the limits $\tau \rightarrow \infty$ and $\omega_2 \rightarrow 0$ do not commute. To summarize, the contact terms in the perturbative expansion of generalized event shapes signal the presence of enhanced terms in the undeformed event shapes. In the example above, $2\delta(\omega_2)/\tau$ gets replaced with 1 after resummation of corrections in $1/\tau$.

7.3 Small ω and the Regge limit

Let us show that the leading behavior of the EEC as $\omega_2 \rightarrow 0$ is related to the behavior of the Mellin amplitude in the Regge limit. We use (4.12), (4.15) and (5.24) to write down the expression for $\text{EEC}(0, \omega_2, z)$ in the Mellin space

$$\begin{aligned} \text{EEC}(0, \omega_2, z) = & \left(1 + \omega_2 + \frac{\omega_2^2}{6}\right) \int \frac{dj}{2\pi i} \frac{1}{2} \frac{\pi}{\sin \pi j} \frac{z^{-j-2} (1-z)^{j-1}}{j^2(j+1)^2} \\ & \times \int \frac{dj_2}{2\pi i} (1 + \omega_2)^{-j_2} \tilde{M}(j - j_2, j_2) . \end{aligned} \quad (7.29)$$

In order to understand the small ω_2 expansion, the relevant integral is thus

$$\int_{-\delta-i\infty}^{-\delta+i\infty} dj_2 (1 + \omega_2)^{-j_2} \tilde{M}(j - j_2, j_2) = \int_0^\infty dj_2 (1 + \omega_2)^{-j_2} \text{Disc}_{j_2} \tilde{M}(j - j_2, j_2) , \quad (7.30)$$

where we evaluated the integral by closing the contour to the right for $\omega_2 > 0$ and picking the contribution from the poles in j_2 , or, equivalently, the discontinuity of the Mellin amplitude. Imagine that the discontinuity of the Mellin amplitude has the following Regge behavior as $j_2 \rightarrow \infty$ ³⁰

$$\text{Disc}_{j_2} \tilde{M}(j - j_2, j_2) \sim j_2^\alpha . \quad (7.31)$$

Via the integral (7.30) it will produce terms as singular as $1/\omega_2^{1+\alpha}$ in the Regge limit. At one loop we get $\text{Disc}_{j_2} \tilde{M}(j - j_1, j_2) \sim j_2$ as $j_2 \rightarrow \infty$, which via (7.30) produces $1/\omega_2^2$. It would be interesting to explore the limit $\omega_2 \rightarrow 0$ and correspondingly the Regge limit of the Mellin amplitude at two and higher loops using the results of [47].

We however did check the relevant scalings by looking at the discontinuity $\text{Disc}_s M(s, t)$ of the corresponding flat space supergravity amplitude $M(s, t)$, where s and t are the standard Mandelstam invariants in flat space. At one loop the supergravity amplitude takes the following form in the Regge limit, see for example formula (39) in [26],

$$\text{Disc}_s M^{1\text{-loop}}(s, t) \sim s . \quad (7.32)$$

The leading term being analytic in t corresponds to scattering at zero impact parameters, which is consistent from the analysis above where it emerged from intermediate operators of fixed spin and large twist. A more familiar eikonal phase in ten dimensions behaves instead as $t^2 \log(-t)/s$. It controls the leading Regge behavior of scattering at non-zero impact parameters which manifests itself in the fact that it is not analytic in t . We observe the same phenomenon for the expansion of $\text{Disc}_{j_2} \tilde{M}(j - j_2, j_2)$ in one loop supergravity. The term $1/j_2$ comes with the j -dependent pre-factor which is non-analytic. Via (7.30) it will contribute to $\log \omega_2$ term in (7.6). As opposed to $1/\omega_2^2$ and $1/\omega_2$ terms, it is non-analytic

³⁰Since $\tilde{M}(j - j_2, j_2)$ is a meromorphic function of j_2 , this formula should be understood as a statement about averaged discontinuity.

in z (due to the presence of $\log z$). This can be traced to non-analyticity in j of the $1/j_2$ term in the large j_2 expansion of $\text{Disc}_{j_2} \tilde{M}(j - j_2, j_2)$. This in turn can be traced back to the universal high energy limit of the eikonal phase in gravity at non-zero impact parameters, see e.g. [48]. It would be interesting to make this connection more explicit using the eikonal phase in the AdS analysis of [49].

8 Ordinary event shapes at finite λ and finite c_T

At weak coupling, given the perturbative expansion of the correlation function one can systematically compute the perturbative corrections to the event shapes. The situation is very different at strong coupling. In this case there is no simple way of translating the perturbative expansion of the correlation function to the perturbative expansion of the event shape. At the technical level, this is related to the fact that both the stringy $1/\lambda$ and the $1/c_T$ gravitational loop corrections yield expressions for the correlation functions that grow too fast in the Regge limit for the event shape of interest to be well defined. In the collider physics setup studied in this paper, the Regge limit divergence is translated to a large detector time effect. It arises because the correlation function describes the energy correlations with the property that the energy flux does not decay with time and generates a divergence when the working time of the detector goes to infinity.

The divergences are absent at finite λ and finite c_T where, based on general arguments, we know that the Regge limit is such that, say, the energy-energy correlation is well defined. Computing the corrections to the event shapes thus requires resummation of the naive perturbative expansion. Let us illustrate this phenomenon with a few examples.

8.1 Stringy corrections

The simplest example of this phenomenon arises when we consider stringy corrections. The leading order correction to the Mellin amplitude takes the form [50, 51]

$$\tilde{M}(j_1, j_2) = \tilde{M}^{\text{strong}}(j_1, j_2) + \frac{60\zeta(3)}{\lambda^{3/2}} + O(\lambda^{-5/2}) . \quad (8.1)$$

Substituting this relation into (7.29) and taking into account (4.44), we can immediately write down the result for the generalized energy-energy correlations with non-zero ω_2 ,

$$\begin{aligned} \text{EEC}(0, \omega_2, z) = & \left(1 + \omega_2 + \frac{\omega_2^2}{6} \right) \\ & \left[\frac{1}{2} \left(\theta(\omega_2) + \theta(-\omega_2) \frac{(1 + \omega_2)^2}{(1 + \omega_2 z)^3} \right) + \frac{120\zeta(3)}{\lambda^{3/2}} \delta(\omega_2) (1 - 6z + 6z^2) + \dots \right] . \end{aligned} \quad (8.2)$$

On the other hand, the direct computation of the $\omega_2 = 0$ event shape in string theory gives [1]

$$\text{EEC}(z) \equiv \text{EEC}(0, 0, z) = \frac{1}{2} \left(1 + \frac{4\pi^2}{\lambda} (1 - 6z + 6z^2) + \dots \right) , \quad (8.3)$$

where dots in this and the previous expression denote corrections suppressed by powers of $\lambda^{-1/2}$.

Let us discuss how the three formulas above are related to each other. The relation (8.3) can be understood by taking into account that the leading correction to the Mellin amplitude (8.1) scales as $\tilde{M}(j_1, j_2)|_{\lambda^{-3/2}} \sim 1$ in the Regge limit $j_2 \rightarrow \infty$. For this reason the integral $\int dj_2 \tilde{M}(j - j_2, j_2)$ that appears in the computation of the energy-energy correlation (7.29) is divergent at $\omega_2 = 0$. The stringy effects effectively cut the Mellin integral off at $j_2 \sim \sqrt{\lambda}$ leading to (8.3). The evaluation of the precise coefficient in (8.3) is a nontrivial task, requiring the resummation of the string perturbative corrections. Yet it can be done explicitly, see [50] for details. In terms of the dispersion relations the mechanism is precisely the same as described above in Section 7.2, which also explains the dependence on z .

Comparing the relations (8.2) and (8.3), we observe that the leading correction to both expressions is proportional to the same function of z but has different dependence on λ . The presence of the $\delta(\omega_2)$ term in (8.2) signifies that the corresponding detector measures a time-independent energy flux. If we imagine a detector with a finite working time T this would produce an effect of order $T/\lambda^{3/2}$. Letting the working time $T \rightarrow \infty$ produces then a divergent result. What happens at finite λ however is that at times $T_{\text{str}} \sim \lambda^{1/2}$ string perturbation theory breaks down and the effect of the resummation is that the energy flux effectively becomes zero for times $T > T_{\text{str}}$.

8.2 Gravitational loops

Let us now try to generalize this discussion to include gravitational loops. It is natural to expect that the same mechanism is at play: the parts of the one-loop result (7.6) that diverge in the $\omega_2 \rightarrow 0$ limit get enhanced by λ or c_T dependent factors coming from the long time effects in the detector. The presence of such terms, which are enhanced compared to the naive expectation coming from the perturbative expansion of the correlation function, is a characteristic feature of strongly coupled conformal field theories with semi-classical gravity duals.

Based on the OPE data of double trace operators and the mechanism discussed in section 7.2, we associate the terms $1/\omega_2^2$ and $1/\omega_2$ with high energy scattering at zero impact parameters. In the flat space limit this manifests itself through the fact that the corresponding terms in the Regge limit of $\text{Disc}_s M(s, t)$ are analytic in t . In string theory, a fixed-angle scattering is very soft in the high energy limit [52]. We therefore expect that the divergences for $\omega_2 \rightarrow 0$ get regularized in the same way as in the example with string corrections above: namely the j_2 integral is cut off at $j_2 \sim \sqrt{\lambda}$. Equivalently, we expect that the divergences to leading order get substituted by $1/\omega_2 \rightarrow \sqrt{\lambda}$. From this argument we expect the leading stringy correction to be³¹

$$\text{EEC}^{\text{QG}}(z) \propto \frac{\lambda}{c_T} (1 - 6z + 6z^2) + \dots \quad (8.4)$$

³¹The same term originates from the correction $c_\infty \delta(\omega_2)$ discussed in the previous section.

Computing the precise coefficient requires a more detailed analysis. The correction (8.4) originates from two different sources: $T\sqrt{\lambda}/c_T$ and T^2/c_T which grow with time and both get saturated at $T \sim T_{\text{str}} \sim \sqrt{\lambda}$.

We expect a different mechanism to be at play for the terms that diverge in the $\omega_i \rightarrow 0$ limit which originate from scattering at non-zero impact parameters. Such divergences will be present in the $1/c_T$ expansion of the event shape even at finite string tension, or, equivalently, λ . These terms get unitarized at finite c_T via the eikonalization of the gravitational loops. Because of this we also expect to have c_T -enhanced terms in the expansion of the event shapes. Effects coming from non-zero impact parameters originates from operators of arbitrary large spin, see e.g. [53, 54]. Given that $\widetilde{\text{EEC}}_{\tau,J}(z, 0, \omega_2)$ are polynomials in z of the maximal power z^J , any non-analyticity in z can only come from the large spin operators. As an example at one loop, the divergent and non-analytic in z piece $\sim \frac{1}{c_T} \log |\omega_2| \log z$ should originate from the expansion of the eikonal phase in AdS [49]. Indeed, the flat space limit of the part of the one-loop supergravity Mellin amplitude that generates $\frac{1}{c_T} \log |\omega_2| \log z$ term matches the expected expansion of the eikonal phase [55, 56].

The $\log |\omega_2|$ divergence in (7.6) corresponds to the long-time tail which grows as $\log T$ as a function of the detector working time T . We thus see that at finite but large working times the leading contribution to the energy correlation takes the form

$$\text{EEC}^{\text{QG}}(z, T) \propto \frac{\log T}{c_T} (1 - 36z + 216z^2 - 400z^3 + 225z^4) \log z. \quad (8.5)$$

This correction is universal (it does not depend on the details of the spectrum of the bulk theory) and originates from the fact that the dual theory is gravitational, with gravity being the leading interaction at high energies and large impact parameters. As a nontrivial consistency check, we verified that (8.6) satisfies the Ward identities (7.7).

To recover the energy-energy correlation $\text{EEC}(z)$ we have to take the limit $T \rightarrow \infty$. Doing it rigorously requires the resummation of the $1/c_T$ perturbation theory. This might be possible using the eikonalization of the gravitational amplitudes in AdS but we do not attempt it in the present paper. Still, let us discuss the simplest possible scenario in which the energy flux that grows as $\log T$ gets saturated at some time T_{QG} . Here T_{QG} is some characteristic time that goes to infinity as $c_T \rightarrow \infty$. From the eikonalization of the gravitational amplitudes we expect that $\log T_{\text{QG}} \sim \log c_T$. In this simple scenario, we get that the leading quantum gravity correction to the energy-energy correlation takes the form

$$\text{EEC}^{\text{QG}}(z) \stackrel{?}{\propto} \frac{\log c_T}{c_T} (1 - 36z + 216z^2 - 400z^3 + 225z^4) \log z. \quad (8.6)$$

It would be very interesting to derive the leading quantum gravity correction to the energy-energy correlation (8.6) rigorously.

9 Conclusions and future directions

In this paper we have introduced a new class of observables in a collider physics setting which we dubbed generalized event shapes. They are defined as the matrix elements of

light-ray operators (1.2) with non-zero momentum, (1.7). These light-ray operators have a finite resolution in time, given by $1/\hat{\omega}$, and thus allow us to probe the longitudinal structure of the state. By setting $\hat{\omega} = 0$ they smoothly transit over to the familiar event shapes.

The generalized event shapes are *not* the standard differential cross sections, since they are sensitive to the relative phases of the various scattering amplitudes. This makes them harder to measure, but from the theoretical point of view they are very natural observables. They are IR safe and can be evaluated both in terms of scattering amplitudes and correlation functions. If defined in terms of integrated Wightman functions, for $\hat{\omega} \neq 0$ the new observables retain all the information contained in the former. We therefore expect that they form a convenient basis of collider-type observables (at least in a CFT). Indeed, many popular jet observables can be restated in terms of energy correlations, see e.g. [11].

The generalized event shapes exhibit new features compared to the usual event shapes. One interesting example is that they develop a bulk point singularity at strong coupling. Approaching the singularity requires analytic continuation of the physical parameters and in this way it is reminiscent of the flat space singularity in the de Sitter correlators, see e.g. [57]. Another characteristic feature of the generalized event shapes is that they are non-analytic around $\hat{\omega} = 0$. This is related to the fact that, depending on the sign of $\hat{\omega}$, the detector operators can either create or annihilate particles. Nonperturbatively this fact manifests itself in Eq. (1.6).

We studied the generalized event shapes perturbatively in planar $\mathcal{N} = 4$ SYM both at weak and strong coupling. The results are summarized in Section 6. First, we considered the case where the source, the sink and the detectors are built out of local scalar operators. In this case, at weak coupling we obtained the leading-order result using both scattering amplitudes and correlation functions. At strong coupling we have only the correlation functions approach at our disposal. Second, we used the $\mathcal{N} = 4$ supersymmetry Ward identities to compute generalized event shapes with detectors defined by conserved currents, namely charge and energy correlations. In the special case where only one of the detectors has $\hat{\omega} \neq 0$, in Section 5.3 we found remarkably simple relations between the various observables. When both detectors carry non-zero momentum we found that relatively simple relations exist not among the observables themselves but among their Mellin kernels, see Eq. (5.13).

Unlike the ordinary event shapes, the generalized event shapes can be computed perturbatively order by order in the $1/c_T$ and $1/\lambda$ at strong coupling. A characteristic feature of the stringy and quantum-gravitational corrections to the generalized event shapes is that they are divergent in the limit $\hat{\omega} \rightarrow 0$. These divergences signify a longitudinal broadening of the state and the presence of long-time tails in the measured radiation. For ordinary event shapes, which perform measurements at arbitrarily late times, this leads to corrections which are enhanced compared to those coming from the perturbative expansion of the correlation function. We studied the one-loop supergravity corrections to the generalized event shapes in Section 7. We also derived a dispersive representation of the generalized event shape and used it to analyze the result. The structure of the ordinary event shapes at finite λ and finite c_T is discussed in Section 8.

Let us list some interesting open questions that we did not address in the present paper:

- Probably the most important question is to understand whether the generalized event shapes, or some of their cousins, can be measured in an experiment. We commented on the special case of low energy elastic scattering, where this should be possible indirectly. It would be interesting to find out if the same or a similar method generalizes to higher energies.
- It would be very interesting to study generalized event shapes in QCD. The computation is analogous to the scattering amplitude one in Section 3. We expect that the final result will be qualitatively similar to that in $\mathcal{N} = 4$ SYM, though the details will differ. This is what happens to the ordinary event shapes and we expect this relation between $\mathcal{N} = 4$ SYM and QCD to hold for the generalized event shapes as well.
- We motivated our study by thinking about energy fluxes in real time, but for technical reasons it was more convenient to work with detectors that carry a definite momentum, rather than detectors that work for a given period of time. We demonstrated the transition between the two pictures on the simple example of the one-point generalized event shapes in Appendix J. We observed the effect of the longitudinal broadening at strong coupling which manifests itself through the divergences in the $\hat{\omega} \rightarrow 0$ limit, or, equivalently, the long-time tails of the radiation measured by the detectors. It would be interesting to connect our results to the broadening picture explored in [7].
- We emphasized that for $\hat{\omega} \neq 0$ we can render a broader class of correlations well defined. A prominent example is the charge-charge correlation which is not IR safe for $\hat{\omega} = 0$ beyond one-loop order. It would be interesting to understand the physics of the $\hat{\omega} \rightarrow 0$ limit of such observables and see if there is a way of constructing an observable that stays finite in that limit.
- We did not discuss the OPE of light-ray operators with non-zero momentum. It would be useful to generalize the analysis of [15, 31, 58] to this case. As we have seen, one obvious difference is that the spin selection rule $J = J_1 + J_2 - 1$ (here J is the spin of a light-ray operator that appears in the OPE of light-ray operators of spin J_1 and J_2) does not hold anymore since $\hat{\omega}$ carries non-zero spin. The light-ray OPE can also shed interesting light on the $\hat{\omega} \rightarrow 0$ limit of the observables discussed in this paper.
- We found that thinking about generalized event shapes is helpful for understanding the stringy and quantum gravity corrections to the ordinary event shapes. The basic phenomenon is that the $1/\hat{\omega}$ divergences present in the generalized event shapes turn into λ or c_T enhanced terms in the ordinary event shapes. To establish this fact it is convenient to use a dispersive representation of the event shapes (we did it for the leading stringy corrections). For gravitational loop corrections that unitarize the scattering amplitudes at large impact parameters, a more thorough analysis should be possible.

- The way how we introduced time dependence in the measurement at infinity is not unique. Our choice of generalized event shapes was dictated by the symmetries of the problem: given a source that carries a definite momentum, it is natural to have detectors that carry definite momenta as well. Another advantage of these detectors is that they naturally suppress the potential divergences at large working times u , see Eq. (2.17). This makes the corresponding matrix elements well defined, even if the original event shape at $\hat{\omega} = 0$ was not. Other bases of time-dependent light-ray operators have been discussed in the literature, see for instance [59].
- It is known that the light transform of the stress-energy tensor, also called ANEC operator, is a non-negative operator in any unitary QFT [5, 6]. If instead we restrict the time integration to some finite interval we get what is known as the quantum null energy condition (QNEC) [60–62]. It bounds the energy flux measured over a time interval T from below by the shape variations of the entanglement entropy. It would be interesting to explore the implications of QNEC to the generalized event shapes.
- In this paper, we only studied one- and two-point correlations. It would be interesting to extend the consideration to multi-point correlations, see e.g. [13, 63]. The computation of the corrections to the lowest order in the coupling within the amplitude approach would require incorporating tree-level form factors with an arbitrary number of on-shell particles. Results for such form factors have been obtained in $\mathcal{N} = 4$ SYM [64, 65]. In the correlation function approach one would need expressions for the multi-point correlation functions involving conserved currents. Such correlation functions can be computed following the approach developed in Refs. [66–68].
- By placing the detector operators with non-zero null momentum both at past and future null infinity we can naturally define transition amplitudes in CFT. It would be interesting to explore the properties of such objects using CFT methods. It would be also very interesting to understand the connection between such objects and the transitions studied in [69, 70].
- Generalized event shapes can be defined and studied in gravity (see [71] for a recent discussion of the ordinary event shapes). Indeed, they are IR safe observables and can be computed using the standard scattering amplitudes techniques. Moreover, in the case of gravitational waves for obvious reasons we cannot place the detectors around the collision point and essentially all the information acquired in the observation comes from the longitudinal, or time-dependent, details of the signal.

Acknowledgments

We are grateful to Alex Belin, Andrei Belitsky, Agnese Bissi, Cyuan-Han Chang, Dima Chicherin, Miguel Correia, Murat Kologlu, Petr Kravchuk, David Simmons-Duffin, Gabriele

Veneziano, Matthew Walters for useful discussions. AZ is grateful to the participants of the SwissMap workshop “Advances in Quantum Gravity” for stimulating discussions on related topics. This project has received funding from the European Research Council (ERC) under the European Union’s Horizon 2020 research and innovation programme (grant agreement number 949077). The work of GK was supported by the French National Agency for Research grant ANR-17-CE31-0001-01.

A Conformal properties of the deformed light-ray operators

Here we recall some key points about the embedding formalism and index-free notation used in Section 2. A more detailed introduction to it can be found, e.g., in [72]. We then apply the formalism to give an alternative derivation of the conformal (2.12) and dilatation (2.14) transformations of the deformed light-ray operators.

Embedding formalism and index-free notation

The embedding formalism provides a redundant description of d –dimensional conformal tensors by raising them to $(d + 2)$ –dimensional ones. For example, a vector $V_A(X)$ with index $A = (+, -, \mu)$ has $d + 2$ components instead of the expected d for a vector $V_\mu(x)$. The $(d + 2)$ –dimensional null vector X^A (with $X \cdot X \equiv X^+ X^- + X^\mu X_\mu = 0$) is also redundant, having $d + 1$ independent coordinates instead of d .

This redundancy is removed in three steps:

1) Require *scale invariance*,

$$\Phi(\lambda X) = \lambda^{-\Delta} \Phi(X) \quad (\text{A.1})$$

with some weight which will later on be identified with the conformal weight. Assuming that $X^+ \neq 0$ this allows us to define the scale invariant field

$$\phi(x) = (X^+)^{\Delta} \Phi(X), \quad (\text{A.2})$$

where the d –dimensional vector x^μ is identified with

$$\frac{X^A}{X^+} = \left(1, \frac{X^-}{X^+} \equiv -x^2, \frac{X^\mu}{X^+} \equiv x^\mu \right) \Rightarrow X \cdot X = 0. \quad (\text{A.3})$$

2) Impose *transversality* of the tensor fields, e.g. for the vector

$$X \cdot V \equiv X^A V_A(X) = \frac{1}{2}(X^+ V^- + X^- V^+) + X^\mu V_\mu = 0. \quad (\text{A.4})$$

This condition removes one degree of freedom.

3) Consider the tensor field modulo *gauge transformations*, e.g. for the vector

$$V_A(X) \rightarrow V_A(X) + X_A s(X), \quad (\text{A.5})$$

where $s(X)$ is an arbitrary scalar field that scales as $s(\lambda X) = \lambda^{-\Delta-1}s(X)$. This is the second redundant degree of freedom of the vector field that needs to be removed. Clearly, the transversality condition (A.4) is invariant under such gauge transformations.

The index-free notation consists in projecting the index A of the vector field with an auxiliary null vector Z^A (with $Z \cdot Z = 0$),

$$V(X, Z) = Z^A V_A(X). \quad (\text{A.6})$$

To respect the gauge invariance (A.5) the vectors X and Z are assumed orthogonal,

$$Z \cdot X = 0. \quad (\text{A.7})$$

Then the transversality (A.4) takes the form of a *gauge invariance* condition (recall (2.5)),

$$V(X, Z + \beta X) = V(X, Z). \quad (\text{A.8})$$

The auxiliary vector Z^A undergoes independent scale transformations reflecting the homogeneous polynomial dependence on Z of the projected tensor. In the example of the vector field (A.6) we obviously have $V(X, \rho Z) = \rho V(X, Z)$. This scaling, together with (A.1), is generalized to the case of arbitrary positive integer spin J , see (2.4), or even to non-integer and negative spins by analytic continuation.

One can reduce the $(d+2)$ -dimensional null vector Z^A , satisfying the orthogonality condition (A.7), to a d -dimensional null vector z^μ by exploiting the gauge invariance (A.8). Indeed, consider the linear combination $Z^A + \beta X^A$ and choose $\beta = -Z^+/X^+$:

$$Z^A + \beta X^A \stackrel{\beta = -\frac{Z^+}{X^+}}{=} \left(0, Z^- - \frac{Z^+}{X^+} X^- \equiv -2z \cdot x, Z^\mu - \frac{Z^+}{X^+} X^\mu \equiv z^\mu \right) \Rightarrow z^2 = 0. \quad (\text{A.9})$$

The vector z^μ is traditionally used for describing symmetric traceless tensors, see e.g. [73].

Conformal transformations

The main point of the embedding formalism is that the d -dimensional conformal group acts linearly on the $(d+2)$ -dimensional vectors, e.g. $X^A \rightarrow \Lambda^A_B X^B$ with $\Lambda \in SO(2, d)$. The benefit is that one can easily build invariants of such linear transformations, see e.g. [72]. The price to pay is the redundancy discussed above and the necessity to fix various gauges, if we want to recover the familiar Lorentz tensors, e.g. the vector field $V(X, Z) \rightarrow V_\mu(x)$.

According to this concept, a Z -projected tensor field is *invariant* under $SO(2, d)$,

$$O(\Lambda X, \Lambda Z) = O(X, Z), \quad (\text{A.10})$$

and in addition has the scaling properties (2.4).

The conformal group $SO(2, d)$ is extended to $O(2, d)$ by adding the discrete operation of *inversion*, $X^{d+2} \rightarrow -X^{d+2}$ or equivalently, $X^+ \leftrightarrow -X^-$. In the fixed frame (A.3) we find

$$x^\mu = \frac{X^\mu}{X^+} \xrightarrow{I} -\frac{X^\mu}{X^-} = -\frac{X^+}{X^-} \frac{X^\mu}{X^+} = \frac{x^\mu}{x^2}. \quad (\text{A.11})$$

The inversion of the vector Z^A in the fixed frame (A.9) is accompanied by a compensating gauge transformation (A.8) with parameter $\beta = Z^-/X^- - Z^+/X^+$. This implies [73]

$$z^\mu \xrightarrow{I} z^\mu - \frac{2z \cdot x}{x^2} x^\mu, \quad (I[z^\mu])^2 = 0, \quad I^2[z^\mu] = z^\mu. \quad (\text{A.12})$$

Infinitesimal translations and conformal boosts

The conformal algebra is generated by d -dimensional translations $P^{+\mu}$ and conformal boosts $K^{-\mu}$. In the embedding space they are realized by $SO(2, d)$ matrices of the block form

$$\Lambda^A{}_B = \left(\begin{array}{c|c} \frac{1}{2}\delta^\pm{}_\pm & 2b^\pm{}_\nu \\ \hline -b^\mu{}_\pm & \delta^\mu{}_\nu \end{array} \right) \quad (\text{A.13})$$

with infinitesimal parameters $b^\pm \equiv b_\mp$. We find

$$\delta X^\pm = 2b^{\pm\mu} X_\mu, \quad \delta X^\mu = -b^{-\mu} X^+ - b^{+\mu} X^- \Rightarrow \delta(X \cdot X) = 0, \quad (\text{A.14})$$

so that

$$\delta x^\mu = \delta \left(\frac{X^\mu}{X^+} \right) = -b^{-\mu} + b^{+\mu} x^2 - 2(b^+ x) x^\mu, \quad (\text{A.15})$$

where $b^{-\mu}$ is the parameter of infinitesimal translations and $b^{+\mu}$ of conformal boosts.

The auxiliary null vector Z^A transforms in the same way,

$$\delta Z^\pm = 2b^{\pm\mu} Z_\mu, \quad \delta Z^\mu = -b^{-\mu} Z^+ - b^{+\mu} Z^- \Rightarrow \delta(Z \cdot Z) = 0. \quad (\text{A.16})$$

Applied to the fixed frame variable z^μ in (A.9) this transformation becomes³²

$$\delta z^\mu = \delta \left(Z^\mu - \frac{Z^+}{X^+} X^\mu \right) = 2b^{+\mu}(xz) - 2x^\mu(zb^+) \Rightarrow \delta(z^2) = 0. \quad (\text{A.17})$$

We see that z^μ transforms only under conformal boosts and $\delta z^\mu|_{x=0} = 0$.

Transformations of tensor fields

As we explained, the Z -projected fields $O(X, Z)$ are inert under conformal transformations, see (A.10). To recover the familiar tensor field transformations we have to ‘undress’ $O(X, Z)$ to an ordinary field with Lorentz indices. Let us see how this works in the example of the vector field (A.6). First, we use the gauge freedom (A.5) and (A.8) to fix the gauges

$$V^-(X) = Z^+ = 0. \quad (\text{A.18})$$

A conformal boost with parameter b^+ should be accompanied by compensating gauge transformations to maintain the gauges (A.18). Then we use the fact that the projected vector field $V(X, Z)$ is invariant under the conformal transformations to write down

$$0 = \delta V(X, Z)$$

³²The transformation (A.17) can also be obtained from the inversion (A.12) and the relation $K = IPI$.

$$= z^\mu \left(\delta V_\mu(x) + \delta x^\nu \partial_\nu V_\mu(x) - 2\Delta(b^+ x) V_\mu(x) + 2b_\mu^+ x^\nu V_\nu(x) - 2x_\mu b^{+\nu} V_\nu(x) \right). \quad (\text{A.19})$$

Here δx^ν is the coordinate transformation (A.15) and the weight factor comes from the definition (A.2) of the ordinary field and from (A.14). We have also used the transformation (A.17) of z^μ . Stripping off z^μ , we find the familiar conformal transformation of a vector field. The generalization to tensors of arbitrary integer spin is straightforward.

Transformations of the deformed light-ray operators

Comparing (2.9) and (2.5), we observe that the light-ray operators acquire a phase under the gauge transformation. When we fix the frame (A.9), the gauge parameter $\beta = -Z^+/X^+$ appears in the exponential factor

$$\mathbf{L}_{\hat{\omega}}[O] \left(X, Z - \frac{Z^+}{X^+} X \right) = e^{i\hat{\omega}Z^+/X^+} \mathbf{L}_{\hat{\omega}}[O](X, Z). \quad (\text{A.20})$$

According to (A.15) and (A.17) both arguments of $O(x - \frac{z}{\alpha}, z)$ in (2.11) are inert under conformal boosts at the origin $x = 0$. However, the exponential factor in (A.20) transforms:

$$\delta_{b^+} \left(\frac{Z^+}{X^+} \right) = \frac{2b^+ \cdot Z}{X^+} - \frac{2b^+ \cdot X Z^+}{(X^+)^2} \xrightarrow[X^+=1, Z^\mu=z^\mu]{x^\mu=X^\mu/X^+=0} 2(b^+ z). \quad (\text{A.21})$$

This leads to the relation (2.12) but its derivation is different from that in (2.13). There we implicitly ‘undressed’ the tensors from the projection variables z^μ and then applied the standard tensor transformation rules like (A.19). Here we treated both x and z on the same footing and we saw that the effect (2.12) originates from the compensating β -gauge transformations needed to restore the special frame (A.9).

The dilatation transformation can be obtained from the commutator $[P^{+\mu}, K^{-\nu}] = \eta^{\mu\nu} D + L^{\mu\nu}$. Commuting two variations with parameters b^+ and b^- , we find

$$\delta_D x^\mu = \tau x^\mu, \quad \delta_D z^\mu = 0, \quad \delta_D X^+ = -\tau X^+, \quad \delta_D Z^+ = -\tau Z^+, \quad (\text{A.22})$$

where $\tau = -2b^+ \cdot b^-$ is the infinitesimal dilatation parameter. The variation of x in the combination $x - z/\alpha$ on the right-hand side of (2.11) is accompanied by a compensating transformation of the integration parameter α , $\delta_D \alpha = -\tau \alpha$. The change of variable in the integral in (2.11) produces the weight λ^{1-J} (with $\lambda = 1 + \tau$) in (2.14). The extra weight $\lambda^{-\Delta}$ is absorbed by the defining factor $(X^+)^{-\Delta}$ in (2.3) (see also (A.2)), which is implicit in (2.11). This reproduces (2.14), without setting $x = 0$ in the dilatation transformations.

B Reality property of generalized event shapes

In this appendix we derive the reality condition for the one-point generalized event shapes (2.38). We have

$$\langle \mathcal{O}(\hat{\omega}, n) \rangle_q = \frac{(-1)^J}{\eta_{\mathcal{O}}} \langle \phi^\dagger(\tilde{q}) \left((\text{CRT}) \mathcal{O}(\hat{\omega}, n) (\text{CRT})^{-1} \right)^\dagger \phi(q) \rangle$$

$$\begin{aligned}
&= \frac{(-1)^J}{\eta_{\mathcal{O}}} \langle (\text{CRT}) \mathcal{O}(\hat{\omega}, n) (\text{CRT})^{-1} \phi(\tilde{q}) | (\text{CRT}) (\text{CRT})^{-1} \phi(q) \rangle \\
&= \frac{(-1)^J}{\eta_{\mathcal{O}}} \langle (\text{CRT})^{-1} \phi(q) | \mathcal{O}(\hat{\omega}, n) (\text{CRT})^{-1} \phi(\tilde{q}) \rangle \\
&= \frac{(-1)^J}{\eta_{\mathcal{O}}} \langle \phi^\dagger(q) (\text{CRT}) \mathcal{O}(\hat{\omega}, n) (\text{CRT})^{-1} \phi(\tilde{q}) \rangle \\
&= \langle \phi(q)^\dagger \mathcal{O}(-\hat{\omega}, n) \phi(\tilde{q}) \rangle = \langle \mathcal{O}(-\hat{\omega}, n) \rangle_{q+\hat{\omega}_1 n_1 + \hat{\omega}_2 n_2}, \tag{B.1}
\end{aligned}$$

Let us set, for example, $\Delta_\phi = 2$, $d = 4$. We then get for the detectors of interest

$$\begin{aligned}
f_S(\omega) &= f_S \left(-\frac{\omega}{\omega+1} \right), \\
f_Q(\omega) &= (1+\omega) f_Q \left(-\frac{\omega}{\omega+1} \right), \\
f_E(\omega) &= (1+\omega)^2 f_E \left(-\frac{\omega}{\omega+1} \right). \tag{B.2}
\end{aligned}$$

The explicit expressions (2.49) and (2.50) satisfy (B.2) indeed.

For the one-point generalized event shapes (2.44) we have

$$\begin{aligned}
\langle \mathcal{O}_1(\hat{\omega}_1, n) \mathcal{O}_2(\hat{\omega}_2, n_2) \rangle_q &= \frac{(-1)^{J_1+J_2}}{\eta_{\mathcal{O}_1} \eta_{\mathcal{O}_2}} \langle \phi^\dagger(\tilde{q}) \left((\text{CRT}) \mathcal{O}_1(\hat{\omega}_1, n_1) \mathcal{O}_2(\hat{\omega}_2, n_2) (\text{CRT})^{-1} \right)^\dagger \phi(q) \rangle \\
&= \frac{(-1)^{J_1+J_2}}{\eta_{\mathcal{O}_1} \eta_{\mathcal{O}_2}} \langle (\text{CRT}) \mathcal{O}_1(\hat{\omega}_1, n_1) \mathcal{O}_2(\hat{\omega}_2, n_2) (\text{CRT})^{-1} \phi(\tilde{q}) | (\text{CRT}) (\text{CRT})^{-1} \phi(q) \rangle \\
&= \frac{(-1)^{J_1+J_2}}{\eta_{\mathcal{O}_1} \eta_{\mathcal{O}_2}} \langle (\text{CRT})^{-1} \phi(q) | \mathcal{O}_1(\hat{\omega}_1, n_1) \mathcal{O}_2(\hat{\omega}_2, n_2) (\text{CRT})^{-1} \phi(\tilde{q}) \rangle \\
&= \frac{(-1)^{J_1+J_2}}{\eta_{\mathcal{O}_1} \eta_{\mathcal{O}_2}} \langle \phi^\dagger(q) (\text{CRT}) \mathcal{O}_1(\hat{\omega}_1, n_1) \mathcal{O}_2(\hat{\omega}_2, n_2) (\text{CRT})^{-1} \phi(\tilde{q}) \rangle \\
&= \langle \phi^\dagger(q) \mathcal{O}_1(-\hat{\omega}_1, n_1) \mathcal{O}_2(-\hat{\omega}_2, n_2) \phi(\tilde{q}) \rangle \\
&= \langle \mathcal{O}_1(-\hat{\omega}_1, n_1) \mathcal{O}_2(-\hat{\omega}_2, n_2) \rangle_{q+\hat{\omega}_1 n_1 + \hat{\omega}_2 n_2}. \tag{B.3}
\end{aligned}$$

Going from the second to the third line we used the anti-unitary property of CRT. Together with (2.41) this results in the relation (2.45).

C One-point function

In this appendix we consider the simplest correlation function involving a single flow operator

$$\langle \phi(\tilde{q}) \mathcal{O}_J(\hat{\omega}, n) \phi(q) \rangle = \int d^d x_1 e^{-i\tilde{q}x_1} \int d^d x_2 e^{-iqx_2} \langle \phi(x_1) \mathcal{O}_J(\hat{\omega}, n) \phi(x_2) \rangle, \tag{C.1}$$

where the scalar operators $\phi(x_2)$ and $\phi(x_1)$ define the source and sink, respectively, and the flow operator is given by (2.22). Its calculation will serve as an illustration of the general formalism for computing more complicated observables from correlation functions.

For simplicity we work in $d = 4$ dimensions, for arbitrary d the formulae become more complicated. For the lowest values of the spin $J = 0, 1, 2$, the flow operator in (C.1) is identified as the scalar, charge or energy detector, respectively. After inserting the definition (2.22) of $\mathcal{O}_J(\hat{\omega}, n)$ in (C.1), we encounter a three-point Wightman correlation function involving two scalar operators ϕ with scaling dimension Δ and the spinning twist-two operator $O_J(x) \equiv \mathcal{O}_{\mu_1 \dots \mu_J}(x) \bar{n}^{\mu_1} \dots \bar{n}^{\mu_J}$. Its form is fixed by conformal symmetry up to an overall normalization factor,

$$\langle \phi(x_1) \mathcal{O}_J(x_3) \phi(x_2) \rangle = \frac{\mathcal{N}_J}{x_{13}^2 x_{32}^2 x_{12}^{2\Delta-2}} \left(\frac{2i(x_{13}\bar{n})}{x_{13}^2} + \frac{2i(x_{32}\bar{n})}{x_{32}^2} \right)^J, \quad (\text{C.2})$$

where we used a shorthand notation for $x_{ij} = x_i - x_j$. The poles of the correlation function come with an ‘ $\pm i0$ ’ prescription whose sign depends on the time separation of the operators:

$$x_{12}^2 \rightarrow x_{12}^2 - i0x_{12}^0, \quad x_{13}^2 \rightarrow x_{13}^2 - i0x_{13}^0, \quad x_{32}^2 \rightarrow x_{32}^2 - i0x_{32}^0. \quad (\text{C.3})$$

In (C.2) we have tacitly assumed that the operator $O_J(x)$ has the canonical scaling dimension $2 + J$. This is certainly true for $J = 1$ and $J = 2$ since the corresponding operators are the conserved $U(1)$ current and the stress-energy tensor. In a generic interacting conformal theory, the operators with $J = 0$ and $J \geq 3$ are not protected and their scaling dimension differs from the canonical dimension $2 + J$, unless there exists an additional symmetry that protects them.³³ Since we are mostly interested in the case $J \leq 2$, we shall assume that the operators $O_J(x)$ are protected.

To obtain $\langle \phi(x_1) \mathcal{O}_J(\hat{\omega}, n) \phi(x_2) \rangle$ from (C.2), we have to replace $x_3 = rn + \alpha \bar{n}$ and apply the operations specified in (2.22) (take the limit $r \rightarrow \infty$ and integrate over α). This can be done using the following identity

$$\frac{1}{x_{13}^2 x_{32}^2} \left(\frac{2i(x_{13}\bar{n})}{x_{13}^2} + \frac{2i(x_{32}\bar{n})}{x_{32}^2} \right)^J = P_J(i(\bar{n}\partial_{x_1}), i(\bar{n}\partial_{x_2})) \frac{1}{x_{13}^2 x_{32}^2}, \quad (\text{C.4})$$

where $P_J(s_1, s_2)$ is a homogenous polynomial in s_i of degree J . Its form can be found by comparing the coefficients in front of the powers of $(x_{13}\bar{n})$ on both sides of (C.4),

$$P_J(s_1, s_2) = \sum_{k=0}^J \binom{J}{k} \frac{(-s_1)^k}{k!} \frac{s_2^{J-k}}{(J-k)!}, \quad (\text{C.5})$$

and can be identified as Gegenbauer polynomials. Replacing $x_3 = rn + \alpha \bar{n}$ we find for $r \gg 1$

$$\begin{aligned} \frac{1}{x_{13}^2 x_{32}^2} &\rightarrow \frac{1}{4r^2(n(x_1 - \alpha \bar{n}) - i0)((n(\alpha \bar{n} - x_2) - i0)} \\ &= -\frac{1}{4r^2} \int_0^\infty ds_1 ds_2 e^{-is_1(n(x_1 - \alpha \bar{n})) - is_2(n(\alpha \bar{n} - x_2))}, \end{aligned} \quad (\text{C.6})$$

³³This happens in particular in $\mathcal{N} = 4$ SYM where the scalar operator with $J = 0$ is half-BPS.

where we only kept the leading term. Here the minus sign in the exponent in the second relation is dictated by the ‘ $-i0$ ’ prescription of the propagator in the first line.

The rationale for using the integral representation (C.6) is that, upon substituting (C.6) into (C.4), the action of the differential operator amounts to inserting the polynomial $P_J(s_1(n\bar{n}), -s_2(n\bar{n})) = (n\bar{n})^J P_J(s_1, -s_2)$ into the integral over s_1 and s_2 . Putting together the above relations and carrying out the α -integration in (2.22) we find

$$\langle \phi(x_1) \mathcal{O}_J(\hat{\omega}, n) \phi(x_2) \rangle = -\frac{\pi \mathcal{N}'_J}{2x_{12}^{2\Delta-2}} \int_0^\infty ds_1 ds_2 e^{-is_1(nx_1) + is_2(nx_2)} \delta(s_1 - s_2 - \hat{\omega}) P_J(s_1, -s_2), \quad (\text{C.7})$$

where the delta function arises from the integration over α in (2.22) and the factor of $1/r^2$ in (C.6) cancels against the analogous factor in (2.22). Note that the dependence on the auxiliary null vector \bar{n} dropped out of this relation, as it should be. The dependence on J resides in the normalization factor and in the polynomial (C.5).

To obtain the correlation (C.1) we have to Fourier transform (C.7) with respect to x_1 and x_2 . This can be done using the following relation

$$\sigma_\Delta(q) = \int \frac{d^4x e^{-i(qx)}}{(-x^2 + i0x^0)^\Delta} = \theta(q) \frac{2\pi^3(q^2/4)^{\Delta-2}}{\Gamma(\Delta)\Gamma(\Delta-1)}, \quad (\text{C.8})$$

where $\theta(q) \equiv \theta(q^0)\theta(q^2)$ ensures that $\sigma_\Delta(q) \neq 0$ only for time-like q 's. In this way we find

$$\begin{aligned} \langle \mathcal{O}_J(\hat{\omega}, n) \rangle_q &\equiv \int d^4x_2 e^{-iqx_2} \langle \phi(0) \mathcal{O}_J(\hat{\omega}, n) \phi(x_2) \rangle \\ &= \mathcal{N}'_J \int_0^\infty ds_1 ds_2 \delta(s_1 - s_2 - \hat{\omega}) P_J(s_1, -s_2) \sigma_{\Delta-1}(q - ns_2), \end{aligned} \quad (\text{C.9})$$

where the proportionality factor \mathcal{N}'_J does not depend on ω and, therefore, it cancels in the ratio $\langle \mathcal{O}_J(\hat{\omega}, n) \rangle_q / \langle \mathcal{O}_J(\omega = 0, n) \rangle_q$. The expression for $\langle \mathcal{O}_J(\omega = 0, n) \rangle_q$ was previously derived in [16, 17].

The relation (C.9) has a simple interpretation in a weakly coupled CFT, as shown in Figure 5. The operator $\phi(x_2)$ excites the vacuum and creates the state $\int d^4x_2 e^{-iqx_2} \phi(x_2)$ containing an arbitrary number of particles with the total momentum q . These particles propagate to the final state and are absorbed by the sink $\phi(x_1)$. The flow operator $\mathcal{O}_J(\hat{\omega}, n)$ plays the role of a detector located on the celestial sphere in the direction n . It selects a particle carrying momentum ns_2 and transfers the light-like momentum $n\hat{\omega}$ to it, so that the momentum of the outgoing particle is $ns_1 = ns_2 + n\hat{\omega}$. Thus, the integration variables s_i in (C.9) have the meaning of particle energies and the polynomial $P_J(s_1, -s_2)$ defines the transition amplitude. Finally, $\sigma_{\Delta-1}(q - ns_2)$ gives the probability for the remaining particles with total momentum $q - ns_2$ to be absorbed by the sink.

Changing the integration variable to $s_2 = q^2/(2(qn))s$ and replacing $\hat{\omega} = q^2/(2(qn))\omega$, we find after some algebra

$$\langle \mathcal{O}_J(\hat{\omega}, n) \rangle_q \sim \frac{(q^2)^{J+\Delta-2}}{(qn)^{J+1}} \int_{\max(0, -\omega)}^1 ds P_J(s + \omega, -s) (1-s)^{\Delta-3}. \quad (\text{C.10})$$

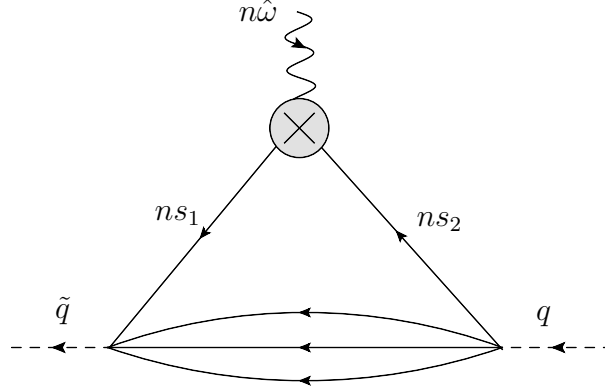


Figure 5. Diagrammatic interpretation of the one-point correlation (C.9). The grey blob represents the detector and the arrows indicate the propagation direction of the particles.

Here the upper integration bound follows from the condition $(q - ns_2)^2 \geq 0$ and the lower bound is due to the condition $s_1 = s_2 + \hat{\omega} \geq 0$. It is easy to check that this relation is in agreement with (2.33). We find that up to a normalization factor the corresponding scaling function is given by

$$f_{\mathcal{O}}(\omega, J) = c_J \int_{\max(0, -\omega)}^1 ds P_J(s + \omega, -s)(1 - s)^{\Delta-3}, \quad (\text{C.11})$$

where the coefficient $c_J = (-1)^J \Gamma(J + \Delta - 1)(J!)^2 / (\Gamma(\Delta - 2)(2J)!)$ is chosen in such a way that $f_{\mathcal{O}}(0, J) = 1$. Notice that the lower integration bound depends on the sign of ω . As we show in a moment, this makes the function $f_{\mathcal{O}}(\omega, J)$ non-analytic around $\omega = 0$.

Replacing the polynomial P_J in (C.11) with its explicit expression (C.5) we find that for the lowest values of the spin $J = 0, 1, 2$ the function $f_{\mathcal{O}}(\omega, J)$ is given by (2.49) and (2.50). It is straightforward to verify that these expressions satisfy the crossing symmetry relation (2.40) (upon replacing $\Delta_\phi = \Delta$, $\Delta_{\mathcal{O}} = J + 2$ and $d = 4$).

The relations (2.49) and (2.50) define the function $f_{\mathcal{O}}(\omega, J)$ on the positive and negative semi-axes of ω , respectively. Although the functions (2.49) and (2.50) are continuous at the origin, their derivatives f'_S , f'''_Q and $f^{(5)}_E$ have a jump at $\omega = 0$. For an arbitrary spin J , this happens for the derivative of order $2J + 1$.

Fixing the one-point function from symmetries

Let us now ask if we can fix the result for the one-point function using symmetries. A similar discussion for the case $\hat{\omega} = 0$ can be found in Section 5.1.3 in [15]. From the formulas above, it is clear that the conditions (2.8), (2.9), and (2.10) are not enough to fix the result. Indeed, consider the following ansatz for the one-point function

$$\langle \phi(X_1) \mathbf{L}_{\hat{\omega}}[O](X_3, Z_3) \phi(X_2) \rangle = \frac{1}{(-2X_1 \cdot X_3)^{\frac{\Delta-J}{2}} (-2X_2 \cdot X_3)^{\frac{\Delta-J}{2}}} \frac{1}{(-2X_1 \cdot X_2)^{\Delta_\phi + \frac{J-\Delta}{2}}}$$

$$\times \int_0^\infty ds_1 ds_2 s_1^{\Delta-2} f\left(\frac{s_2}{s_1}\right) \delta(s_1 - s_2 - \hat{\omega}) e^{\frac{i}{2} \left(s_2 \frac{Z_3 \cdot X_2}{X_2 \cdot X_3} - s_1 \frac{Z_3 \cdot X_1}{X_1 \cdot X_3} \right)}, \quad (\text{C.12})$$

where $f(s_2/s_1)$ is an unknown function. We note that (C.12) has the correct transformation properties for any $f(s_2/s_1)$. Moreover, assuming that $f(1) \neq 0$, for $\hat{\omega} = 0$ it yields the known expression for the three-point function.

We can fix the function $f(s_2/s_1)$ in (C.12) by noting that the light-ray operator in (C.12) is polynomial in the polarization vector Z . To implement this condition, we observe that a local operator satisfies the shortening condition

$$(w \cdot \partial_z)^{J+1} O(x, z) = 0, \quad (\text{C.13})$$

where we introduced an extra polarization vector which is null and transverse to z^μ , see section 3.1 in [58] for more details,

$$z^2 = z \cdot w = w^2 = 0. \quad (\text{C.14})$$

In writing (C.13) we assumed that $O(x, z)$ is a local operator with spin J . The relation (C.13) is just an economic way of saying that $O(x, z)$ is a polynomial in the polarization tensor z of degree J . We can now pull $(w \cdot \partial_z)^{J+1}$ through the ω -deformed light transform to get a shortening condition when acting on (C.12). This fixes the unknown function $f(s_2/s_1)$.

Let us do this exercise explicitly for the simplest case $J = 0$. In this case we get the relation

$$\left((z \cdot \partial_x)(w \cdot \partial_z) - (z \cdot \partial_z)(w \cdot \partial_x) \right) \mathbf{L}_{\hat{\omega}}[O](x, z) = 0, \quad (\text{scalar } O), \quad (\text{C.15})$$

which was also discussed in [58]. It leads to the following equation for the three-point function

$$\left((z \cdot \partial_x)(w \cdot \partial_z) - (z \cdot \partial_z)(w \cdot \partial_x) \right) \langle \phi(x_1) \mathbf{L}_{\hat{\omega}}[O](x, z) \phi(x_2) \rangle = 0. \quad (\text{C.16})$$

Plugging (C.12) into (C.16) we find

$$f(x) = c_0 x^{\frac{\Delta-2}{2}}, \quad (\text{C.17})$$

which is indeed the correct expression. Analogous computations can be done for $J > 0$ as well.

D Free scalar field at null infinity

Let us consider a free massless real scalar field in $d = 4$ dimensions. It can be represented in terms of creation and annihilation operators,

$$\varphi(x) = \int_{-\infty}^{\infty} \frac{d^4 p}{(2\pi)^3} \delta_+(p^2) (a_p e^{-i(px)} + a_p^\dagger e^{i(px)}), \quad (\text{D.1})$$

where $\delta_+(p^2) = \theta(p^0)\delta(p^2)$.

Following the discussion in Section 3.1, we send the scalar field to null infinity by replacing $x = rn + \alpha\bar{n}$ and taking the limit $r \rightarrow \infty$

$$\lim_{r \rightarrow \infty} r\varphi(rn + \alpha\bar{n}) = \lim_{r \rightarrow \infty} r \int_{-\infty}^{\infty} \frac{d^4p}{(2\pi)^3} \delta_+(p^2) \left[a_p e^{-ir(pn) - i\alpha(p\bar{n})} + a_p^\dagger e^{ir(pn) + i\alpha(p\bar{n})} \right]. \quad (\text{D.2})$$

It is convenient to apply Sudakov's decomposition of the momenta

$$p = p_+n + p_-\bar{n} + p_\perp, \quad (\text{D.3})$$

where $n^2 = \bar{n}^2 = 0$ and $(p_\perp n) = (p_\perp \bar{n}) = 0$. Switching to the variables (p_+, p_-, p_\perp) in (D.2) we get

$$\begin{aligned} \lim_{r \rightarrow \infty} r(n\bar{n}) \int_{-\infty}^{\infty} \frac{dp_+ dp_- d^2p_\perp}{(2\pi)^3} \theta(p_+) \theta(p_-) \delta(2p_+p_-(n\bar{n}) - p_\perp^2) \\ \times \left[a_{p_+, p_-, p_\perp} e^{-i(n\bar{n})(p_-r + p_+\alpha)} + a_{p_+, p_-, p_\perp}^\dagger e^{i(n\bar{n})(p_-r + p_+\alpha)} \right]. \end{aligned} \quad (\text{D.4})$$

Next we rescale $p_- \rightarrow p_- / ((n\bar{n})r)$ and take the limit $r \rightarrow \infty$ to get

$$\int_{-\infty}^{\infty} \frac{dp_+ dp_- d^2p_\perp}{(2\pi)^3} \theta(p_+) \theta(p_-) \delta(p_\perp^2) \left[a_{p_+, 0_-, p_\perp} e^{-i(p_- + (n\bar{n})p_+\alpha)} + a_{p_+, 0_-, p_\perp}^\dagger e^{i(p_- + (n\bar{n})p_+\alpha)} \right]. \quad (\text{D.5})$$

Integrating over p_- and using the identity $\int d^2p_\perp \delta(p_\perp^2) = \pi \int dp_\perp^2 \delta(p_\perp^2) = \pi$ we arrive at

$$\lim_{r \rightarrow \infty} r\varphi(rn + \alpha\bar{n}) = i \int_0^\infty \frac{dp_+}{8\pi^2} \left[a_{p_+, 0_-, 0_\perp}^\dagger e^{i(n\bar{n})p_+\alpha} - a_{p_+, 0_-, 0_\perp} e^{-i(n\bar{n})p_+\alpha} \right]. \quad (\text{D.6})$$

Here the creation and annihilation operators are defined for the momentum $(p_+, 0_-, 0_\perp)$ that is aligned along the null vector n . Denoting this momentum by sn^μ we can rewrite the relation (D.6) in a covariant form,

$$\lim_{r \rightarrow \infty} r\varphi(rn + \alpha\bar{n}) = i \int_0^\infty \frac{ds}{8\pi^2} \left[a_{sn}^\dagger e^{i(n\bar{n})s\alpha} - a_{sn} e^{-i(n\bar{n})s\alpha} \right]. \quad (\text{D.7})$$

The complex scalar field satisfies a similar relation with the only difference that the operator a_{sn}^\dagger is replaced by the annihilation operator b_{sn}^\dagger with opposite charge. Then, substituting (D.7) into (3.7) and performing the integration over α we obtain a representation of the scalar flow operator that coincides with the second line of (3.7).

E Derivation of the SSC kernels

Here we present the details of the derivation of the scalar-scalar kernels, Eqs. (4.13) and (4.14), in Mellin space. The derivation is a direct generalization of the analysis in [16]. We

start with the four-point correlation function (4.3), in which we retain only the interaction part. It is described by the function $\Phi(u, v)$ which has the Mellin representation (4.6). Using the symmetry properties of the Mellin amplitude $M(j_1, j_2)$ and doing the crossing transformation $j_1 \rightarrow -1 - j_1 - j_2$, we can recast (4.6) as follows:

$$\Phi(u, v) = \int_{c_0} \frac{dj_1 dj_2}{(2\pi i)^2} [\Gamma(1 - j_1) \Gamma(1 - j_2) \Gamma(j_1 + j_2)]^2 M(j_1, j_2) u^{-1-j_1-j_2} v^{j_2}, \quad (\text{E.1})$$

where the integration contour satisfies $\text{Re}(j_1), \text{Re}(j_2) < 0$ and $\text{Re}(j_1 + j_2) > -1$.

The relevant integral takes the form³⁴

$$\begin{aligned} & \int_{c_0} \frac{dj_1 dj_2}{(2\pi i)^2} [\Gamma(1 - j_1) \Gamma(1 - j_2) \Gamma(j_1 + j_2)]^2 M(j_1, j_2) \\ & \times \frac{1}{(2\pi)^4} \int d^4 x_3 d^4 x_4 e^{i(\tilde{q}x_4) - i(qx_3)} \int_{-\infty}^{\infty} d\alpha_1 d\alpha_2 e^{-i\alpha_1 \hat{\omega}_1 (n_1 \bar{n}_1) - i\alpha_2 \hat{\omega}_2 (n_2 \bar{n}_2)} \\ & \times \frac{1}{x_{12}^4 x_{34}^4} \left(\frac{x_{14}^2 x_{23}^2}{x_{13}^2 x_{24}^2} \right)^{j_2-1} \left(\frac{x_{12}^2 x_{34}^2}{x_{13}^2 x_{24}^2} \right)^{2-j_1-j_2}, \end{aligned} \quad (\text{E.2})$$

where we kept the ordering of the operators implicit. Next we set $x_i = r_i n_i + \alpha_i \bar{n}_i$ (for $i = 1, 2$) at the detector points and take the limit $r_i \rightarrow \infty$ according to (2.22). We also rescale $\alpha_i \rightarrow \alpha_i / (n_i \bar{n}_i)$ to get (skipping the first line of (E.2))

$$\begin{aligned} & \frac{1}{(2\pi)^4} \int d^4 x_3 d^4 x_4 e^{i(\tilde{q}x_4) - i(qx_3)} \int_{-\infty}^{\infty} d\alpha_1 d\alpha_2 e^{-i\alpha_1 \hat{\omega}_1 - i\alpha_2 \hat{\omega}_2} \frac{2^{j_1+j_2-4}}{(n_1 n_2)^2 x_{34}^4} \\ & \times \left[\frac{x_{34}^2 (n_1 n_2)}{(\alpha_1 - (x_4 n_1) - i\epsilon)((x_3 n_2) - \alpha_2 - i\epsilon)} \right]^{1-j_2} \left[\frac{x_{34}^2 (n_1 n_2)}{(\alpha_2 - (x_4 n_2) - i\epsilon)((x_3 n_1) - \alpha_1 - i\epsilon)} \right]^{1-j_1}. \end{aligned} \quad (\text{E.3})$$

Here we introduced the $i\epsilon$ prescription that captures the ordering of the operators according to (4.1). Note that the dependence on \bar{n}_i has dropped out, as expected. The identity

$$\begin{aligned} & \int_{-\infty}^{\infty} d\alpha \frac{e^{-i\hat{\omega}\alpha}}{(\alpha - n \cdot x_3 - i\epsilon)^a (n \cdot x_4 - \alpha - i\epsilon)^b} \\ & = \frac{i^{a+b}}{\Gamma(a)\Gamma(b)} \int_0^{\infty} ds_1 ds_2 s_1^{a-1} s_2^{b-1} 2\pi \delta(s_1 - s_2 + \hat{\omega}) e^{is_1(nx_3) - is_2(nx_4)}, \end{aligned} \quad (\text{E.4})$$

where $\text{Re}(a), \text{Re}(b) > 0$, allows us to perform the integral over the detector times, or equivalently the light transform.

As a result we get the following expression

$$\begin{aligned} & \frac{1}{(2\pi)^2} \int d^4 x_3 d^4 x_4 e^{i(\tilde{q}x_4) - i(qx_3) + is_1(x_3 n_1) + is_1'(x_3 n_2) - is_2(x_4 n_1) - is_2'(x_4 n_2)} \frac{2^{j_1+j_2-4}}{\Gamma(1-j_2)^2 \Gamma(1-j_1)^2} \\ & \times \int_0^{\infty} ds_1 ds_1' ds_2 ds_2' \delta(s_1 - s_2 + \hat{\omega}_1) \delta(s_1' - s_2' + \hat{\omega}_2) \frac{1}{(n_1 n_2)^{j_1+j_2}} \frac{1}{(-x_{34}^2 + i\epsilon x_{43}^0)^{j_1+j_2}}. \end{aligned} \quad (\text{E.5})$$

³⁴The relation between (E.1) and the variables used in [58] is $\gamma_{12} = j_1 + j_2$, $\gamma_{14} = 1 - j_2$.

One of the space-time integrations produces the momentum conserving delta function $(2\pi)^4 \delta^4(\tilde{q} - q - \hat{\omega}_1 n_1 - \hat{\omega}_2 n_2)$ as in (2.28). The remaining integral over x_{34} can be done using the formula

$$\int d^d x \frac{e^{-i(qx)}}{(-x^2 + i\epsilon x^0)^\Delta} = \theta(q) \frac{2\pi^{d/2+1}}{\Gamma(\Delta)\Gamma(\Delta+1-\frac{d}{2})} (q^2/4)^{\Delta-d/2}. \quad (\text{E.6})$$

In this way we arrive at the desired formula for the scalar-scalar correlation

$$\langle \mathcal{O}(\omega_1, n_1) \mathcal{O}(\omega_2, n_2) \rangle_q = \frac{1}{8\pi^2} \frac{\text{SSC}(z, \omega_1, \omega_2)}{(qn_1)(qn_2)}, \quad (\text{E.7})$$

where

$$\text{SSC}(z, \omega_1, \omega_2) = \int_{\mathcal{C}_0} \frac{dj_2 dj_1}{(2\pi i)^2} K_{\text{SS}}(z, \omega_1, \omega_2) M(j_1, j_2), \quad (\text{E.8})$$

and the kernel admits the following representation

$$\begin{aligned} K_{\text{SS}} &= \frac{(j_1 + j_2 - 1)(qn_1)(qn_2)}{2^{j_1+j_2-1}(n_1 n_2)^{j_1+j_2}} \int_0^\infty ds_1 ds_2 \theta(s_1 + \hat{\omega}_1) \theta(s_1 + \hat{\omega}_2) \theta(q - n_1 s_1 - n_2 s_2) \\ &\times [(s_1 + \hat{\omega}_1)s_2]^{-j_2} [s_1(s_2 + \hat{\omega}_2)]^{-j_1} [(q - n_1 s_1 - n_2 s_2)^2]^{j_1+j_2-2}. \end{aligned} \quad (\text{E.9})$$

We rescale the integration variables $s_i \rightarrow 2(qn_i)s_i/q^2$ and introduce the dimensionless variables (2.34) and the cross ratio (2.42) to get

$$\begin{aligned} K_{\text{SS}}(z, \omega_1, \omega_2) &= \frac{1}{2} (j_1 + j_2 - 1) z^{-j_1-j_2} \int_0^\infty ds_1 ds_2 \theta(s_1 + \omega_1) \theta(s_2 + \omega_2) \theta(1 - s_1 - s_2 + s_1 s_2 z) \\ &[(s_1 + \omega_1)s_2]^{-j_2} [s_1(s_2 + \omega_2)]^{-j_1} (1 - s_1 - s_2 + s_1 s_2 z)^{j_1+j_2-2}, \end{aligned} \quad (\text{E.10})$$

As explained in the bulk of the paper, it is sufficient to consider two choices of the signs of ω_1, ω_2 , namely $+-$ and $++$. The two other choices are obtained from the relations (2.55). Here we restrict ourselves to the case $\omega_1 > 0$, so that the integration range of s_1 in (E.10) is

$$0 \leq s_1 \leq \frac{1 - s_2}{1 - s_2 z}. \quad (\text{E.11})$$

The result takes the following form

$$\begin{aligned} K_{\text{SS}}(z, \omega_1, \omega_2) &= \frac{\Gamma(j_1 + j_2) \Gamma(1 - j_1)}{2\Gamma(j_2)} z^{-j_1-j_2} \omega_1^{1-j_1-j_2} \\ &\times \int_{\max[0, -\omega_2]}^1 ds_2 s_2^{-j_1} (1 - s_2)^{j_2-1} (s_2 + \omega_2)^{-j_1} \left(1 + \omega_1 - s_2(1 + \omega_1 z)\right)^{j_1-1}. \end{aligned} \quad (\text{E.12})$$

Note that we first compute the kernel in the region where the integrals converge, namely $\text{Re}(j_1 + j_2) > 1$, and then define it in the region where we use the Mellin amplitude via analytic continuation.

Next we switch to the more convenient integration variable $s_2 = (1 + \frac{1+\omega_2}{|\omega_2|}X)^{-1}$ to get

$$K_{\text{SS}} = \frac{\Gamma(j_1 + j_2)\Gamma(1 - j_1)}{2\Gamma(j_2)} z^{-j_1-j_2} \omega_1^{1-j_1-j_2} |\omega_2|^{1-j_1-j_2} (1 + \omega_1)^{j_1-1} (1 + \omega_2)^{j_2-1} \\ \times \int_0^\infty dX \theta(1 + \text{sign}(\omega_2)X) X^{j_2-1} (1 + \text{sign}(\omega_2)X)^{-j_1} \left(X + \frac{(1-z)\omega_1|\omega_2|}{(1+\omega_1)(1+\omega_2)} \right)^{j_1-1}. \quad (\text{E.13})$$

At this point we can in principle simply evaluate the last integral in terms of hypergeometric functions. The convergence of the integral requires first considering the region $\text{Re}(j_2) > 0$ and then analytically continuing to the region of interest, $\text{Re}(j_2) < 0$.

To do this more explicitly it is convenient to perform the integration in a slightly different manner. We first represent the last factor on the right-hand side of (E.13) in Mellin form:

$$\left(X + \frac{(1-z)\omega_1|\omega_2|}{(1+\omega_1)(1+\omega_2)} \right)^{j_1-1} = \int \frac{ds}{2\pi i} \frac{\Gamma(1 - j_1 + s)\Gamma(-s)}{\Gamma(1 - j_1)} X^{j_1-1-s} \left(\frac{(1-z)\omega_1|\omega_2|}{(1+\omega_1)(1+\omega_2)} \right)^s. \quad (\text{E.14})$$

After that we integrate over X ,

$$\omega_2 > 0 : \quad \int_0^\infty dX X^{j_1+j_2-s-2} (1+X)^{-j_1} = \frac{\Gamma(1 - j_2 + s)\Gamma(j_1 + j_2 - 1 - s)}{\Gamma(j_1)}, \\ \omega_2 < 0 : \quad \int_0^1 dX X^{j_1+j_2-s-2} (1-X)^{-j_1} = \frac{\Gamma(1 - j_1)\Gamma(j_1 + j_2 - 1 - s)}{\Gamma(j_2 - s)}. \quad (\text{E.15})$$

Finally, we shift the Mellin variable $s \rightarrow j_1 + j_2 - 1 + s$ to get

$$K_{\text{SS}}^{++} = \frac{1}{2} \Gamma(j_1 + j_2)\Gamma(1 - j_1 - j_2) z^{-j_1-j_2} (1-z)^{1-j_1-j_2} (1 + \omega_1)^{-j_2} (1 + \omega_2)^{-j_1} \\ \times \int \frac{ds}{2\pi i} \frac{\Gamma(-s)\Gamma(j_2 + s)\Gamma(j_1 + s)\Gamma(1 - j_1 - j_2 - s)}{\Gamma(1 - j_1 - j_2)\Gamma(j_2)\Gamma(j_1)} \left(\frac{(1-z)\omega_1\omega_2}{(1+\omega_1)(1+\omega_2)} \right)^s. \quad (\text{E.16})$$

This is precisely the formula (4.22) we quoted in the bulk of the paper. The integration contour in (E.16) is fixed as follows: we first consider a straight line for $\text{Re}(j_2) > 0$ that runs parallel to the imaginary axis and separates the poles generated by the product of gamma functions in the numerator, i.e. the poles coming from $\Gamma(\cdots - s)$ from the left and the poles coming from $\Gamma(\cdots + s)$ from the right. We then deform the contour to the region of interest $\text{Re}(j_2) < 0$.

Let us also write down the explicit result of the integration

$$K_{\text{SS}}^{++} = \frac{\pi}{2 \sin \pi(j_1 + j_2)} (1 + \omega_1)^{-j_2} (1 + \omega_2)^{-j_1} z^{-j_1-j_2} (1-z)^{j_1+j_2-1} \\ \times {}_2F_1 \left(j_2, j_1, j_1 + j_2, \frac{(1-z)\omega_1\omega_2}{(1+\omega_1)(1+\omega_2)} \right) \\ + \frac{\Gamma(1 - j_2)\Gamma(1 - j_1)\Gamma(j_1 + j_2)\Gamma(j_1 + j_2 - 1)}{2\Gamma(j_2)\Gamma(j_1)} z^{-j_1-j_2} (\omega_1\omega_2)^{1-j_1-j_2} (1 + \omega_1)^{j_1-1} (1 + \omega_2)^{j_2-1}$$

$$\times {}_2F_1\left(1-j_2, 1-j_1, 2-j_1-j_2, \frac{(1-z)\omega_1\omega_2}{(1+\omega_1)(1+\omega_2)}\right). \quad (\text{E.17})$$

In the case $\omega_2 < 0$ we get instead

$$K_{\text{SS}}^{+-} = \frac{\pi}{2 \sin \pi(j_1 + j_2)} z^{-j_1-j_2} (1-z)^{j_1+j_2-1} (1+\omega_1)^{-j_2} (1+\omega_2)^{-j_1} \\ \times \int \frac{ds}{2\pi i} \Gamma(-s) \frac{\Gamma(1-j_1)\Gamma(j_2+s)\Gamma(1-j_1-j_2-s)}{\Gamma(1-j_1-s)\Gamma(j_2)\Gamma(1-j_1-j_2)} \left(-\frac{(1-z)\omega_1\omega_2}{(1+\omega_1)(1+\omega_2)}\right)^s, \quad (\text{E.18})$$

which is the formula (4.16) quoted in the bulk of the paper. Doing the integral we get

$$K_{\text{SS}}^{+-} = \frac{1}{2} z^{-j_1-j_2} (1-z)^{j_1-1} (-\omega_1\omega_2)^{-j_2} (1+\omega_2)^{j_2-j_1} \frac{\Gamma(1-j_1)^2 \Gamma(j_1+j_2)}{\Gamma(1+j_2-j_1)} \\ \times {}_2F_1\left(j_2, 1-j_1, 1+j_2-j_1, \frac{(1+\omega_1)(1+\omega_2)}{(1-z)\omega_1\omega_2}\right). \quad (\text{E.19})$$

This form is not particularly convenient for taking the limit $\omega_i \rightarrow 0$. Using a standard identity for the hypergeometric functions we can instead write it as follows

$$K_{\text{SS}}^{+-} = \frac{\pi}{2 \sin \pi(j_1 + j_2)} (1+\omega_1)^{-j_2} (1+\omega_2)^{-j_1} z^{-j_1-j_2} (1-z)^{j_1+j_2-1} \\ \times {}_2F_1\left(j_2, j_1, j_1+j_2, \frac{(1-z)\omega_1\omega_2}{(1+\omega_1)(1+\omega_2)}\right) \\ + \frac{\Gamma(1-j_1)^2 \Gamma(j_1+j_2) \Gamma(j_1+j_2-1)}{2\Gamma(j_2)^2} z^{-j_1-j_2} (-\omega_1\omega_2)^{1-j_1-j_2} (1+\omega_1)^{j_1-1} (1+\omega_2)^{j_2-1} \\ \times {}_2F_1\left(1-j_2, 1-j_1, 2-j_1-j_2, \frac{(1-z)\omega_1\omega_2}{(1+\omega_1)(1+\omega_2)}\right). \quad (\text{E.20})$$

Null limit of the kernel

Here we comment on the existence of a special simplifying limit in which the momentum of the sink becomes null. The representation (4.22) suggests to consider the limit

$$\frac{\omega_1\omega_2(1-z)}{1+\omega_1+\omega_2+\omega_1\omega_2} = 1, \quad (\text{E.21})$$

which corresponds to

$$z = -\frac{1+\omega_1+\omega_2}{\omega_1\omega_2}. \quad (\text{E.22})$$

Physically, this condition means that either the source or the sink carries null momentum,

$$(\text{E.21}) : \quad q^2 = 0 \quad \text{or} \quad (q + \hat{\omega}_1 n_1 + \hat{\omega}_2 n_2)^2 = 0. \quad (\text{E.23})$$

Keeping q^2 timelike and requiring that z takes the physical values $0 < z < 1$ yields the constraint $\omega_i < 0$ and $\omega_1 + \omega_2 < -1$.

In this kinematics the Mellin integral in (4.22) simplifies dramatically and can be immediately computed using Barnes' lemma with the following result

$$K_{\text{SS}}^{\text{null}}(j_1, j_2 | \omega_1, \omega_2) = \frac{\omega_1 \omega_2}{2(1 + \omega_1)(1 + \omega_2)} \left(-\frac{1 + \omega_1 + \omega_2}{(1 + \omega_1)(1 + \omega_2)} \right)^{-j_1 - j_2} \Gamma(1 - j_1) \Gamma(1 - j_2) \Gamma(j_1 + j_2), \quad (\text{E.24})$$

where we have set $z = -\frac{1 + \omega_1 + \omega_2}{\omega_1 \omega_2}$ according to (E.21). Note that on this locus two-point generalized event shape becomes one-dimensional since the kernel depends nontrivially only on the combination $\frac{z}{1 - z} = -\frac{1 + \omega_1 + \omega_2}{(1 + \omega_1)(1 + \omega_2)}$.

F Computing SSC_{++} using correlation functions

Here we show the details of the computation of the correlation SSC_{++} in (4.24) and (4.25). The starting point is the following representation of the relevant Mellin kernel

$$K_{\text{SS}}^{++}(j_1, j_2 | z, \omega_1, \omega_2) = -\frac{1}{2} \frac{j_1 j_2}{j_1 + j_2} \int_0^\infty dX \int_0^1 dt \frac{(1 - t)^2}{t^2 z^2 (1 + \omega_1 \omega_2 X)} Y_1^{j_2 - 1} Y_2^{j_1 - 1}, \quad (\text{F.1})$$

where

$$Y_1 = \frac{(1 - t)(1 - z + (1 + \omega_1)(1 + \omega_2)X)}{tz(1 + \omega_2)(1 + \omega_1 \omega_2 X)} \geq 0, \quad Y_2 = \frac{(1 - t)(1 + \omega_2)X}{z} \geq 0. \quad (\text{F.2})$$

The advantage of this representation is that for simple Mellin amplitudes like (4.9) the integrals over j_i are now very easy to take both at weak and at strong coupling. The basic integrals that we need are

$$\begin{aligned} \int_{-\epsilon - i\infty}^{-\epsilon + i\infty} \frac{dj}{2\pi i} Y^{j-1} &= \delta(1 - Y) - \delta(Y), \\ \int_{-\epsilon - i\infty}^{-\epsilon + i\infty} \frac{dj}{2\pi i} \frac{1}{j} Y^{j-1} &= -\frac{\theta(1 - Y)}{Y_+}, \end{aligned} \quad (\text{F.3})$$

where $\epsilon > 0$ and $\frac{\theta(1 - Y)}{Y_+}$ is the distribution that acts on test functions as $\int_0^1 \frac{dY}{Y} (f(Y) - f(0))$.

At weak coupling we get the distribution

$$\begin{aligned} &\int \frac{dj_2 j_1}{(2\pi i)^2} \left(\frac{1}{j_2} + \frac{1}{j_1} \right) Y_1^{j_2 - 1} Y_2^{j_1 - 1} \\ &= -\frac{\theta(1 - Y_1)}{(Y_1)_+} \left(\delta(1 - Y_2) - \delta(Y_2) \right) - \frac{\theta(1 - Y_2)}{(Y_2)_+} \left(\delta(1 - Y_1) - \delta(Y_1) \right). \end{aligned} \quad (\text{F.4})$$

We then act with this distribution on the test function

$$g(Y_1, Y_2) = -\frac{\partial(t, X)}{\partial(Y_1, Y_2)} \frac{(1 - t)^2}{2t^2 z^2 (1 + \omega_1 \omega_2 X)} \Big|_{t=t(Y_1, Y_2), X=X(Y_1, Y_2)} \quad (\text{F.5})$$

and obtain the result (4.24).

At strong coupling we get instead

$$\begin{aligned} & \int_{-\epsilon-i\infty}^{-\epsilon+i\infty} \frac{dj_2 j_1}{(2\pi i)^2} (j_1 + j_2)(1 + j_1 + j_2) Y_1^{j_2-1} Y_2^{j_1-1} \\ &= (\hat{j}_1 + \hat{j}_2)(1 + \hat{j}_1 + \hat{j}_2) \int_{-\epsilon-i\infty}^{-\epsilon+i\infty} \frac{dj_2 j_1}{(2\pi i)^2} Y_1^{j_2-1} Y_2^{j_1-1}, \end{aligned} \quad (\text{F.6})$$

where $\hat{j}_2 = Y_1 \partial_{Y_1} + 1$ and $\hat{j}_1 = Y_2 \partial_{Y_2} + 1$. Using (F.3) and (F.6) one can check that the result takes the form

$$\text{SSC}_{++}^{\text{strong}} = \frac{1}{2} (\partial_{Y_1}^2 g(1, 0) + \partial_{Y_2}^2 g(0, 1) - \partial_{Y_1}^2 g(1, 1) - \partial_{Y_2}^2 g(1, 1) - 2 \partial_{Y_1} \partial_{Y_2} g(1, 1)) \quad (\text{F.7})$$

yielding (4.25).

G Bulk point singularity

According to (4.25), the expressions for the correlations at strong coupling with ω_1 and ω_2 of the same sign contain a new scale $\omega_1 + \omega_2 + z\omega_1\omega_2$. To elucidate its origin, we revisit the calculation of the SSC with the Mellin amplitude of the form (4.39). For $p = 0$ and $p = 1$ it coincides with the expression at weak and strong coupling. For $p \geq 1$ the corresponding expression for the four-point correlation function has a bulk singularity.

Applying (E.12) and (E.8), we change the integration variable as $s_2 = 1/(1 + \omega_1 s)$ and obtain for $\omega_1 > 0$

$$\begin{aligned} \text{SSC}_p(\omega_1, \omega_2) &= \int_{\text{Re } j_i = -\delta} \frac{dj_1 dj_2}{(2\pi i)^2} [j_1 j_2 (1 + j_1 + j_2)]^p \frac{(j_1 + j_2)}{j_1 j_2} \frac{\Gamma(-j_2) \Gamma(1 + j_1 + j_2)}{\Gamma(1 + j_1)} z^{-j_1 - j_2} \\ &\times \int_0^{s_{\max}} ds s^{j_1-1} (1 + \omega_2(1 + \omega_1 s))^{-j_2} (s(1 + \omega_1) + (1 - z))^{j_2-1}, \end{aligned} \quad (\text{G.1})$$

where s_{\max} is given by ∞ and $-(1 + \omega_2)/(\omega_1 \omega_2)$ for positive and negative ω_2 , respectively. The integration over small s produces a pole $1/j_1$. For $p > 1$ it is compensated by the prefactor and, therefore, does not contribute. This implies that $\text{SSC}_p(\omega_1, \omega_2) = 0$ for negative ω_2 whereas for positive ω_2 it does not contain powers of $1/(1 + \omega_1 z)$ and $1/(1 + \omega_2 z)$.

For $p \geq 2$ we rewrite the previous relation as

$$\text{SSC}_p(\omega_1, \omega_2) = (\partial_1 \partial_2)^{p-1} (1 + \partial_1 + \partial_2)^p (\partial_1 + \partial_2) I(\epsilon_1, \epsilon_2) \Big|_{\epsilon_i=0}, \quad (\text{G.2})$$

where $\partial_i = \partial_{\epsilon_i}$ and the notation was introduced for

$$\begin{aligned} I(\epsilon_1, \epsilon_2) &= \int_{\text{Re } j_i = -\delta} \frac{dj_1 dj_2}{(2\pi i)^2} \frac{\Gamma(-j_2) \Gamma(1 + j_1 + j_2)}{\Gamma(1 + j_1)} z^{-j_1 - j_2} e^{\epsilon_1 j_1 + \epsilon_2 j_2} \\ &\times \int_0^{s_{\max}} ds s^{j_1-1} (1 + \omega_2(1 + \omega_1 s))^{-j_2} (s(1 + \omega_1) + (1 - z))^{j_2-1}. \end{aligned} \quad (\text{G.3})$$

Using the identity

$$\int_{\text{Re } j_i = -\delta} \frac{dj_1 dj_2}{(2\pi i)^2} \frac{\Gamma(-j_2)\Gamma(1+j_1+j_2)}{\Gamma(1+j_1)} X_1^{j_1} X_2^{j_2} = \delta(1+X_2-X_1), \quad (\text{G.4})$$

we obtain

$$I(\epsilon_1, \epsilon_2) = \int_0^{s_{\max}} \frac{ds}{s(s(1+\omega_1)+1-z)} \delta\left(1 + \frac{s(1+\omega_1)+1-z}{z(1+\omega_2(1+\omega_1 s))} e^{\epsilon_1} - \frac{s}{z} e^{\epsilon_2}\right). \quad (\text{G.5})$$

The integral is localized on the solution of the equation

$$1 + \frac{s_*(1+\omega_1)+1-z}{z(1+\omega_2(1+\omega_1 s_*))} e^{\epsilon_1} - \frac{s_*}{z} e^{\epsilon_2} = 0 \quad (\text{G.6})$$

satisfying the condition $0 \leq s_* \leq s_{\max}$ and it is given by

$$I(\epsilon_1, \epsilon_2) = \frac{z(1+\omega_2(1+\omega_1 s_*))}{s_*(s_*(1+\omega_1)+1-z)(\omega_1\omega_2 z - e^{\epsilon_1}(1+\omega_2(1+2s_*\omega_1)) + e^{\epsilon_2}(1+\omega_1))}. \quad (\text{G.7})$$

At small ϵ_i we have

$$s_* = \frac{1}{\omega_2} + z + O(\epsilon_i), \quad I(\epsilon_1, \epsilon_2) = -\frac{\omega_2^2 z}{(1+\omega_2 z)(\omega_1 + \omega_2 + \omega_1 \omega_2 z)} (1 + O(\epsilon_i)). \quad (\text{G.8})$$

Notice that $s_* < 0$ for $-1 < \omega_2 < 0$ and, therefore, $I(\epsilon_1, \epsilon_2) = 0$ in this case. For $\omega_2 > 0$ we observe that $I(\epsilon_1, \epsilon_2)$ contains two factors in the denominator. As mentioned above, the first one $(1+\omega_2 z)$ disappears in the final expression for $\text{SSC}_p(\omega_1, \omega_2)$. The derivatives in (G.2) increase the power of $\omega_1 + \omega_2 + \omega_1 \omega_2 z$ in the denominator. The close examination shows that each power of ϵ_i in the expansion of $I(\epsilon_1, \epsilon_2)$ is accompanied by a factor of $1/(\omega_1 + \omega_2 + \omega_1 \omega_2 z)^2$. This leads to (4.41). For $p = 2$ we obtain from (G.2) the relation (4.43) with the coefficient functions given by

$$\begin{aligned} c_0 &= 2520 (\omega_1 + \omega_2)^2, \\ c_1 &= 1260 (\omega_1 + \omega_2) (5\omega_1 + 5\omega_2 - 4), \\ c_2 &= 280 (20\omega_1^2 + 40\omega_2\omega_1 - 43\omega_1 + 20\omega_2^2 - 43\omega_2 + 9), \\ c_3 &= 140 (15\omega_1^2 + 30\omega_2\omega_1 - 72\omega_1 + 15\omega_2^2 - 72\omega_2 + 41), \\ c_4 &= 60 (5\omega_1^2 + 10\omega_2\omega_1 - 58\omega_1 + 5\omega_2^2 - 58\omega_2 + 75), \\ c_5 &= 10 (\omega_1^2 + 2\omega_2\omega_1 - 44\omega_1 + \omega_2^2 - 44\omega_2 + 141), \\ c_6 &= -4 (3\omega_1 + 3\omega_2 - 38), \\ c_7 &= 3. \end{aligned} \quad (\text{G.9})$$

H Details of the derivation in Section 5

Summary of the SSC correlation

In this subsection we recall some of the key steps in obtaining the SSC correlation as an integrated correlation function.

It proves very efficient to go to new coordinates $x^\mu \rightarrow y^\mu$ by performing a conformal transformation [1, 49] (see Section 2.2),

$$y^+ = -\frac{1}{x^+}, \quad y^- = x^- - \frac{\vec{x}^2}{x^+}, \quad \vec{y} = \frac{\vec{x}}{x^+}, \quad dy^2 = \frac{dx^2}{(x^+)^2}, \quad (\text{H.1})$$

where the notation was introduced for the light-like coordinates x^\pm and $\vec{x} = (x, \bar{x})$,

$$x_{\alpha\dot{\alpha}} = x_\mu(\sigma^\mu)_{\alpha\dot{\alpha}} = \begin{bmatrix} x^+ & \bar{x} \\ x & x^- \end{bmatrix}, \quad dx^2 = dx^+ dx^- - dx d\bar{x}. \quad (\text{H.2})$$

Then sending the detectors at points 1 and 2 to null infinity is equivalent to setting $y_{1,2}^+ = 0$. The calculations are greatly simplified by using conformal invariance to ‘gauge away’ some of the coordinates at the source points 3 and 4. So, we work in the special frame

$$y_1^+ = y_2^+ = 0, \quad y_3^+ = 1, \quad \vec{y}_3 = \vec{y}_4 = y_4^- = 0, \quad y_4^+ \rightarrow \infty. \quad (\text{H.3})$$

At the end the covariant form can be easily restored by undoing the gauges and switching back to the coordinates $x_{3,4}$.

The next step is the Fourier transform from the detector times to frequencies, $y_{1,2}^- \rightarrow \hat{\omega}_{1,2}$. Applied to the correlation function G_{00} in (5.1), this procedure results in

$$\begin{aligned} \mathbb{G}_{00}(y; n_i, \hat{\omega}_i) &= \int_{-\infty}^{\infty} dy_1^- dy_2^- e^{-i(y_1^- \hat{\omega}_1 + y_2^- \hat{\omega}_2)} \langle \phi^\dagger(y_4) O(0^+, y_1^-, \vec{y}_1) O(0^+, y_2^-, \vec{y}_2) \phi(y_3) \rangle \\ &= \int_{-\infty}^{\infty} dy_1^- dy_2^- e^{-i(y_1^- \hat{\omega}_1 + y_2^- \hat{\omega}_2)} F(y), \end{aligned} \quad (\text{H.4})$$

where the function F was defined in (5.4). After integrating over y_1^-, y_2^- we restore the covariant notation and obtain

$$\mathbb{G}_{00}(x; \gamma, \Omega_i) = \frac{1}{x^2} \mathcal{G}(\gamma, \Omega_i), \quad (\text{H.5})$$

where $x \equiv x_{34}$. The function \mathcal{G} generalizes that in (5.11). It depends on the dimensionless variables

$$\gamma = \frac{2(xn_1)(xn_2)}{x^2(n_1n_2)}, \quad \Omega_i = \hat{\omega}_i(xn_i). \quad (\text{H.6})$$

The Mellin kernel for the dimensionless function $\mathcal{G}(\gamma, \Omega_i)$ in the coordinate representation is given by the double Schwinger integral (see Appendix E)

$$K_{\mathcal{G}}(j_i|x) = (-\gamma)^{j_1+j_2-1} \int_0^\infty dS_1 dS_2 e^{-i(S_1+S_2)} (S_2 (S_1 + \Omega_1))_+^{-j_2} (S_1 (S_2 + \Omega_2))_+^{-j_1}, \quad (\text{H.7})$$

where the parameters $S_i = s_i(xn_i)$ are dimensionless (see (H.6)). The S -factors are understood as the $+$ distribution $1/S_+^j$ and $1/(S + \Omega)_+^j$. This makes differentiating with respect to S or Ω safe, as long as $j \neq -1, -2, \dots$.

After the Fourier transform to momentum space $x \rightarrow q$ we get (see (E.9))

$$K_{\text{SS}}(j_i|q) = ((n_1 n_2)/2)^{-j_1-j_2} \mathbb{I}_{j_1, j_2} \left\{ \sigma_{j_1+j_2}(q - n_1 s_1 - n_2 s_2) \right\}, \quad (\text{H.8})$$

where

$$\mathbb{I}_{j_1, j_2} \{ \sigma \} = \int_0^\infty ds_1 ds_2 (s_2 (s_1 + \hat{\omega}_1))_+^{-j_2} (s_1 (s_2 + \hat{\omega}_2))_+^{-j_1} \sigma, \quad (\text{H.9})$$

$$\sigma_j(\hat{q}) = \int \frac{d^4 x e^{-i\hat{q}x}}{(-x^2 + i0x^0)^j} = C_j \theta(\hat{q}^0) \theta(\hat{q}^2) (\hat{q}^2)^{j-2}, \quad \hat{q} = q - n_1 s_1 - n_2 s_2 \quad (\text{H.10})$$

and $C_j = \pi^3 / (2^{2j-3} \Gamma(j) \Gamma(j-1))$. The variables s_i have the same dimension and Lorentz charge as the frequencies $\hat{\omega}_i$. It is convenient to introduce new dimensionless variables z and ω_i (cf. (2.42) and (2.34)), as well as to rescale the integration variables $s_i \rightarrow (q^2/2(qn_i))s_i$. After this the scalar kernel becomes

$$K_{\text{SS}} = C_{j_1+j_2} z^{1-j_1-j_2} \mathbb{I}_{j_1, j_2} \left\{ \theta(q^0 - n_i^0 s_i) \theta(1 - s_1 - s_2 + z s_1 s_2) (1 - s_1 - s_2 + z s_1 s_2)^{j_1+j_2-2} \right\}, \quad (\text{H.11})$$

where the integral operator \mathbb{I}_{j_1, j_2} is defined in (H.9) but now with $\hat{\omega} \rightarrow \omega$. In the rest frame $q^\mu = (q^0, \vec{0})$ with $q^0 > 0$ and $n_i^\mu = (1, \vec{n}_i)$ with $\vec{n}_i^2 = 1$ we have $q^2 = (q^0)^2$, $(qn_i) = q^0$. The condition $\hat{q}^0 \geq 0$ becomes $2 - s_1 - s_2 \geq 0$, thus reducing the integration domain to $0 \leq s_i \leq 1$. The conditions $s_i + \omega_i \geq 0$ restrict the domain further, if one or both $\omega_i < 0$. In this section most of the time we will consider the simplest case $\omega_i \geq 0$ and will comment on the choice $\omega_1 < 0$, $\omega_2 > 0$ in Section H. The last condition $\hat{q}^2 \geq 0 \Rightarrow 1 - s_1 - s_2 + z s_1 s_2 \geq 0$ can be resolved by the following change of variables:

$$s_1 \rightarrow u, \quad s_2 \rightarrow \frac{(1-u)v}{1-zu}; \quad u \in [\max(0, -\omega_1), 1], \quad v \in [0, 1]. \quad (\text{H.12})$$

Relations QSC/SSC and ESC/SSC

In this subsection we work out the simplest example QSC/SSC in detail and explain the main steps. The principal difference compared to the standard case is that instead of integrating over the detector time x^- , we now Fourier transform it into the energy $\hat{\omega}$. Thus, if earlier we could neglect the total time derivative ∂_{x^-} contained in the operator (5.7), now it contributes to the Fourier transform terms $\sim \hat{\omega}$. This calls for a more efficient formalism.

Spinor formalism

We introduce the following notation for the λ -projections consistent with their Lorentz charges. The auxiliary spinors $\lambda_\pm \equiv \langle \pm |$ and $\tilde{\lambda}_\pm \equiv [\pm |$ satisfy completeness conditions

$$\begin{aligned} |+\rangle^\alpha \langle -|_\beta - |-\rangle^\alpha \langle +|_\beta &= \delta_\beta^\alpha \Rightarrow \langle +|^\alpha |-\rangle_\alpha \equiv \langle +|-\rangle = 1, \\ |+\rangle^{\dot{\alpha}} [-|_{\dot{\beta}} - | -|_{\dot{\beta}}]^{\dot{\alpha}} [+|_{\dot{\beta}} &= \delta_{\dot{\beta}}^{\dot{\alpha}} \Rightarrow [+|^{\dot{\alpha}} | -]_{\dot{\alpha}} \equiv [+| -] = 1. \end{aligned} \quad (\text{H.13})$$

The four-vectors have the projections

$$\begin{aligned} y^+ &= \langle -|^\alpha y_{\alpha\dot{\alpha}}|-\rangle^{\dot{\alpha}} = [-|\dot{\alpha}\tilde{y}^{\dot{\alpha}\alpha}|-\rangle_\alpha \equiv \langle -|y|-\rangle = [-|\tilde{y}|-\rangle, \\ y^- &= \langle +|y|+\rangle = [+|\tilde{y}|+\rangle, \quad y = \langle +|y|-\rangle = [-|\tilde{y}|+\rangle, \quad \bar{y} = \langle -|y|+\rangle = [+|\tilde{y}|-\rangle. \end{aligned} \quad (\text{H.14})$$

In terms of projected variables and in the frame (H.3) the matrices (5.8) become

$$\begin{aligned} \mathcal{X}_{1[234]} &\equiv \begin{pmatrix} \langle -|\mathcal{X}_{1[234]}|-\rangle & \langle -|\mathcal{X}_{1[234]}|+\rangle \\ \langle +|\mathcal{X}_{1[234]}|-\rangle & \langle +|\mathcal{X}_{1[234]}|+\rangle \end{pmatrix} \\ &= \begin{pmatrix} \bar{y}_{12}(y_2\bar{y}_1 - y_3^-) & y_2\bar{y}_{12}y_1^- \\ y_2(\bar{y}_1y_{13}^- + \bar{y}_2y_3^-) - y_1(\bar{y}_1y_{23}^- + \bar{y}_2y_3^-) + y_{21}y_3^- & y_1^-(y_2y_{13}^- + y_1y_{32}^-) \end{pmatrix}, \\ \mathcal{X}_{[12]3} &= \begin{pmatrix} \bar{y}_{12} & -y_2\bar{y}_1 - y_{23}^- \\ y_1\bar{y}_2 + y_{13}^- & y_1y_{23}^- + y_2y_{31}^- \end{pmatrix}, \quad \mathcal{X}_{[12]4} = \begin{pmatrix} \bar{y}_{12} & -y_2^- \\ y_1^- & 0 \end{pmatrix}. \end{aligned} \quad (\text{H.15})$$

The operator (5.7) is decomposed into two projections:

$$\begin{aligned} \mathcal{D} &= \tilde{\lambda}_{-\dot{\alpha}} \tilde{\partial}_y^{\dot{\alpha}\alpha} \frac{\partial}{\partial \lambda_-^\alpha} = \partial_{y^-} \partial_+ + \partial_{\bar{y}} \partial_0, \\ \mathcal{D}^2 &= \partial_{\bar{y}}^2 \partial_0 (\partial_0 - 1) + 2\partial_{y^-} \partial_{\bar{y}} \partial_+ (\partial_0 - 1) + \partial_{y^-}^2 \partial_+^2, \end{aligned} \quad (\text{H.16})$$

where the projected spinor derivatives act as follows:

$$\begin{aligned} \partial_0|\pm\rangle &= \mp|\pm\rangle, \quad \partial_+|-\rangle = |+\rangle, \quad \partial_+|+\rangle = 0, \\ \partial_0 y^\pm &= \pm y^\pm, \quad \partial_0 \bar{y} = \bar{y}, \quad \partial_0 y = -y, \quad \partial_+ y^+ = y, \quad \partial_+ \bar{y} = y^-, \quad \partial_+ y^- = \partial_+ y = 0, \\ \partial_{y^-} &\equiv [-|\tilde{\partial}_y|-\rangle \Rightarrow \partial_{y^-} y^- = 1, \quad \partial_{\bar{y}} \equiv [-|\tilde{\partial}_y|+\rangle \Rightarrow \partial_{\bar{y}} \bar{y} = 1, \text{ otherwise } 0. \end{aligned} \quad (\text{H.17})$$

These rules allow us to expand out the differential operators in (5.6) and are easily automatized. Below we show in detail how this is done for the simplest relation QSC/SSC.

QSC differential operator in coordinate space

The QSC correlation is obtained from the relations (5.6)–(5.9) and is given by

$$\begin{aligned} \text{QSC} &= (\partial_{y_1^-} \partial_+ + \partial_{\bar{y}_1} \partial_0) \left[\langle -|\mathcal{X}_{1[234]}|-\rangle \frac{\mathcal{G}(\gamma, \Omega_i)}{(y_{12}\bar{y}_{12}y_3^-)^2} \right] \\ &= \partial_{y_1^-} \left[\left(\langle +|\mathcal{X}_{1[234]}|-\rangle + \langle -|\mathcal{X}_{1[234]}|+\rangle \right) \frac{\mathcal{G}}{(y_{12}\bar{y}_{12}y_3^-)^2} \right] + \partial_{\bar{y}_1} \left[2\langle -|\mathcal{X}_{1[234]}|-\rangle \frac{\mathcal{G}}{(y_{12}\bar{y}_{12}y_3^-)^2} \right], \end{aligned} \quad (\text{H.18})$$

where (see (H.6))

$$\Omega_i = (y_3^- - y_i \bar{y}_i) \hat{\omega}_i, \quad \gamma = -\frac{(y_3^- - y_1 \bar{y}_1)(y_3^- - y_2 \bar{y}_2)}{y_{12}\bar{y}_{12}y_3^-}. \quad (\text{H.19})$$

The next step is the Fourier transform $y^- \rightarrow \hat{\omega}$ (recall (H.4)). The first term in (H.18) with the total detector time derivative $\partial_{y_1^-}$ gives rise to terms proportional to Ω_1 . This is in

contrast with the standard case (i.e. $\hat{\omega}_i = 0$) where the time derivatives were suppressed by the time integral. We distribute the derivatives in (H.18) and restore the covariant form to obtain the generalization of the first relation in (5.11),

$$\text{QSC}(x) = \frac{(xn_2)}{(n_1n_2)^2x^4} \left[\frac{\Omega_1}{2\gamma} \left((\gamma - 2)\mathcal{G}_{\Omega_1} - \gamma\mathcal{G}_{\Omega_2} + i\mathcal{G} \right) + (\gamma - 1)\mathcal{G}_\gamma + \mathcal{G} \right]. \quad (\text{H.20})$$

On the other hand, we have the identity

$$\frac{(n_2\partial_x)}{2(n_1n_2)^2} \left[\frac{\mathcal{G}(\gamma, \Omega)}{x^2} \right] = \frac{(xn_2)}{(n_1n_2)^2x^4} \left[(1 - \gamma)\mathcal{G}_\gamma + \frac{\Omega_1}{\gamma}\mathcal{G}_{\Omega_1} - \mathcal{G} \right]. \quad (\text{H.21})$$

Recalling that $\text{SSC}(x) = \mathcal{G}(x)/x^2$ (see (H.5)), we can combine (H.20) and (H.21) into

$$\text{QSC}(x) = -\frac{1}{(n_1n_2)} (n_2\partial_x)\text{SSC}(x) + \frac{(xn_2)}{(n_1n_2)^2x^4} \Omega_1 \left[\mathcal{G}_{\Omega_1} - \mathcal{G}_{\Omega_2} + \frac{i}{\gamma}\mathcal{G} \right]. \quad (\text{H.22})$$

QSC differential operator in momentum space

Our final goal is to express the QSC kernel as a differential operator in momentum space acting on the SSC kernel. We start by inserting the Mellin kernel $K_{\mathcal{G}}(x)$ defined in (H.7) into the right-hand side of (H.20) and then we switch back to the dimensionfull variables s_i and $\hat{\omega}_i$:

$$\begin{aligned} K_{\text{QS}}(x) = & \frac{1}{(n_1n_2)^2} (-x^2(n_1n_2)/2)^{-j_1-j_2} \mathbb{I}_{j_1, j_2} \left\{ e^{-is_k(xn_k)} \left[\frac{i\hat{\omega}_1}{2} + \left(1 - j_1 - \frac{j_2s_1}{s_1 + \hat{\omega}_1} \right) \frac{1}{(xn_1)} \right. \right. \\ & \left. \left. + \frac{j_1\hat{\omega}_1}{(n_1n_2)x^2(s_2 + \hat{\omega}_2)}(xn_1) + \frac{2j_1(s_1 + \hat{\omega}_1) + j_2(2s_1 + \hat{\omega}_1)}{(n_1n_2)x^2(s_1 + \hat{\omega}_1)}(xn_2) \right] \right\}. \end{aligned} \quad (\text{H.23})$$

When Fourier transforming the right-hand side of (H.23), $K_{\text{QS}} = \int d^4x e^{-ixq} K_{\text{QS}}(x)$, we encounter the basic Fourier integral (H.10) and two new ones:

$$\int d^4x e^{-ix\hat{q}} (xn_k)(-x^2)^{-j-1} = -i\partial_{s_k} \sigma_{j+1} = \frac{i}{j} [(qn_k) - (n_k n_i) s_i] \sigma_j, \quad (\text{H.24})$$

$$\int d^4x e^{-ix\hat{q}} \frac{(-x^2)^{-j}}{(xn_1)} \xrightarrow{-i\partial/\partial s_1} \sigma_j. \quad (\text{H.25})$$

We use the relation (H.25) in (H.23) by pulling out a total derivative ∂_{s_1} from the pole $1/(xn_1)$,

$$(s_1 + \hat{\omega}_1)^{-j_2} s_1^{-j_1} \left(1 - j_1 - \frac{j_2s_1}{s_1 + \hat{\omega}_1} \right) = \partial_{s_1} \left[(s_1 + \hat{\omega}_1)^{-j_2} s_1^{-j_1} \right] \quad (\text{H.26})$$

and integrating it by parts.³⁵ Thus, all the terms in (H.23) are reduced to the basic Fourier integral (H.10). Switching over to the dimensionless variables $s_i \rightarrow (q^2/2(qn_i))s_i$, we obtain the following Schwinger integral with the measure defined in (H.11):

$$K_{\text{QS}} =$$

³⁵The boundary terms vanish under suitable conditions on the parameters j_i .

$$\frac{i(qn_2)}{2(n_1n_2)(j_1+j_2)}\mathbb{I}_{j_1,j_2}\left\{\left[2(j_1+j_2+j_2z\omega_1)-\frac{j_2\omega_1(z\omega_1+1)}{s_1+\omega_1}+\frac{j_1\omega_1(z\omega_2+1)}{s_2+\omega_2}\right]\sigma_{j_1+j_2}\right\}. \quad (\text{H.27})$$

The terms with poles $1/(s_i + \omega_i)$ can be interpreted as derivatives of $K_{\text{SS}}(q) \sim \mathbb{I}_{j_1,j_2}\{\sigma_{j_1+j_2}\}$ with respect to ω_i . In this way we arrive at the final result

$$K_{\text{QS}} = \frac{i(qn_2)}{(n_1n_2)}\left\{1 + \frac{\omega_1}{2(j_1+j_2)}\left[2j_2z + (1+z\omega_1)\partial_{\omega_1} - (1+z\omega_2)\partial_{\omega_2}\right]\right\}K_{\text{SS}}. \quad (\text{H.28})$$

This is our first example of a differential operator (5.13) relating two correlations. We remark that Eq. (H.28) contains the kinematic prefactor $i(qn_2)/(n_1n_2)$ which has been stripped off the kernels in (5.10), (5.12) and (5.13). Setting $\omega_i = 0$ reproduces the standard relation (5.12).

ESC differential operator

The case ESC/SSC is treated in a similar way. The analog of (H.18), after doing the spinor variables algebra is (recall (H.15)–(H.17))

$$\begin{aligned} \text{ESC} = & 12\partial_{\bar{z}_1}^2 \left[\langle -|\mathcal{X}_{1[234]}|-\rangle^2 G \right] + 12\partial_{z_1^-}\partial_{\bar{z}_1} \left[\left(\langle +|\mathcal{X}_{1[234]}|-\rangle + \langle -|\mathcal{X}_{1[234]}|+\rangle \right) \langle -|\mathcal{X}_{1[234]}|-\rangle G \right] \\ & + 2\partial_{z_1^-}^2 \left[\left(2\langle +|\mathcal{X}_{1[234]}|+\rangle \langle -|\mathcal{X}_{1[234]}|-\rangle + \left(\langle +|\mathcal{X}_{1[234]}|-\rangle + \langle -|\mathcal{X}_{1[234]}|+\rangle \right)^2 \right) G \right], \end{aligned} \quad (\text{H.29})$$

with $G = \mathcal{G}/(z_{12}\bar{z}_{12}z_3^-)^3$. After distributing the derivatives and restoring the covariant notation, the analog of (H.23) contains a pole $1/(xn_1)$ (the measure $\hat{\mathbb{I}}_{j_1,j_2}$ is not shown):

$$\begin{aligned} & \frac{\hat{\omega}_1}{4(xn_1)} \left[\frac{j_2(xn_2)((j_1+j_2)s_1 + (j_1-1)\hat{\omega}_1)}{zx^2(s_1+\hat{\omega}_1)^2} - \frac{i((j_1+j_2-1)s_1 + (j_1-1)\hat{\omega}_1)}{(s_1+\hat{\omega}_1)} \right] \\ & \xrightarrow{\int ds_1 \partial_{s_1}} -\frac{1}{4}s_1\hat{\omega}_1 \left(1 + \frac{ij_2(xn_2)}{zx^2(s_1+\hat{\omega}_1)} \right). \end{aligned} \quad (\text{H.30})$$

Here we pulled ∂_{s_1} out and integrated it by parts (recall (H.26)). The remaining terms are polynomial of the type $(xn_1)^p(xn_2)^q$. Their Fourier transforms are done by repeated use of the relations (H.10), (H.24) and (H.25). The sum of all the terms contains poles in $s_i + \omega_i$ (but no positive powers!) which are converted to derivatives with respect to ω_i . The result for the coefficients of the differential operator (5.13) is shown in (5.16). Setting $\omega_i = 0$ we recover the standard relation (5.12).

Remarks

We conclude this subsection by a couple of remarks. The first term in (H.22) is a total x -space derivative with a simple Fourier transform, so we might have saved some work by using the shorter form (H.22) of the relation (H.20). However, the Fourier transform of the

total derivative term is not so obvious in the cases QQC, EQC and EEC, as we explain in the next subsection.

A related issue is a key feature of the right-hand side of (H.27), namely the absence of positive powers of $s_i + \omega_i$. They would have been an obstruction for the interpretation of the right-hand side as a differential operator, as we did for example in (H.28). This property is automatic in the cases QSC and ESC. However, in the cases QQC, EQC and EEC positive powers do appear, already in the total derivative term written as a Schwinger integral. Since we know the expected result of its Fourier transform, we can derive highly non-trivial identities relating the obstruction terms to simpler ones. It turns out that these identities suffice for eliminating the obstruction terms also in the main (non-derivative) part. In this way we derive a differential operator for the relation to the SSC kernel. We illustrate this phenomenon in the next subsection on the simplest case QQC.

Relation QQC/SSC

Differential operator in coordinate space

The QQC correlation is obtained from (5.6)–(5.9) (see (H.15) and (H.19)):

$$\text{QQC} = (\partial_{y_1^-} \partial_{1_+} + \partial_{\bar{y}_1} \partial_{1_0})(\partial_{y_2^-} \partial_{2_+} + \partial_{\bar{y}_2} \partial_{2_0}) \left[\langle 1_- | \mathcal{X}_{[12]3} | 2_- \rangle \langle 1_- | \mathcal{X}_{[12]4} | 2_- \rangle \frac{\mathcal{G}(\gamma, \Omega_i)}{(y_{12} \bar{y}_{12} y_3^-)^2} \right]. \quad (\text{H.31})$$

Notice that the spinor derivatives ∂_+, ∂_0 act separately at points 1 and 2. Doing the algebra and restoring the covariant form we obtain a differential operator that consists of two parts:

(i) total derivative applied to a function of γ and Ω (the generalization of (5.11)):

$$\begin{aligned} \text{QQC}_{\text{tot.der.}} &= \frac{1}{(n_1 n_2)^2 x^4} \square_x \left(\frac{\mathcal{G}(\gamma, \Omega)}{x^2} \right) = \frac{1}{(n_1 n_2)^2 x^4} \left\{ \partial_\gamma [(1 - \gamma) \gamma \partial_\gamma] \right. \\ &\quad \left. - ((\gamma - 1) \partial_\gamma + 1) \Omega_1 \partial_{\Omega_1} - ((\gamma - 1) \partial_\gamma + 1) \Omega_2 \partial_{\Omega_2} + \frac{1}{\gamma} \Omega_1 \Omega_2 \partial_{\Omega_1, \Omega_2} \right\} \mathcal{G}; \quad (\text{H.32}) \end{aligned}$$

(ii) deviation from the total derivative by terms proportional to Ω :

$$\begin{aligned} \text{QQC}_{\text{dev.}} &= \frac{1}{(n_1 n_2)^2 x^4} \frac{i \Omega_1}{4 \gamma} \\ &\quad \times \left\{ \frac{i}{2} \Omega_2 + 2 \gamma + 2 \gamma (\gamma - 1) \partial_\gamma + (\gamma - 2) \Omega_2 \partial_{\Omega_1} + i \gamma \Omega_2 \partial_{\Omega_1, \Omega_2} \right\} \mathcal{G} + (1 \leftrightarrow 2). \quad (\text{H.33}) \end{aligned}$$

Differential operator in momentum space. Total derivative identity

The deviation term (H.33) is treated as in Section H. The analog of (H.27) contains no positive powers of $s_i + \omega_i$, so it can be turned into a differential operator. The latter is simplified with the help of the differential equation for the scalar kernel (5.17) with the result shown in (5.15).

The total derivative term (H.32) requires special care. Although its Fourier transform is expected to be very simple, this is by no means obvious. Indeed, in order to obtain this Fourier transform we need to prove the following highly non-trivial identity:

$$\mathbb{I}_{j_1, j_2} \left\{ \left[j_1 (z\omega_1\omega_2 + \omega_1 + 2\omega_2 + 2) - \omega_1 - 1 - \frac{j_2\omega_1 (z\omega_1\omega_2 + \omega_1 + \omega_2 + 1)}{s_1 + \omega_1} \right. \right. \\ \left. \left. + (s_2 + \omega_2) \left(\frac{j_2\omega_1 (z\omega_1 + 1)}{s_1 + \omega_1} - (zj_2\omega_1 + j_1 + j_2 - 1) \right) \right] \sigma_{j_1+j_2} + (1 \leftrightarrow 2) \right\} = 0. \quad (\text{H.34})$$

Notice the presence of positive power of $s_i + \omega_i$ in the second line. This is an example of ‘obstruction’ terms being replaced by terms of the differential operator type.

The proof of (H.34) makes use of the variables (H.12) spanning the interval $u, v \in [0, 1]$ if $\omega_i \geq 0$. We can rewrite the integrand in (H.34) as a sum of total derivatives:³⁶

$$\int_0^1 du dv \left\{ \partial_v \left[v^{1-j_2} (1-v)^{j_1+j_2-1} (\omega_2(1-uz) + v(1-u))^{-j_1} \right] \right. \\ \times u^{-j_1} (1-u)^{j_1-1} (1-zu)^{j_1+j_2-2} (zu^2 - 2zu + 1) (\omega_1 + u)^{-j_2} \\ \left. + \partial_u \left[u^{1-j_1} (1-u)^{j_1} (1-zu)^{j_1+j_2-1} (\omega_1 + u)^{-j_2} (\omega_2(1-uz) + v(1-u))^{-j_1} \right] v^{-j_2} (1-v)^{j_1+j_2-1} \right\}. \quad (\text{H.35})$$

The boundary terms in the two integrals vanish if $0 < \text{Re}(j_1) < 1$, $\text{Re}(j_2) < 1$ and $\text{Re}(j_1 + j_2) > 1$. If $\omega_1 < 0$ and $\omega_2 \geq 0$, the variable u is in the interval $u \in [-\omega_1, 1]$. In this case the factor $(\omega_1 + u)^{-j_2}$ in (H.35) vanishes at the boundary $u = -\omega_1$ provided that $\text{Re}(j_2) < 0$. The application domain of this identity can be extended by analytic continuation in j_1, j_2 .

Relations EQC/SSC and EEC/SSC

The new feature in the cases EQC/SSC and EEC/SSC is that obstruction terms with positive powers of $s_i + \omega_i$ appear not only in the Fourier transform of the total derivative part but also in the deviation terms. Requiring that the Fourier transforms of the total derivative terms equal the expressions originating from (5.11), we find two new identities of the type (H.34). More identities are generated by differentiating the existing ones with respect to ω_i , thus lowering the powers of $s_i + \omega_i$. For example, the derivative $\partial_{\omega_1, \omega_2}$ of (H.34) removes all the positive powers, resulting in a differential equation for $K_{\text{SS}}(q)$. We find altogether 11 linearly independent identities. Adding the appropriate linear combinations of identities to the deviation terms, we succeed in removing all the obstruction terms. The resulting differential operators for EQC and EEC are listed in the ancillary file.

An interesting byproduct of the procedure is a particular linear combination of identities that amounts to a simple homogeneous partial differential equation for the scalar kernel K_{SS} ,

³⁶ES is grateful to Dima Chicherin for a discussion on this point.

see (5.17). It arises as a consistency condition for the Fourier transform of the Schwinger integral in (H.7) and its space-time derivatives.

Equation (5.17) can be solved by separation of variables. For example, we can substitute

$$K_{\text{SS}}(z, \omega_i) = (\omega_2 + 1)^{j_2 - j_1} (\omega_1 \omega_2)^{-j_2} F(X), \quad X = \frac{z\omega_1\omega_2 + \omega_1 + \omega_2 + 1}{\omega_1\omega_2(z - 1)}. \quad (\text{H.36})$$

We obtain an ordinary differential equation for the function $F(X)$:

$$(1 - X)XF''(X) + ((j_1 - j_2 - 2)X + 1)F'(X) + (j_1 - 1)j_2F(X) = 0. \quad (\text{H.37})$$

The relevant solution

$$F(X) = c_1 {}_2F_1(1 - j_1, j_2; 1; X) \quad (\text{H.38})$$

is selected by the requirement that it be regular at $X = 0$. This boundary condition amounts to setting $z\omega_1\omega_2 + \omega_1 + \omega_2 + 1 = 0$ in the integral (H.11). The constant c_1 is fixed by taking the limit $\omega_i \rightarrow 0$ and comparing with the value of the integral (H.8).

An alternative substitution is

$$K_{\text{SS}}(z, \omega_i) = (\omega_1 + 1)^{j_1 - j_2} (-\omega_1\omega_2)^{-j_1} G(Y), \quad Y = \frac{(\omega_1 + 1)(\omega_2 + 1)}{\omega_1\omega_2(1 - z)}, \quad (\text{H.39})$$

yielding the differential equation

$$(Y - 1)YG''(Y) + ((j_1 - j_2 + 2)Y - j_1 + j_2 - 1)G'(Y) - j_1(j_2 - 1)G(Y) = 0 \Rightarrow \\ G(Y) = c_2 {}_2F_1(j_1, 1 - j_2; 1 + j_1 - j_2; Y). \quad (\text{H.40})$$

Again, the relevant solution is selected by the boundary condition of regularity at $Y = 0$. This condition amounts to setting $\omega_1 = -1$. Both the solution and the integral (H.11) vanish at this point. The integration constant c_2 can be fixed as before.

We remark that using well-known identities, these solutions can be rewritten in an alternative form involving two hypergeometric functions each. For example, the solution (H.36), (H.38) becomes (cf. (E.17))

$$K_{\text{SS}}(z, \omega_i) = (1 - z)^{j_1 + j_2 - 1} z^{-j_1 - j_2} \frac{(\omega_1 + 1)^{-j_2} (\omega_2 + 1)^{-j_1} \Gamma(1 - j_1 - j_2)}{[\Gamma(1 - j_1) \Gamma(1 - j_2)]^2 \Gamma(j_1 + j_2)} \\ \times {}_2F_1\left(j_1, j_2; j_1 + j_2; \frac{\omega_1\omega_2(1 - z)}{(\omega_1 + 1)(\omega_2 + 1)}\right) \\ + z^{-j_1 - j_2} \frac{(\omega_1\omega_2)^{-j_1 - j_2 + 1} (\omega_1 + 1)^{j_1 - 1} (\omega_2 + 1)^{j_2 - 1} \sin(\pi j_1) \sin(\pi j_2)}{\pi^2 (j_1 + j_2 - 1)} \\ \times {}_2F_1\left(1 - j_1, 1 - j_2; 2 - j_1 - j_2; \frac{\omega_1\omega_2(1 - z)}{(\omega_1 + 1)(\omega_2 + 1)}\right). \quad (\text{H.41})$$

Both terms in this expression are particular solutions of the differential equation (5.17). The boundary conditions are less obvious in this form. The first term admits a power series expansion $\sum_{m,n=0}^{\infty} c_{m,n} \omega_1^m \omega_2^n$ while the second term has a non-analytic behavior near the origin. It can be shown that the regular solution of (5.17) is unique up to normalization. So, the scalar kernels share the same regular part but differ by their non-analytic parts.

I Singular terms in the energy-energy correlation

In this appendix we explain the origin of the last two terms in the expression (6.16) for the energy-energy correlation. A feature of these terms is that they scale at small z as $\log z/z$,

$$\text{EEC}_{++}^{(1)} \sim -\frac{\log z}{z} \omega_1^2 \omega_2^2 \left(\frac{1}{72(\omega_1 + 1)} + \frac{1}{72(\omega_2 + 1)} + \frac{1}{12\sqrt{(\omega_1 + \omega_2)^2 - 4\omega_1\omega_2 z}} \right). \quad (\text{I.1})$$

As explained in Section 3.3, such singular terms come from the detector cross talk.

Applying (5.10) and (4.9) we get

$$\text{EEC}_{++}^{(1)}(\omega_1, \omega_2, z) = - \int \frac{dj_1 dj_2}{(2\pi i)^2} K_{\text{EE}}(j_1, j_2 | z, \omega_1, \omega_2) \frac{(j_1 + j_2)^2}{j_1^2 j_2^2}, \quad (\text{I.2})$$

where the kernel K_{EE} can be obtained from the analogous kernel for the scalar detectors K_{SS} using the relation (5.13). Replacing K_{SS} with its integral representation (E.10) and going to the limit $z \rightarrow 0$, we find after some algebra

$$\begin{aligned} \text{EEC}_{++}^{(1)}(\omega_1, \omega_2, z) \sim & - \int \frac{dj_1 dj_2}{(2\pi i)^2} \frac{z^{-2-j}}{(1+j)} \int_0^\infty ds_1 ds_2 f(s_1, s_2 | \omega_1, \omega_2) \\ & \times (s_1(s_2 + \omega_2))_+^{-j_1-2} (s_2(s_1 + \omega_1))_+^{-j+j_1-2} \\ & \times (1 - s_1 - s_2 + z s_1 s_2)^j \theta(1 - s_1 - s_2 + z s_1 s_2), \end{aligned} \quad (\text{I.3})$$

where we changed the integration variable $j = j_1 + j_2$ and introduced the function

$$f(s_1, s_2 | \omega_1, \omega_2) = \frac{\omega_1^2 \omega_2^2}{72} (s_1^2 \omega_2^2 + s_2^2 \omega_1^2 + 4s_2 s_1 \omega_1 \omega_2 + 6s_2 s_1^2 \omega_2 + 6s_2^2 s_1 \omega_1 + 6s_2^2 s_1^2). \quad (\text{I.4})$$

The integration contour in the Mellin integral in (I.3) satisfies $\text{Re}(j_1) < 0$ and $\text{Re } j > -1$. The two factors in the second line of (I.3) are defined with the ‘+’ prescription, see (I.5). This is needed to make the integral over small s_1 and s_2 in (I.3) well defined.

Closing the integration contour over j in (I.3) to the left half-plane, we find that the leading contribution for $z \rightarrow 0$ comes from the pole at $j = -1$. An additional pole arises after the integration over small $w \equiv 1 - s_1 - s_2 + z s_1 s_2$. Applying the identity

$$\frac{1}{w^{-j}} = -\frac{1}{1+j} \delta(w) + \left[\frac{1}{w} \right]_+ + O(1+j) \quad (\text{I.5})$$

and taking the residue at the double pole, we obtain from (I.3)

$$\begin{aligned} \text{EEC}_{++}^{(1)}(\omega_1, \omega_2, z) \stackrel{z \rightarrow 0}{\sim} & -\frac{\log z}{z} \int \frac{dj_1}{2\pi i} \int_0^\infty ds_1 ds_2 f(s_1, s_2 | \omega_1, \omega_2) \\ & \times (s_1(s_2 + \omega_2))_+^{-j_1-2} (s_2(s_1 + \omega_1))_+^{j_1-1} \delta(1 - s_1 - s_2 + z s_1 s_2). \end{aligned} \quad (\text{I.6})$$

As in the previous case, the integration over small s_1 and s_2 yields additional poles at $j_1 = -1$ and $j_1 = 0$, respectively. Their contribution to the right-hand side of (I.6) is

$$-\frac{\log z}{z} \times \frac{\omega_1^2 \omega_2^2}{72} \left(\frac{1}{1 + \omega_1} + \frac{1}{1 + \omega_2} \right). \quad (\text{I.7})$$

The remaining contribution from nonzero s_i looks as

$$\begin{aligned} & -24 \frac{\log z}{z} \omega_2^4 \int_0^\infty ds_1 ds_2 \frac{(s_1 + \omega_1)^2}{(s_2 + \omega_2)^2} \delta(s_1 \omega_2 - s_2 \omega_1) \delta(1 - s_1 - s_2 + z s_1 s_2) \\ &= -\frac{\log z}{z} \frac{\omega_1^2 \omega_2^2}{12} \int_0^\infty ds_1 ds_2 \delta(s_1 \omega_2 - s_2 \omega_1) \delta(1 - s_1 - s_2 + z s_1 s_2) \\ &= -\frac{\log z}{z} \frac{\omega_1^2 \omega_2^2}{12} \frac{1}{\sqrt{(\omega_1 + \omega_2)^2 - 4z\omega_1\omega_2}}, \end{aligned} \quad (\text{I.8})$$

where $\delta(s_1 \omega_2 - s_2 \omega_1)$ results from the integration over j_1 in (I.6). Putting together the last two relations we recover (I.1). Notice that the integral (I.8) vanishes for ω_1 and ω_2 of opposite signs. This explains why the expression (6.15) for EEC_{+-} does not contain terms like (I.8).

J Time profile in the detector

In this appendix we address the question what is the longitudinal profile observed by a calorimeter in the physical state

$$|\Psi\rangle \simeq \int d^4x \, e^{iP \cdot x} e^{-\frac{t^2 + \vec{x}^2}{4\sigma^2}} J(x) |\Omega\rangle. \quad (\text{J.1})$$

We only consider here the simplest case of the one-point energy correlation. Consider the energy calorimeter centered around the retarded time t_0 and working in the interval $t_0 - T \leq t \leq t_0 + T$

$$\mathcal{E}_{t_0, T}(n) = \int_{-T}^T du \, T_{uu}(u - t_0, \vec{n}) = \int_{-\infty}^{\infty} \frac{d\hat{\omega}}{\pi} \frac{\sin \hat{\omega} T}{\hat{\omega}} e^{i\hat{\omega} t_0} \mathcal{E}(\hat{\omega}, n). \quad (\text{J.2})$$

We can easily relate the one-point function of $\mathcal{E}_{t_0, T}(n)$ to the one-point function studied in the bulk of the paper

$$\langle \Psi | \mathcal{E}_{t_0, T}(n) | \Psi \rangle = \int d^4q \int \frac{d\hat{\omega}}{\pi} f_\sigma(q + \hat{\omega}n) f_\sigma(q) \frac{\sin \hat{\omega} T}{\hat{\omega}} e^{i\hat{\omega} t_0} \langle \langle J(q + \hat{\omega}n) \mathcal{E}(\hat{\omega}, n) J(q) \rangle \rangle, \quad (\text{J.3})$$

where it is natural to choose the wave function to be centered around a given momentum P^μ with some spread $1/\sigma$,

$$f_\sigma(q) \sim e^{-\sigma^2 [(q^0 - P^0)^2 + (\vec{q} - \vec{P})^2]}. \quad (\text{J.4})$$

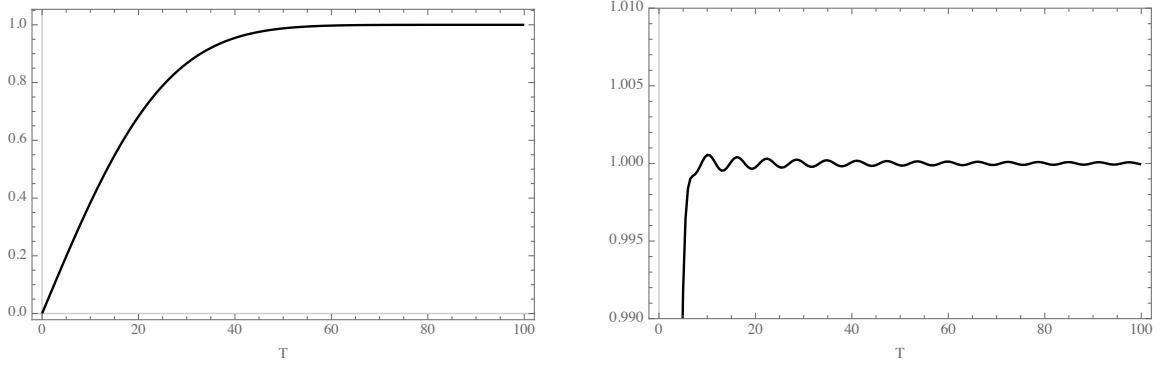


Figure 6. Time dependence of the energy measurement for $P^\mu = (P^0, \vec{0})$ with $P^0 = 1$. We set $\sigma = 10$ (the left panel) and for $\sigma = 1$ (the right panel). In the latter case we observe small quantum oscillations around the asymptotic value.

In the coordinate space such a wave function is localized around the origin with a spread σ both in space and time.

Let us choose the source to have the scaling dimension $\Delta_\phi = 2$ for simplicity and use (2.49) and (2.50). We go to the center-of-mass frame and set $P^\mu = (P^0, \vec{0})$ with $P^0 = 1$. We also consider a narrow wave packet so that $\sigma P^0 \gg 1$. In this limit, the integral over q is localized at $q = P$. Finally, we set $t_0 = 0$ since its effect is simply to shift the origin of the plots considered below. In this regime the result is captured by the following integral

$$\int_{-1}^{\infty} \frac{d\hat{\omega}}{\pi} e^{-2\sigma^2 \hat{\omega}^2} \frac{\sin \hat{\omega} T}{\hat{\omega}} \left(1 + \hat{\omega} + \frac{1}{6} \hat{\omega}^2 \right), \quad (\text{J.5})$$

where we used the fact that $f_\sigma(P + \hat{\omega}n) = e^{-2\sigma^2 \hat{\omega}^2}$. The lower limit on the integral comes from the condition that the time component of $P + \hat{\omega}n$ is non-negative, which is necessary for $\langle\langle J(P + \hat{\omega}n) \mathcal{E}(\hat{\omega}, n) J(P) \rangle\rangle$ to be non-zero.

We plot (J.5) in Figure 6 for different values of σ . The response of the calorimeter starts at 0 and then goes to its asymptotic value 1 on time scales set by the size of the spread of the wave function in the coordinate space σ . As σ decreases two effects occur: first, the asymptotic value of the energy detector response is reached faster; second, quantum oscillations develop around the asymptotic value 1.³⁷

References

- [1] D. M. Hofman and J. Maldacena, *Conformal collider physics: Energy and charge correlations*, *JHEP* **05** (2008) 012 [[0803.1467](#)].
- [2] N. A. Sveshnikov and F. V. Tkachov, *Jets and quantum field theory*, *Phys. Lett. B* **382** (1996) 403 [[hep-ph/9512370](#)].

³⁷We say quantum because in a classical field theory, where the energy flux is locally positive, the one-point function is monotonically increasing as we increase T .

- [3] G. P. Korchemsky, G. Oderda and G. F. Sterman, *Power corrections and nonlocal operators*, *AIP Conf. Proc.* **407** (1997) 988 [[hep-ph/9708346](#)].
- [4] G. P. Korchemsky and G. F. Sterman, *Power corrections to event shapes and factorization*, *Nucl. Phys. B* **555** (1999) 335 [[hep-ph/9902341](#)].
- [5] T. Hartman, S. Kundu and A. Tajdini, *Averaged Null Energy Condition from Causality*, *JHEP* **07** (2017) 066 [[1610.05308](#)].
- [6] T. Faulkner, R. G. Leigh, O. Parrikar and H. Wang, *Modular Hamiltonians for Deformed Half-Spaces and the Averaged Null Energy Condition*, *JHEP* **09** (2016) 038 [[1605.08072](#)].
- [7] Y. Hatta, E. Iancu, A. H. Mueller and D. N. Triantafyllopoulos, *Jet evolution from weak to strong coupling*, *JHEP* **12** (2012) 114 [[1210.1534](#)].
- [8] A. Belin, D. M. Hofman, G. Mathys and M. T. Walters, *On the stress tensor light-ray operator algebra*, *JHEP* **05** (2021) 033 [[2011.13862](#)].
- [9] A. Martin and J.-M. Richard, *New result on phase shift analysis*, *Phys. Rev. D* **101** (2020) 094014 [[2004.11156](#)].
- [10] P. Kravchuk and D. Simmons-Duffin, *Light-ray operators in conformal field theory*, *JHEP* **11** (2018) 102 [[1805.00098](#)].
- [11] H. Chen, I. Moulton, X. Zhang and H. X. Zhu, *Rethinking jets with energy correlators: Tracks, resummation, and analytic continuation*, *Phys. Rev. D* **102** (2020) 054012 [[2004.11381](#)].
- [12] L. J. Dixon, I. Moulton and H. X. Zhu, *Collinear limit of the energy-energy correlator*, *Phys. Rev. D* **100** (2019) 014009 [[1905.01310](#)].
- [13] H. Chen, I. Moulton and H. X. Zhu, *Spinning Gluons from the QCD Light-Ray OPE*, [2104.00009](#).
- [14] H. Chen, I. Moulton and H. X. Zhu, *Quantum Interference in Jet Substructure from Spinning Gluons*, *Phys. Rev. Lett.* **126** (2021) 112003 [[2011.02492](#)].
- [15] M. Kologlu, P. Kravchuk, D. Simmons-Duffin and A. Zhiboedov, *Shocks, Superconvergence, and a Stringy Equivalence Principle*, *JHEP* **11** (2020) 096 [[1904.05905](#)].
- [16] A. V. Belitsky, S. Hohenegger, G. P. Korchemsky, E. Sokatchev and A. Zhiboedov, *From correlation functions to event shapes*, *Nucl. Phys. B* **884** (2014) 305 [[1309.0769](#)].
- [17] A. V. Belitsky, S. Hohenegger, G. P. Korchemsky, E. Sokatchev and A. Zhiboedov, *Event shapes in $\mathcal{N} = 4$ super-Yang-Mills theory*, *Nucl. Phys. B* **884** (2014) 206 [[1309.1424](#)].
- [18] A. V. Belitsky, S. Hohenegger, G. P. Korchemsky, E. Sokatchev and A. Zhiboedov, *Energy-Energy Correlations in $\mathcal{N}=4$ Supersymmetric Yang-Mills Theory*, *Phys. Rev. Lett.* **112** (2014) 071601 [[1311.6800](#)].
- [19] J. M. Henn, E. Sokatchev, K. Yan and A. Zhiboedov, *Energy-energy correlation in $\mathcal{N}=4$ super Yang-Mills theory at next-to-next-to-leading order*, *Phys. Rev. D* **100** (2019) 036010 [[1903.05314](#)].
- [20] A. V. Belitsky, S. Hohenegger, G. P. Korchemsky and E. Sokatchev, *$\mathcal{N}=4$ superconformal Ward identities for correlation functions*, *Nucl. Phys. B* **904** (2016) 176 [[1409.2502](#)].

- [21] G. P. Korchemsky and E. Sokatchev, *Four-point correlation function of stress-energy tensors in $\mathcal{N} = 4$ superconformal theories*, *JHEP* **12** (2015) 133 [[1504.07904](#)].
- [22] G. P. Korchemsky and A. Zhiboedov, *On the light-ray algebra in conformal field theories*, [2109.13269](#).
- [23] L. F. Alday and A. Bissi, *Loop Corrections to Supergravity on $AdS_5 \times S^5$* , *Phys. Rev. Lett.* **119** (2017) 171601 [[1706.02388](#)].
- [24] F. Aprile, J. M. Drummond, P. Heslop and H. Paul, *Quantum Gravity from Conformal Field Theory*, *JHEP* **01** (2018) 035 [[1706.02822](#)].
- [25] L. F. Alday and S. Caron-Huot, *Gravitational S-matrix from CFT dispersion relations*, *JHEP* **12** (2018) 017 [[1711.02031](#)].
- [26] L. F. Alday, *On genus-one string amplitudes on $AdS_5 \times S^5$* , *JHEP* **04** (2021) 005 [[1812.11783](#)].
- [27] J. Penedones, J. A. Silva and A. Zhiboedov, *Nonperturbative Mellin Amplitudes: Existence, Properties, Applications*, *JHEP* **08** (2020) 031 [[1912.11100](#)].
- [28] J. D. Qualls, *Lectures on Conformal Field Theory*, [1511.04074](#).
- [29] E. Witten, *APS Medal for Exceptional Achievement in Research: Invited article on entanglement properties of quantum field theory*, *Rev. Mod. Phys.* **90** (2018) 045003 [[1803.04993](#)].
- [30] G. P. Korchemsky, *Energy correlations in the end-point region*, *JHEP* **01** (2020) 008 [[1905.01444](#)].
- [31] M. Kologlu, P. Kravchuk, D. Simmons-Duffin and A. Zhiboedov, *The light-ray OPE and conformal colliders*, *JHEP* **01** (2021) 128 [[1905.01311](#)].
- [32] P. Kravchuk, J. Qiao and S. Rychkov, *Distributions in CFT. Part I. Cross-ratio space*, *JHEP* **05** (2020) 137 [[2001.08778](#)].
- [33] V. M. Braun, G. P. Korchemsky and D. Müller, *The Uses of conformal symmetry in QCD*, *Prog. Part. Nucl. Phys.* **51** (2003) 311 [[hep-ph/0306057](#)].
- [34] M. Gary, S. B. Giddings and J. Penedones, *Local bulk S-matrix elements and CFT singularities*, *Phys. Rev. D* **80** (2009) 085005 [[0903.4437](#)].
- [35] J. Maldacena, D. Simmons-Duffin and A. Zhiboedov, *Looking for a bulk point*, *JHEP* **01** (2017) 013 [[1509.03612](#)].
- [36] J. Penedones, *Writing CFT correlation functions as AdS scattering amplitudes*, *JHEP* **03** (2011) 025 [[1011.1485](#)].
- [37] F. Aprile and P. Vieira, *Large p explorations. From SUGRA to big STRINGS in Mellin space*, *JHEP* **12** (2020) 206 [[2007.09176](#)].
- [38] S. M. Chester, *Genus-2 holographic correlator on AdS_5 times S^5 from localization*, *JHEP* **04** (2020) 193 [[1908.05247](#)].

- [39] D. Carmi and S. Caron-Huot, *A Conformal Dispersion Relation: Correlations from Absorption*, *JHEP* **09** (2020) 009 [[1910.12123](#)].
- [40] D. Mazáč, L. Rastelli and X. Zhou, *A Basis of Analytic Functionals for CFTs in General Dimension*, [1910.12855](#).
- [41] S. Caron-Huot, D. Mazac, L. Rastelli and D. Simmons-Duffin, *Dispersive CFT Sum Rules*, *JHEP* **05** (2021) 243 [[2008.04931](#)].
- [42] G. Mack, *D-independent representation of Conformal Field Theories in D dimensions via transformation to auxiliary Dual Resonance Models. Scalar amplitudes*, [0907.2407](#).
- [43] G. Mack, *D-dimensional Conformal Field Theories with anomalous dimensions as Dual Resonance Models*, *Bulg. J. Phys.* **36** (2009) 214 [[0909.1024](#)].
- [44] M. S. Costa, V. Goncalves and J. Penedones, *Conformal Regge theory*, *JHEP* **12** (2012) 091 [[1209.4355](#)].
- [45] R. Gopakumar, A. Sinha and A. Zahed, *Crossing Symmetric Dispersion Relations for Mellin Amplitudes*, *Phys. Rev. Lett.* **126** (2021) 211602 [[2101.09017](#)].
- [46] A. L. Fitzpatrick, J. Kaplan, M. T. Walters and J. Wang, *Eikonalization of Conformal Blocks*, *JHEP* **09** (2015) 019 [[1504.01737](#)].
- [47] A. Bissi, G. Fardelli and A. Georgoudis, *All loop structures in Supergravity Amplitudes on $AdS_5 \times S^5$ from CFT*, [2010.12557](#).
- [48] D. Amati, M. Ciafaloni and G. Veneziano, *Higher Order Gravitational Deflection and Soft Bremsstrahlung in Planckian Energy Superstring Collisions*, *Nucl. Phys. B* **347** (1990) 550.
- [49] L. Cornalba, M. S. Costa and J. Penedones, *Eikonal approximation in AdS/CFT: Resumming the gravitational loop expansion*, *JHEP* **09** (2007) 037 [[0707.0120](#)].
- [50] V. Gonçalves, *Four point function of $\mathcal{N} = 4$ stress-tensor multiplet at strong coupling*, *JHEP* **04** (2015) 150 [[1411.1675](#)].
- [51] D. J. Binder, S. M. Chester, S. S. Pufu and Y. Wang, *$\mathcal{N} = 4$ Super-Yang-Mills correlators at strong coupling from string theory and localization*, *JHEP* **12** (2019) 119 [[1902.06263](#)].
- [52] D. J. Gross and P. F. Mende, *String Theory Beyond the Planck Scale*, *Nucl. Phys. B* **303** (1988) 407.
- [53] L. Cornalba, M. S. Costa, J. Penedones and R. Schiappa, *Eikonal Approximation in AdS/CFT: From Shock Waves to Four-Point Functions*, *JHEP* **08** (2007) 019 [[hep-th/0611122](#)].
- [54] L. Cornalba, M. S. Costa, J. Penedones and R. Schiappa, *Eikonal Approximation in AdS/CFT: Conformal Partial Waves and Finite N Four-Point Functions*, *Nucl. Phys. B* **767** (2007) 327 [[hep-th/0611123](#)].
- [55] P. Di Vecchia, A. Luna, S. G. Naculich, R. Russo, G. Veneziano and C. D. White, *A tale of two exponentiations in $\mathcal{N} = 8$ supergravity*, *Phys. Lett. B* **798** (2019) 134927 [[1908.05603](#)].
- [56] P. Di Vecchia, S. G. Naculich, R. Russo, G. Veneziano and C. D. White, *A tale of two*

- exponentiations in $\mathcal{N} = 8$ supergravity at subleading level, *JHEP* **03** (2020) 173 [[1911.11716](#)].
- [57] N. Arkani-Hamed and J. Maldacena, *Cosmological Collider Physics*, [1503.08043](#).
 - [58] C.-H. Chang, M. Kologlu, P. Kravchuk, D. Simmons-Duffin and A. Zhiboedov, *Transverse spin in the light-ray OPE*, [2010.04726](#).
 - [59] M. Beşken, J. De Boer and G. Mathys, *On Local and Integrated Stress-Tensor Commutators*, [2012.15724](#).
 - [60] R. Bousso, Z. Fisher, S. Leichenauer and A. C. Wall, *Quantum focusing conjecture*, *Phys. Rev. D* **93** (2016) 064044 [[1506.02669](#)].
 - [61] R. Bousso, Z. Fisher, J. Koeller, S. Leichenauer and A. C. Wall, *Proof of the Quantum Null Energy Condition*, *Phys. Rev. D* **93** (2016) 024017 [[1509.02542](#)].
 - [62] S. Balakrishnan, T. Faulkner, Z. U. Khandker and H. Wang, *A General Proof of the Quantum Null Energy Condition*, *JHEP* **09** (2019) 020 [[1706.09432](#)].
 - [63] H. Chen, M.-X. Luo, I. Moulton, T.-Z. Yang, X. Zhang and H. X. Zhu, *Three point energy correlators in the collinear limit: symmetries, dualities and analytic results*, *JHEP* **08** (2020) 028 [[1912.11050](#)].
 - [64] L. V. Bork, *On form factors in $\mathcal{N} = 4$ SYM theory and polytopes*, *JHEP* **12** (2014) 111 [[1407.5568](#)].
 - [65] L. Bianchi, A. Brandhuber, R. Panerai and G. Travaglini, *Form factor recursion relations at loop level*, *JHEP* **02** (2019) 182 [[1812.09001](#)].
 - [66] D. Chicherin, R. Doobary, B. Eden, P. Heslop, G. P. Korchemsky and E. Sokatchev, *Bootstrapping correlation functions in $N=4$ SYM*, *JHEP* **03** (2016) 031 [[1506.04983](#)].
 - [67] D. Chicherin, R. Doobary, B. Eden, P. Heslop, G. P. Korchemsky, L. Mason et al., *Correlation functions of the chiral stress-tensor multiplet in $\mathcal{N} = 4$ SYM*, *JHEP* **06** (2015) 198 [[1412.8718](#)].
 - [68] T. Fleury and R. Pereira, *Non-planar data of $\mathcal{N} = 4$ SYM*, *JHEP* **03** (2020) 003 [[1910.09428](#)].
 - [69] G. P. Korchemsky, *Exact scattering amplitudes in conformal fishnet theory*, *JHEP* **08** (2019) 028 [[1812.06997](#)].
 - [70] M. Gillioz, M. Meineri and J. Penedones, *A scattering amplitude in Conformal Field Theory*, *JHEP* **11** (2020) 139 [[2003.07361](#)].
 - [71] R. Gonzo and A. Pokraka, *Light-ray operators, detectors and gravitational event shapes*, *JHEP* **05** (2021) 015 [[2012.01406](#)].
 - [72] M. S. Costa, J. Penedones, D. Poland and S. Rychkov, *Spinning Conformal Correlators*, *JHEP* **11** (2011) 071 [[1107.3554](#)].
 - [73] V. K. Dobrev, G. Mack, V. B. Petkova, S. G. Petrova and I. T. Todorov, *Harmonic Analysis on the n -Dimensional Lorentz Group and Its Application to Conformal Quantum Field Theory*, vol. 63. 1977, [10.1007/BFb0009678](#).